GEOCHEMISTRY AND PETROGENESIS OF GRANITIC ROCKS AROUND HUTTI SCHIST BELT, DHARWAR CRATON

A THESIS
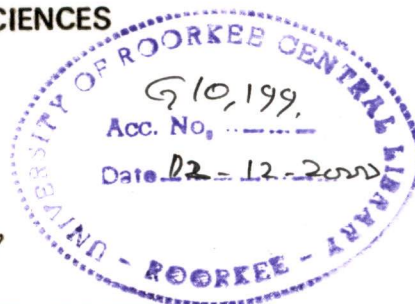
Submitted in fulfilment of the
requirements for the award of the degree
of
DOCTOR OF PHILOSOPHY
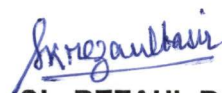*in*

EARTH SCIENCES

By

Sk. REZAUL BASIR

DEPARTMENT OF EARTH SCIENCES
UNIVERSITY OF ROORKEE
ROORKEE-247 667 (INDIA)

JANUARY, 2000

CANDIDATE'S DECLARATION

I, hereby, certify that the work which is being presented in this thesis entitled **"GEOCHEMISTRY AND PETROGENESIS OF GRANITIC ROCKS AROUND HUTTI SCHIST BELT, DHARWAR CRATON"** in fulfilment of the requirement for the award of the Degree of **Doctor of Philosophy**, submitted in the **Department of Earth Sciences** of the university, is an authentic record of my own work carried out during a period from July, 1996 to January, 2000 under the supervision of Dr. S. Balakrishnan and Dr. D.C. Srivastava.

The matter embodied in this thesis has not been submitted by me for the award of any other degree.

Sk. REZAUL BASIR

This is to certify that the above statement made by the candidate is correct to the best of our knowledge.

Dr. D.C. SRIVASTAVA

Associate Professor
Department of Earth Sciences
University of Roorkee
Roorkee - 247 667, U.P.
INDIA

Dr. S. BALAKRISHNAN

Professor
Department of Earth Sciences
Pondicherry University
Pondicherry - 605 014
INDIA

Date: 04.01.2000.

The Ph.D. viva-voce examination of **Mr. Sk. Rezaul Basir**, Research Scholar has been held on 27.9.2000

Signature of Supervisors Signature of H.O.D. Signature of External Examiner

Acknowledgement

Sk. Rezual Basir

ABSTRACT

The Dharwar craton of south India is one of the major Archean cratons that consists of low to high grade supracrustals within a sea of tonalite-trondhjemite-granodiorite (TTG) suite of rocks. The eastern Dharwar craton consists of several gold mineralized schist belts (e.g. Kolar, Ramagiri, and Hutti) that are essentially composed of pillowed metabasalts, rhyolites, polymictic conglomerates, grits, phyllites and Banded Iron Formation (BIF) at various stratigraphic levels. Of these, the Hutti schist has attained greenschist to amphibolite grade of metamorphism. The typical hook shaped map pattern of the Hutti schist belt is a consequence of two co-axial phases of folding.

Geochemically the granoitiods surrounding the Hutti schist belt are divided into four distinct groups: (1) quartz monzodiorite (2) granodiorite, (3) granite, and (4) monzodiorite.

The quartz monzodiorites have SiO_2 content of the order of 62 wt.%. They have higher MgO, CaO and Ba and lower Na_2O and K_2O content as compared to that of the granodiorites. Their Mg# (0.6-0.66) are much higher than that of any other rock types analyzed from the study area. They show LREE enriched (Ce_N/Yb_N = 14.14) and HREE depleted (Er_N/Yb_N = 0.89) rare earth element patterns with slight or no Eu anomaly.

On the basis of geochemical modeling, it is argued that the magmas parental to quartz monzodiorites can neither be derived by partial melting of tholeiitic metabasalts occurring in the Hutti schist belt nor they represent the residual magmas formed by fractional crystallization of common mineral phases from tholeiitic magmas. [Mg]-[Fe] modeling suggests that the parental magmas of quartz monzodiorites are derived by partial melting of

a composite mantle source that is compositionally similar to komatiite. But the trace element modeling suggests that the sources, formed by mixing of garnet lherzolite and basaltic magmas, must have been enriched in incompatible trace elements prior to melting. It is argued that partial melting of composite sources in the mantle wedge, similar in composition to that of komatiite enriched in LILEs and LREEs might have given rise to the magmas parental to the quartz monzodiorites.

Granodiorites are the most dominant rock types amongst the granitoids around the Hutti schist belt. They are silica saturated to oversaturated rocks (65.25 to 72.49 wt.%). Na_2O abundance in these rocks is invariably higher than K_2O. The rocks are meta-aluminous in nature and define a calc-alkaline trend. In general, these rocks have high concentration of Ba (454 to 918 ppm) and Sr (> 450 ppm). Though the granodiorites occurring to east, west and north of the belt have broadly similar major element chemistry but they differ in their trace element, REE abundance, and chondrite normalized REE patterns.

Western granodiorites have chondrite normalized REE patterns parallel to that of quartz monzodiorites with no Eu anomaly. Their major and trace element abundance as well as geochemical modeling suggest that they can be derived by fractional crystallization processes including liquid immiscibility from quartz monzodiorites.

The eastern granodiorites (named as Kavital granodiorites) have higher MgO, FeO, TiO_2, and higher Mg# than that of western granodiorites. They have highly fractionated chondrite normalized REE patterns with slight negative or no Eu anomaly. It is suggested that they might have been derived by partial melting of intermediate rocks similar in composition to that of sanukitoids, high magnesian andesites or adakites.

Granodiorites occurring to the north of the belt are named as Northern granodiorites. Although their major and trace element abundance are comparable to that of Kavital granodiorites, their chondrite normalized REE patterns are less fractionated and show negative Eu anomaly. On the basis of geochemical modeling it is suggested that Northern granodiorites are derived by low pressure partial melting of Hutti metabasalts having island arc affinities.

The granites of Hutii schist belt are classified into two categories: high alkali granites and low alkali granites that occur towards northeast and northwest parts of the belt, respectively. In general, the low alkali granites have higher abundance of CaO, Ba and

lower Sr than the high alkali granites. They show fractionated chondrite normalized REE patterns with strong negative Eu anomaly. In contrast, the high alkali granites show more negative Eu anomaly as compared to the low alkali granites. Geochemical modeling suggests that both type of granites could have been derived by low extents partial melting of granodiorites similar in composition to that of Kavital granodiorites under hydrous conditions of melting ($P_{H2O} = P_{total}$) at pressures ≥ 0.5 GPa.

Although the major element abundance in the monzodiorite occurring east and west of the Hutti schist belt are similar, these two monzodiorites differ in their REE patterns. The eastern monzodiorite is characterized by highly fractionated chondrite normalized REE pattern ($Ce_N/Yb_N = 37.0$) with slight negative Eu anomaly ($Eu/Eu^* = 0.78$), whereas, the western monzodiorite is characterized by less fractionated chondrite normalized REE patterns ($Ce_N/Yb_N = 7.07$) and almost no Eu anomaly ($Eu/Eu^* = 0.97$). On the basis of geochemical modeling it implies that the eastern monzodiorite could have been derived by partial melting of LREE enriched basaltic andesites, whereas, the western monzodiorite can be generated by partial melting of Hutti metabasalts.

On the basis of field, petrographic and geochemical characteristics it is shown that the granodiorites occurring to east, west and north of the belt have distinct petrogenetic characteristics and they form three disparate granitoid terranes. It is suggested that these unrelated granitoid terranes that are separated by the schist belt might have been emplaced in island arc tectonic settings. The tholeiitic basalts occurring in the Hutti schist belt have evolved in the island arc environment.

CONTENTS

LIST OF TABLES

LIST OF FIGURES

LIST OF PLATES

CHAPTER 1

INTRODUCTION

Most Archean Shield areas consist of linear supracrustal belts that are surrounded by granitoid rocks. Although some supracrustal belts may represent intracratonic rift basins formed due to crustal thinning, for others the age relationship between the supracrustal belts and the surrounding granitoids is ambiguous. More than 60 to 80% of the Archean continental crust is composed of trondjemite-tonalite-granodiorite (TTG) suite that plays an important role in the evolution and growth of the continental crust (Drummond and Defant, 1990). Hence, study of the granitoids surrounding Archean supracrustal belts is important in understanding the growth and evolution of the continental crust as well as mineralization usually associated with the supracrustal-granite terranes.

It is now widely regarded that the plate tectonic processes could have been responsible for the growth of the early continental crust (Burke, et al., 1976; Tarney, et al 1976; Condie, 1981, 1986, 1988; Windley, 1984; Nisbet, 1987; Krogstad et al., 1989). Prominent views to explain the evolution of the Archean continental crust include: I) growth by juvenile addition of materials directly or indirectly derived from the mantle up to 3 Ga and subsequent growth by recycling of the continental crust (Taylor and McLeanan, 1981). II) growth by continuous inputs from the mantle throughout the Archean (Shirey and Hanson 1984).

Several hypotheses exist on the petrogenesis of Archean to recent TTG. But, generally they are considered to be the product of island arc and continental margin magmatism associated with subduction zones (Barker and Arth, 1976; Barker, 1979; Drummond and Defant, 1990). The elevated rate of continental crustal growth during the Archean as compared to the post-Archean indicates that heat flow and consequently plate

movements were greater in the Archean (Sleep and Windley, 1982). Hence, it has been suggested that the partial melting of the subducting oceanic crust was possible during the Archean (Parson and Sclater, 1977; Drummond and Defant, 1990) and such melts constituted the major component of the magmas parental to Archean TTG suite (Drummond and Defant, 1990). However, in present day, partial melting of mantle wedge above the subducting slab is the main source for generating arc magmas. In the subduction zone, the subducting oceanic crust undergoes dehydration and releases volatiles which react with the mantle wedge that gets enriched in LILEs and REEs prior to melting (Thompson, 1992; Kay et al., 1993).

The granitoid rocks that are formed by partial melting of subducting oceanic slab can be identified by geochemical modeling. Experimental studies by Rapp and Watson (1995) and Tatsumui and Eggins (1995) show that the subducting slab melts at 0.22-0.30 GPa pressure, at which garnet is one of the major residual phases along with ortho-pyroxene, clinopyroxene and plagioclase. Since the REE K_d values of garnet are very high for HREEs, there is greater depletion of HREEs in the melt and the chondrite normalized REE pattern of the melt will be highly fractionated. The melts formed by subducting slab will be having its own geochemical characteristics, particularly for REEs as compared to those formed by partial melting of other sources, such as the mantle wedge. Hence, geochemical studies on Archean granitoids are very useful in deciphering the extent of contribution to the continental crustal growth by way of partial melting of oceanic crust at subduction zones. A detailed geochemical study on Archean granitoids is helpful in placing constraints on the possible sources and tectonic settings for granitoid magma generation. From this, it is possible to infer about the geothermal gradient and rate of tectonic processes that prevailed during the Archean.

The eastern Dharwar craton consists of several gold mineralized schist belts (e.g. Kolar, Ramagiri, Hutti etc.). Extensive geological, geochemical and geochronological studies have been carried out on Kolar and Ramagiri schist belts and on granitoids surrounding these belts. These studies show that the Kolar schist belt is a volcanic dominated supracrustal belt which comprises amphibolites of tholeiitic and komatitic affinities and minor felsic volcanics and BIF (Anantha Iyer and Vasudev, 1979; Anantha Iyer et al., 1980; Rajamani et al., 1985) On the basis of structural, geochemical and isotopic studies this belt is considered to be suture that formed between two granitoid terranes with distinct

evolutionary histories that have been juxtaposed by the end of Archean (Krogstad et al., 1989, 1991; Balakrishnan et al., 1990).

The Ramagiri schist belt consists predominantly of tholeiitic metabasalts and felsic volcanics with minor metasediments. On the basis of field, petrographic, geochemical and isotopic studies, it has been suggested that the granitoids occurring to east, west and central of the belt form three unrelated granitoid terranes that were assembled together by accretionary processes by the end of late Archean (Zachariah et al., 1995, 1996; Mohanta, 1998; Balakrishnan et al., 1999). Further, these authors suggest that Ramagiri schist belt forms boundary between the three disparate granitoid terranes.

Hutti schist belt occurs ca. 200 km north of Ramagiri, and it is also a volcanic dominated supracrustal belt which is surrounded by granitoids. The granitoid terranes occurring to east, west and north of the Hutti schist belt have distinct rock associations and field characteristics (Srikantia, 1995). The eastern terrane consists of predominantly equigranular granitoids with minor intrusive granites. The western terrane has several rock types including monzodiorites, granodiorites and granites which are foliated at places. The northern terrane consists of porphyritic K-feldspar bearing granodiorites. The objective of the study is to carry out detailed field, petrographic and geochemical studies in order to understand the petrogenesis of the granitoids.

Geochemical studies using major and trace elements including the rare earth elements are important to understand the petrogenesis of these rocks. Such studies can be used as a tool to understand the crustal evolution. Amongst the trace elements, rare earth elements are particularly useful in deciphering the petrogenetic processes because they are relatively less mobile, and their equilibrium distribution values are known. An attempt has been made to understand the crustal evolution of the Hutti area by using the petrogenetic information of the granitoids. This is integrated with the previous studies on Kolar and Ramagiri schist belts to infer the crustal evolution in the eastern Dharwar craton.

CHAPTER 2

GEOLOGY OF THE DHARWAR CRATON

2.1 DHARWAR CRATON

Precambrian rocks constitute most of the Peninsula of India and partly the Himalaya and related mountain regions (Naqvi and Rogers, 1987). The Indian Peninsular shield comprises of Aravalli craton in the west, Singhbhum craton in the east, Bastar in the central, region and Dharwar craton in the south.

The Dharwar craton covers an area of about 238,000 sq. km and it is divisible into two blocks (Fig. 2.1) : Western Block and Eastern Block, separated by Chitradurga boundary fault (Swaminath et al., 1976, Swaminathan and Ramakrishnan, 1981). These two blocks are different in respect of lithology, environment of deposition of sediments, type of volcanisms, character of supracrustal belts and type of metamorphism.

2.2 WESTERN BLOCK

The Western Block is predominantly composed of tonalite–trondjemite–granodiorite (TTG) gneisses. Older supracrustal of Sargur Group occur as small enclaves and narrow belts within the TTG suite. The rocks of Sargur Group consists of amphibolites, serpentinised komatiites, ultramafic intrusive complex and BIF with subordinate amounts of fuchsite quartzites and pelites, marbles and rare chromiferous quartzites and bedded barytes (Radhakrishna, 1993). Several extensive supracrustal in the Western Block are named after the localities such as Bababudan, Chitradurga, Shimoga, Holenarasipur, Javanahalli. Each of these belts is having clear-cut stratigraphy starting with quartz pebble conglomerate that demarcates an unconformity between older granitic gneisses and younger supracrustals.
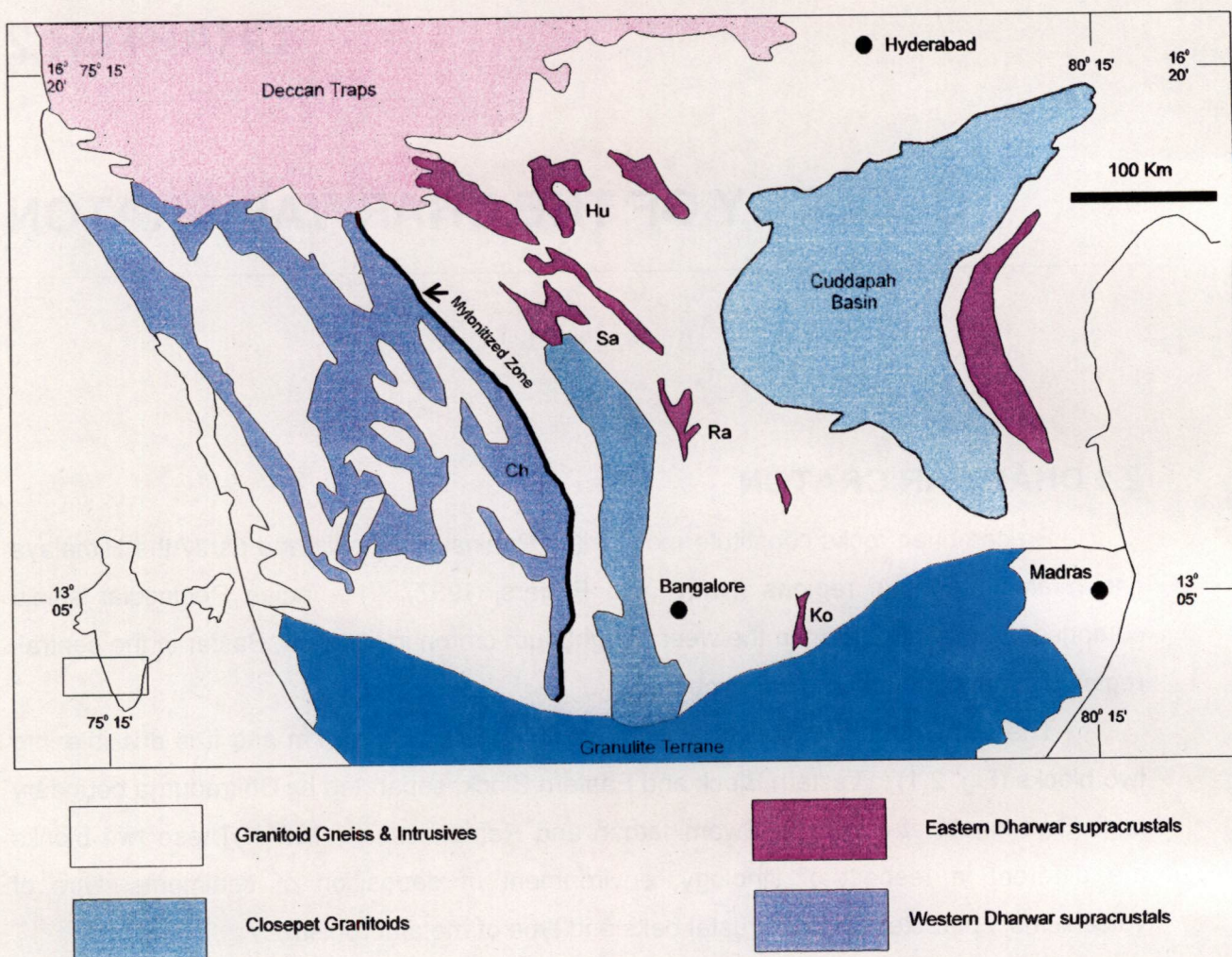
Fig. 2.1 Geological map of southern India (modified after Chadwick et al., 1996). Hu=Hutti, Sa=Sandur, Ra=Ramagiri, Ko=Kolar and Ch=Chitradrga schist belts. Inset shows location of the Dharwar craton.

The Bababudan belt (Group) starts with an unconformity (?) and at places directly overlies Peninsular Gneisses. The rocks of this belt include amygdular basalts–quartzite–phyllite alternations, acid volcanics, ultramafic rocks and prominent BIF (Radhakrishna, 1993). The geology of the 450 km long Chitradurga belt (Group) is highly controversial. A variety of terms have been applied to different parts of the belt. The Chitradurga Group of rocks mainly consists of quartzite, marble, pelite, BIF, pillowed basalt and rhyolite with polymictic conglomerate (containing fragments of the older gneisses) at the base. The Bababudan and Chitradurga Groups together constitute the Dharwar Supergroup. The

5

Bababudan Group is older than the Chitradurga Group (e.g. Viswanatha and Ramakrishna, 1981), but the correlations are controversial (Naqvi and Rogers, 1987)

2.2.1 Structure

Three major parallel N–S shears have been recognized in the Western Block. They are as follows : (i) Chitradurga fault between the western and Eastern Blocks (ii) Bababudan fault at the eastern margin of the Bababudan belt and (iii) Balehonnur fault between Bababudan and Western Ghat belts (Radhakrishna, 1993).

The structures in the Chitradurga belt show north–south orientation throughput the Western Block and affects rocks of widely different ages (Krishna Murthy, 1974, 1978; Chadwick et al., 1978; Roy and Biswas, 1979; Naha and Chatterjee, 1982).

The rocks of Western Block have experienced at least three generations of folding. The first or first two sets of fold are commonly tight and isoclinal whereas the youngest set tends to be more open. The folds of first generation (F_1) are characterized by their steep plunges. The interference of F_1 and F_2 folds resulting in the development of dome and basin structure as evidence in the Bababudan belt (Naqvi and Rogers, 1987). At least three generation of folding were recognized in the Chitradurga belt that is having a more complex view. F_1 folds are isoclinal and reclined with their axial plane schistosity parallel to the bedding whereas F_2 folds are coaxial with F_1 folds. F_2 folds are open to isoclinal and accompanied by development of crenulation cleavage. The F_3 folds in the Chitradurga belt are broad wraps on the limbs of both F_1 and F_2 folds (Naqvi, 1973; Mukhopadhyay and Ghosh, 1983; Mukhopadhyay and Baral, 1985). Naha et al. (1993) have reported that the supracrustal rocks of the Dharwar Supergroup have undergone three main episodes of deformation.

2.2.2 Metamorphism

Rocks of Western Block have undergone low grade greenschist to granulite facies of metamorphism. A change in metamorphic facies has been noticed from north to south in these schist belts (Raase et al., 1986). At the southern edge of the craton geobarometers commonly indicate pressure in the range of 0.5 to 0.6 GPa in the gneiss–granulite transition zone. On the basis of equilibrium in the system Harris and Jayaram et al. (1984) have shown a pressure range of 0.26 to 0.38 GPa and temperature of $570^0C \pm 50^0C$ in the

Sandur schist belt occurring to the north-central parts of the craton. Based largely on breakdown of phengite and phengite-biotite equilibrium Sivaprakash (1983) has calculated 0.2 to 0.4 GPa pressure and 300^0 C to 400^0 C temperature in schists occurring to the northern parts of the Dharwar craton.

2.2.3 Geochemistry

Detailed studies have been carried out pertaining to supracrustal belts while gneissic rocks that constitute more than 80% of the Dharwar craton, have received little attention. It is necessary to characterize these gneissic rocks with respect to their composition, mode of origin and evolution, in order to understand the crustal development of the craton. Jayaram et al. (1984) have carried out a systematic geochemical studies of the gneissic rocks occurring in the Western Block. They classify these gneisses into three spatial groups *viz.,* (I) Gneisses bordering the supracrustal belts, (II) Gneisses and granites far away from the supracrustal belts and, (III) Gneisses occurring as islands within the supracrustal belts.

Compositionally, the gneisses of all the three groups range from tonalite to granite and define a calc-alkaline trend. Some of the gneiss samples such as, gneisses from Chitradurga area, are quartz-monzodiorite to granite in compostion. The gneisses of group III are mainly granodiorite. Most of the gneisses in all the three groups are meta-aluminous in nature.

Though the gneisses of three groups are more or less similar in their major element concentration, they differ in their trace element contents. The tonalitic gneisses bordering Kudremukh-Bababudan belts (Group I) show low Rb (30-83 ppm), lower Ba, Zr and Y and higher Sr where as gneisses away from supracrustal belts (Group II) show a wide range for Rb, Sr and Y and are characterized by higher Ba (30-1200 ppm) and Zr (90-550 ppm). The gneisses of Group III have comparable Rb and Sr to that of Group I and Group II, but higher Y (19.7 ppm) content.

The gneisses of three groups show REE pattern characteristics of granitoids, all show LREE enriched fractionated trend with negative Eu anomaly, but some show a positive Eu anomaly. The tonalite gneisses of Group I are generally low in REE content ($\Sigma REE=47-77$ ppm) while Group II gneisses have higher REE abundance ($\Sigma REE=107-353$ ppm). The gneisses of group III show both high and low REE content ($\Sigma REE=33-44$ ppm; $\Sigma REE=109-$

139 ppm). The gneisses of group I and III have higher Eu/Eu* values (0.7-1.23) while Eu/Eu* ratios are lower and the values ranging from 0.47-0.54 in Group II gneissses (Jayaram, et al. 1984).

2.2.4 Geochronology

The age of so called Peninsular Gneisses occurring near Hasan in the Western Block (On the basis of Rb-Sr isochron) lies between 3.4 to 3.0 Ga (Beckinsale et al. 1980, 1982; Stroth et al. 1983; NGRI, 1992). They have reported Rb-Sr ages of ca. 3000-2900 Ma for the base of Dharwar Supergroup and an age of 2565 $\pm$ 28 Ma for the acid volcanics of the "Ranibennur Formation". Later on Taylor et al. (1988) have reported the Sm-Nd ages of 2.99-3.06 Ga for the Dharwar acid volcanics, whereas Bhaskar Rao et al. (1992) reported Rb-Sr ages of 2520 $\pm$ 20 Ma for the same unit. U-Pb isotopic ages of zircons from the Dharwar acid volcanics have yielded 2614 $\pm$ 18 Ma (Nutman et al., 1996) and 2606 $\pm$ 6 Ma (Trendall et al., 1997). Kumar et al. (1996) have reported Sm-Nd ages of 2911 $\pm$ 49 Ma and 2848 $\pm$ 70 Ma for Kalasapur and Santaveri Formations of Bababudan belt are, respectively. Zircons from rhyolitic flow of the Holenarsipur belt have yielded ages of 3298 $\pm$ 7 Ma (Peucat et al., 1995). The gneisses of Gorur and Hunasekatte have been dated at 3204 $\pm$ 30 Ma and 3121 $\pm$ 63 Ma, respectively (Naha et al., 1993), whereas the post tectonic granite intrusions have yielded a younger age of ca. 2.5 Ga (Meen et al., 1992; Naha et al,. 1993). The Pb-Pb ages of tonalitic and trondjemitic gneisses range from 3.1 Ga to 3.0 Ga (Meen et al., 1992). The U-Pb ages of zircons from the metasediments of the older schist belts range from 3.4 Ga to 2.9 Ga (Nutman et al., 1992).

2.2.5 Mineralization

Most of the ore deposits in the Western Block are sulfides (Vasudev̂ and Naganna, 1973) and the principal metal is copper (Raddhakrishnan, 1967). The deposits are of two types viz., Stratiform and hydrothermal (vein-type). The former types occur in the schist belts and the latter types occur both in the schist belts and in the gneisses and granites. The principal ore deposit is in Ingaldhal area (Mookherjee and Philip, 1979). Isotopic studies of Ingaldhal rocks have been carried out by Menon et al. (1981). Their studies show that the value of $\delta^{34}S/^{32}S$ for most of the samples is approximately zero, indicating that the

8

mineralizing fluids are of mantle derived. But $\delta^{34}S/^{32}S$ value for some of the samples is as high as ± 10, indicating a different source or a large variation in temperature and composition of the precipitating fluid.

2.3 EASTERN BLOCK

As compared to the Western Block, the Eastern Block has been paid less attention by the geologists. Like Western Block, the Eestern Block also contains TTG suite but it is volumetrically minor compared to the vast terrane of younger granitoids (Radhakrishna, 1993). The number of schist belts is also less as compared to that of Western Block but the schist belts of Eastern Block are economically more important. The supracrustal belts are essentially composed of pillowed basalts, rhyolites, polymictic conglomerates, grits, phyllites and BIF at various stratigraphic level. The famous auriferous schist belts *viz.*, Kolar, Ramagiri and Hutti are included in these supracrustal belts.

It is considered that the Eastern Block had experienced large scale crustal remobilization as compared to that of Western Block and this obscured the basement-cover relationship in the Eastern Block (Viswanathan and Ramakrishnan, 1981). The crustal remobilization might have resulted from anomalous heat flow from the mantle, probably in the form of plumes and this gave rise to andalusite-sillimanite type metamorphism unlike kyanite-sillimanite type in the Western Block (Rollinson et al., 1981).

2.3.1 Structure

The major structural trends are very much similar to that of Western Block. Roy (1979) has carried out a detail structural analysis of Hutti schist belt and described two major episodes of tight folding. Out of these the second one is oriented in northwest-southeast direction with steep plunges. The Kolar schist belt is a multiple refolded synform plunging towards north and shows structures such as minor isoclinal fold (F_1) and refolded F_2 structures in the BIF. A banded ferruginous quartzite near the western margin of the Kolar schist belt shows a wide variety of small-scale structures. These structures vary in shape, style as well as orientation. Mukhopadhay (1988, 1989) and Mukhopadhay and Haimanot (1989) carried out the analysis of these small-scale structures and concluded that the schist belt has undergone four phases of folding (F_1-F_4). The F_1 and F_2 folds are nearly co-axial with north-northeast strike and are tight to isoclinal folds. Whereas, F_3 folds

are open and recumbent with axes trending N-S; F_4 folds are cross folds with subvertical axial planes. The superposition of F_3 and F_4 folds gave rise to irregular domes and basins on subvertical foliation planes (Ghosh and Sengupta, 1985).

The belt and the surrounding gneisses are characterized by ductile shear zones. These shear zones are dextral as well as sinistral in nature. Displacements caused by these shear zones can be seen along the contacts of different rock types, aplitic and pegmatitic veins as well as in pre-shear foliations. These shear zones are oriented in the same direction (N-S) in gneisess of both the sides of the belt and Mukhopadhay (1990) concluded that they must have developed during the same deformational episode. Shear zones of considerable dimensions have also been reported from the amphibolites of the schist belt (Hamilton and Hodgson, 1986; Mukherjee et al., 1986). On the basis of the structural studies on the gold ore lodes of Kolar schist belt Hamilton and Hodgson (1986) suggested that the belt was subjected to two episodes of ductile deformation along east west direction.

Foliations are well developed in the coarse grained gneisses with strike dominantly in the N-S direction as that of the foliations in the schist belt rocks. The overall pre-shear structural pattern is similar to that of the schist belt. It implies that the early structural history of these two rock groups is somewhat similar (Mukhopadhay, 1990).

The Ramagiri schist belt has been divided into three blocks viz., eastern, central and Western Blocks. In the Eastern Blocks both the gniesses as well as the schist belt rocks show subvertical foliations in $N20^0E$ direction whereas the foliations trend in the central block are in between $N10^0E$ to $N10^0W$ with steep dip (Zachariah et al., 1996). The contact zone between the rocks of the schist belt and gneisses shows sheared deformation. But the granitic rocks occurring to west of the belt are generally massive and show occasional shear zones.

2.3.2 Metamorphism

The rocks of the Eastern Block have also undergone greenschist to granulite grade of metamorphism. Most of the studies show the metamorphic condition in the gneiss-granulite transition zone in the range of to 0.8 GPa and 700^0C to 800^0C (Naqvi and Rogers, 1987). Deformation and metamorphism of the Hutti, Maski and Pamidi schist belts are so intense that a stratigraphy cannot be well established. The rocks of these belts are

metamorphosed to greenschist to amphibolite facies (Ballal, 1975; Roy,1979; Anantha Iyer et al., 1980). The supracrustal enclaves around Kolar belt show mineral assemblages like codierite-sillimanite-biotite, cordierite-anthophylite (Viswanatha and Ramakrishna, 1981), and Narayan Kutty and Anantha Iyer (1977a, 1977b) estimated metamorphic conditions of about 600^0 C and 0.3 to 0.5 GPa.

The southern part of the Closepet granite schistose enclaves are characterized by cordierite bearing assemblages (Radhakrishna, 1954; Jayaram et al., 1976; Naqvi and Rogers, 1987). Rollinson et al. (1981) estimated metamorphic pressures of about 0.6 GPa and temperature of about 800^0 C for the western enclaves of the Kunigal and related belts. However, peak metamorphic conditions of 690^0 C to 730^0 C and 0.45 to 0.5 GPa pressure has been estimated for these enclaves (Harris and Jayaram, 1982).

2.3.3 Geochronology

The U-Pb ages of the gneisses occurring to west and east of the Kolar schist belt ranges from 2631 ± 6.5 Ma to 2551 ± 2.5 Ma and 2532 ± 3 Ma to 2520 ± 2 Ma, respectively (Krogstad et al., 1991). Balakrishnan et al (1990) have reported an age of ca. 2700 Ma for the mafic-ultramafic rocks of the schist belt. The Pb-Pb isotopic age on the metavolcanics of the central block of Ramagiri schist belt is 2746 ± 66 Ma (Zachariah et al., 1995). Krogstad et al. (1992) have reported U-Pb ages of sphenes from the gneisses occurring to east and west of the Ramagiri schist belt are 2552 ± 2 Ma and 2523 ± 2 Ma, respectively. Balakrishnan et al. (1999) have reported U-Pb ages for the gneisses occurring to east, central and west of the Ramagiri schist belt are 2650 ± 7 Ma, 2613 ± 7 Ma and 2528 ± 1 Ma, respectively. U-Pb ages on zircon from Vibhuti Formation (acid volcanic) of Sandur Group which constitutes the Sandur schist belt has been dated at 2658 ± 14 Ma (Nutman et al., 1996). Bhaskar Rao et al. (1992) have reported an Rb-Sr isochron age of 2452 ± 50 Ma for a granite pluton occurring in the northeast of the Sandur schist belt.

2.3.4 Mineralization

A variety of commercially important deposits including gold, diamond, barite and asbestos occur in the Eastern Block (Kurein, 1980). Gold occurs in Hutti, Kolar and Ramagiri schist belts. The gold-quartz vein of Hutti deposit contains pyrite, arsenopyrite and

sphalerite in shear zones in metamorphosed rocks (Naqvi and Rogers, 1987). Sulfur isotopic studies of Menon et al. (1981) indicate that the ore bearing fluids were derived from primitive mantle. Fluid inclusion studies of Kolar samples reveal the mineralizing condition of the fluid: the temperature was in the range of 250^0C to 300^0C and pressure varied from 0.18 GPa to 0.35 GPa (Safonov et al., 1984). The sulfur isotopic studies of Safonov et al. (1984) show the derivation of mineralizing fluids from the mantle. Two types of gold mineralization *viz.*, gold quartz sulfide lodes and gold quartz calcite lodes have been identified in the Kolar schist belt. Out of these the latter is more important and formed dominantly from magmatic fluids derived from granitic intrusions whereas, the sulfide lodes have been deposited by complex sedimentary processes (Siva Siddaiah and Rajamani, 1989).

Many sulfide minerals like pyrite, arsenopyrite, chalcopyrite, pyrrhotite and tetrahedrite-tennaite are associated with gold mineralized veins of Ramagiri schist belt. The gold deposits are considered to be magmatic hydrothermal origin (Reddy et al., 1992).

2.3.5 Kolar and Ramgiri schist belts and surrounding Granitoids

Kolar schist belt

The Kolar schist belt is a N-S trending volcanic dominated Archean supracrustal belt comprises mafic and ultramafic rocks of tholeiitic affinity with minor pyroclastic rocks (Anantha Iyer and Vasudev, 1979; Rajamani et al., 1985). The belt is considered to be a suture zone along which two gneissic terranes and two amphibolite terranes with distinct histories have been juxtaposed (Krogstad et al., 1989). The rocks of the schist belt have undergone greenschist to amphibolite facies of metamorphism. There are four textural varieties of amphiboles *viz.*, schistose, granular, massive and fibrous have been found (Rajamani et al., 1985). Amphibolites of western and eastern side of the belt have distinct geochemical characteristics. Rajamani et al. (1985) suggested that the western side amphibolites were derived from LREE depleted source whereas the eastern side amphibolites were derived from LREE enriched sources. The high Mg-amphibolites were dated at ca. 2700 Ma on Sm-Nd isochron (Balakrishnan et al., 1990), whereas the ages of gneisses occurring east and west of the belt are ca. 2530 Ma and 2630 Ma, respectively

(Krogstad et al., 1991). Balakrishnan et al. (1990) have suggested an ocean floor and island arc setting for the evolution of western and eastern parts this belt, respectively.

The Kolar schist belt is surrounded by granitoid rocks ranging from tonalitic to granodioritic in composition (Working Group of GSI, AMD and NGRI, 1977; Viswanatha and Ramakrishna, 1981; Balakrishnan, 1982).

Four distinct varieties of gneisses *viz.,* Dod, Dosa, Banded gneiss and Patna granite occur to the western side of the belt, whereas the gneisses occur the eastern side are named as Kambha and Champion gneisess (Balakrishnan, 1982; Balakrishnan and Rajamani, 1987). The contact zones between the schist belt rocks and the gneisses on both the sides are mylonitized. Banded gneisses, the name itself implies that the gneisses are having bands of leucocratic and melanocratic minerals. Dod gneisses are tonalitic to quartz monzodioritic in composition, whereas Dosa gneiss is granodioritic. The gneisses of the eastern side of the belt are dominantly granodioritic in composition. Balakrishnan and Rajamani (1987) have suggested that liquid immiscibility is the process by which these rocks (except Banded gneisses) could have originated from parental magmas whereas, Banded gneisses might have been derived by low degrees of partial melting of granitiod rocks and therefore had a crustal origin. Their studies showed that these rocks could not be derived by partial melting of the amphibolites of the belt.

The U-Pb ages on zircons from gneisses suggest that the gneisses occurring to east of the belt are 83 Ma years younger than the gneisses occurrung to west of it (Krogstad et al., 1989; Hanson et al., 1986; Krogstad et al., 1991). Balakrishnan et al. (1990) report an age of ca. 2700 Ma for the amphibolites of Kolar schist belt and show that the schist belt rocks are older than the gneisses on either side of the belt. Therefore the gneisses cannot form the basement of these supracrustals. The geochemical studies of amphiboles (Balakrishnan et al., 1985; Rajamani et al., 1985) and gniesses (Balakrishnan and Rajamani, 1987) suggest that they have come from different mantle sources and at different times (as evidenced by the isotopic studies of Krogstad et al., 1986, 1991; Hanson et al., 1986; Balakrishnan et al., 1990).

Ramagiri schist belt

Ramagiri schist belt is a Y-shaped volcanic dominated Archean supracrustal belt located at Anantapur district of Andhra Pradesh. The volcanic rocks range from mafic to

13

felsic in composition. Each of the arms of this belt has its distinct geological and geochemical characteristics (Zachariah et al., 1996). The eastern arm consists predominantly of well foliated amphibolites with subordinate amount of banded ferruginous quartzite (BFQ). The central arm has mafic and felsic volcanics of greenschist facies and western arm is made up of fine grained massive and pillowed metabasalts. On the basis of geochemical signatures of these rocks Zachariah et al. (1996) and Zachariah (1992) have suggested an island arc setting for the origin of these rocks. U-Pb isotope studies on zircon separated from a pyroclastic unit of this belt gave an age of 2707 ± 8 Ma (Balakrishnan et al., 1999).

The Ramagiri schist belt has three arms separated by granitoid rocks. The Granitoids surrounding each arm is having its own geochemical and geochronological characters (Zachariah et al., 1996; Mohanta, 1998; Krogstad et al., 1992). They are named as Gangam complex (gneisses to the west of the belt), Ramagiri complex (central gneisses) and Chenna gneisses (occurring to the east of the belt). The Chenna gneisses belong to typical TTG (tonalite-trondjemite-granodiorite) suite. They are peraluminous to meta-aluminous in nature and show LREE enriched and HREE fractionated rare earth pattern with negative or no Eu anomaly (Mohanta, 1998). The Chenna gneisses occurring east of Cherlopalle is light to dark grey, banded and folded, whereas, those occurring to west of Cherlopalle are having migmatitic apperance (Balakrishnan et al., 1999).

The Gangam gneissic complex consists of quartz monzodiorite, granodiorite and granite rocks. The rocks are weakly foliated and are meta-aluminous in nature with high abundance of Ba, Sr and REE. These rocks show LREE enriched and variably fractionated REE pattern. They might have generated by partial melting of crustal materials such as basalts or granodiorites (Mohanta, 1998).

The Ramagiri complex is having three components *viz.,* quartz diorite, granodiorite and granite. Granitoids of Ramagiri complex are inferred as intrusives but their contact with the central and western arms of the schist belt is sheared (Balakrishnan et al., 1999). The gneissic rocks of this complex have been grouped into a broad field of tonalite-granodiorite-granite. The granodiorites are meta-aluminous in nature with relatively high alkali content. Ba content is highly variable (130 ppm to 1300 ppm) and Sr content is very low within the range of 100 to 200 ppm. They show LREE enriched and HREE fractionated REE pattern with almost no negative Eu anomaly (Mohanta, 1998).

14

The granites of Ramagiri complex are leucocratic and rich in silica (of the order of 78 wt.%) with high alkali content. They are grouped into meta-aluminous to sub-aluminous variety. REE abundance are very low and these rocks show LREE enriched but concave up HREE chondrite normalized REE pattern (Mohanta, 1998).

The U-Pb ages on zircon and titanite show that Chenna gneisses (2650±7 Ma) are ca. 100 Ma older than the Gangam complex (2528 ± 1 Ma), whereas, Central Ramagiri complex has yielded a U-Pb zircon age of 2613 ± 6 Ma (Balakrishnan et al., 1999). These authors also report a U-Pb isochron age of 2707 ± 18 Ma from a pyroclastic unit of the belt. The ages of rocks of the schist belt and the surrounding granitoids implies that the granitoids are younger than the rocks of the schist belt and cannot form the basement for the schist belt rocks.

The geological, geochemical and geochronolgical information suggest that there are three disparate granitoid terranes surrounding the Ramagiri schist belt and each of these might have evolved distinctly and later accreted at the end of Archean to the older cratonic nucleus (Balakrishnan et al., 1999).

2.3.6 Hutti schist belt

Most of the work undertaken at the Hutti Gold Mines before 1970 is in the form of unpublished reports by the mining and exploration agencies. The first available published information on Hutti schist belt is by Vasudev and Naganna (1973) who recognize three distinct stages of mineralization in the quartz-sulfide reefs. The schist belt consists predominantly of volcanic suite of rocks with subordinate metabasalts. Pillowed basalts, acid to intermediate volcanics and quartz/rhyolite porphyry occur in decreasing order of abundance (Biswas et al., 1985). The schist belt is surrounded by granitoids, which show intrusive relationship at many places. The rocks of the schist belt have undergone up to amphibolite facies of metamorphism.

Ziauddin and Narayanaswamy (1974) and Mohanty and Raju (1974) show that en-'echelon shear fractures host the gold-quartz mineralization. Roy (1979) and Curtis et al. (1990) demonstrate that the gold mineralization is controlled by first phase of folding (F_1), and the associated green schist facies of metamorphism on the regional scale.

A conglomerate horizon with pebbles and cobbles embedded in a fine grained, well foliated matrix occurs as a conformable bed within the volcano-sedimentary sequence of the

Hutti schist belt at Palkhanmaradi village. The pebbles and cobbles are granitic in composition. At some places they are rounded but at many places they are stretched and elongated parallel to the foliation (N-S) of the matrix. The matrix is an admixture of basalt and arkosic material. The presence of such conglomeratic horizon imply a possible existence of a sialic crust older than the schist belt (Roy and Biswas, 1982).

The metabasalts from the Hutti schist belt are enriched in large ion lithophile elements with higher Rb/Sr and Ba/Sr and lower K/Ba and K/Rb ratios (Anantha Iyer and Vasudev, 1979), which are characteristics of Marginal basin basalt (MBB). These metabasalts exhibit slightly LREE enriched chondrite normalized patterns, and show higher Ce_N/Yb_N (1.63-1.81) and La_N/Sm_N ratios than the average Ocean ridge basalt (Ce_N/Yb_N = 0.87; and La_N/Sm_N = 0.55). These ratios are comparable to basalts (Ce_N/Yb_N = 1.35; and La_N/Sm_N = 1.15) erupted in Marginal basin tectonic environment (Anantha Iyer et al., 1980). On the basis of major and trace element including REE geochemistry Anantha Iyer et al. (1980) suggest a back arc spreading centre (marginal basin) for the evolution of Hutti metabasalts. But, on the basis of trace element modeling Giritharan and Rajamani (1998) suggest that these metabasalts are derived by different extent of partial melting of mantle sources at ~2.5 Gpa pressure and are emplaced in an island arc environment.

As compared to Kolar and Ramgiri schist belts less attention has been paid to Hutti schist belt. So far no major geochemical study has been carried out on granitoids surrounding the Hutti schist belt. A major objective of this study is to compare the chemical characteristics of the granitoids surrounding the Hutti, Ramagiri and Kolar schist belts to understand their petrogenesis and put constraints on the existing evolutionary models of the Eastern Block, particularly in the Hutti area.

FIELD STUDY AND PETROGRAPHY

3.1 LOCATION AND ACCESSIBILITY

The Hutti supracrustal belt, an important auriferous belt of India, is named after village Hutti (Lat. 16^0 12′ N and Long. 76^0 43′ E) in Lingsugur Taluk of Raichur District in Karnataka State. Hutti is about 400 km north of the state capital of Karnataka, Bangalore, and about 80 km west of Raichur. It is connected to Raichur and Bangalore by metalled roads. The nearest railway head is Raichur (Southern Division of the Indian Railways). Hutti is almost at midway between Western and Eastern Ghats. The area is generally flat, largely covered by black cotton soil, but with numerous outcrops of granite are conspicuous. The average elevation above mean sea level is about 523 meters. Average rainfall is about 500 mm received mostly during SW monsoon period (June-September) and maximum and minimum temperatures are about 40^0 C and 10^0 C, respectively.

The area under investigation falls between Lat. 15^0 55′ N to 16^0 20′ N and Long. 76^0 30′ E to 77^0 0′ E on Survey of India toposheets Nos. 57 A/9, 56 D/11, 56 D/12, 56 D/15 and 56 D/16.

3.1.1 Introduction

The main objectives of this field study are to: (1) classify the granitic rocks occurring in and around Hutti schist belt, (2) decipher the contact relationship between the Hutti schist belt and the surrounding granitoid rocks, and (3) collect representative samples for petrographic and geochemical analysis. The study is aimed to place constraints on various models available for petrogenesis and to understand the crustal evolution of the eastern Dharwar craton during Archean.

3.1.2 Field Study

The fieldwork was carried out along seven major traverses with Hutti as the base camp . These traverses are:

1) Hutti-Chinchargi-Uti-Galaga traverse
2) Hutti-Gurgunta-Golapalli-Yellagatti traverse
3) Hutti-Pamankallur-Kavital-Potepur traverse
4) Hutti-Anwari-Hussainpur traverse
5) Hutti-Bullapur-Kasamdudi traverse
6) Hutti-Lingsugur-Ankasdoddi-Maski traverse
7) Hutti-Pamankallur-Bhagalvad traverse

Apart from these several other smaller traverses were also made in the area.

Representative samples were collected for petrographic and geochemical studies (Fig. 3.1). The rocks of the Hutti schist belt show different grades of metamorphism in different parts. The metamorphism is more intense in the eastern part than that of western and southern parts. Whereas amphibolite is the predominant rock type in the eastern part, chlorite-schist is the major rock type in the western part of the Hutti schist belt. The amphibolites are mainly two types. One of these is fine grained, and folded amphibolite, whereas, the other one is coarse grained and massive amphibolite. In most places the contact between the schist belt rocks and the surrounding granitoids is concealed under the soil cover.

The granitic rocks surrounding the Hutti schist belt are massive to weakly foliated with or without mafic xenoliths. The size of these xenoliths varies from a few cm to half a meter in diameter. These granitic rocks are dark grey, medium to coarse grained, and consist of plagioclase, quartz, K-feldspars, hornblede and biotite.

A outcrop of schist belt rock and granitic rock exposes on the Hutti River bed, at the location of sample GR-2 (½ km north of Madrainkota village). The nature of the contact is ambiguous and it cannot be inferred as intrusive or tectonic. Both schist belt and granitic rocks on either side of the contact are mylonitized. The foliation in the schist belt as well as in the granitic rocks strikes nearly E-W with a dip of 78^0 towards north. The granitic rocks are leucocratic, medium grained, and consists of plagioclase, K-feldspars, quartz, biotite and hornblende. These rocks are, in general, free from xenoliths.
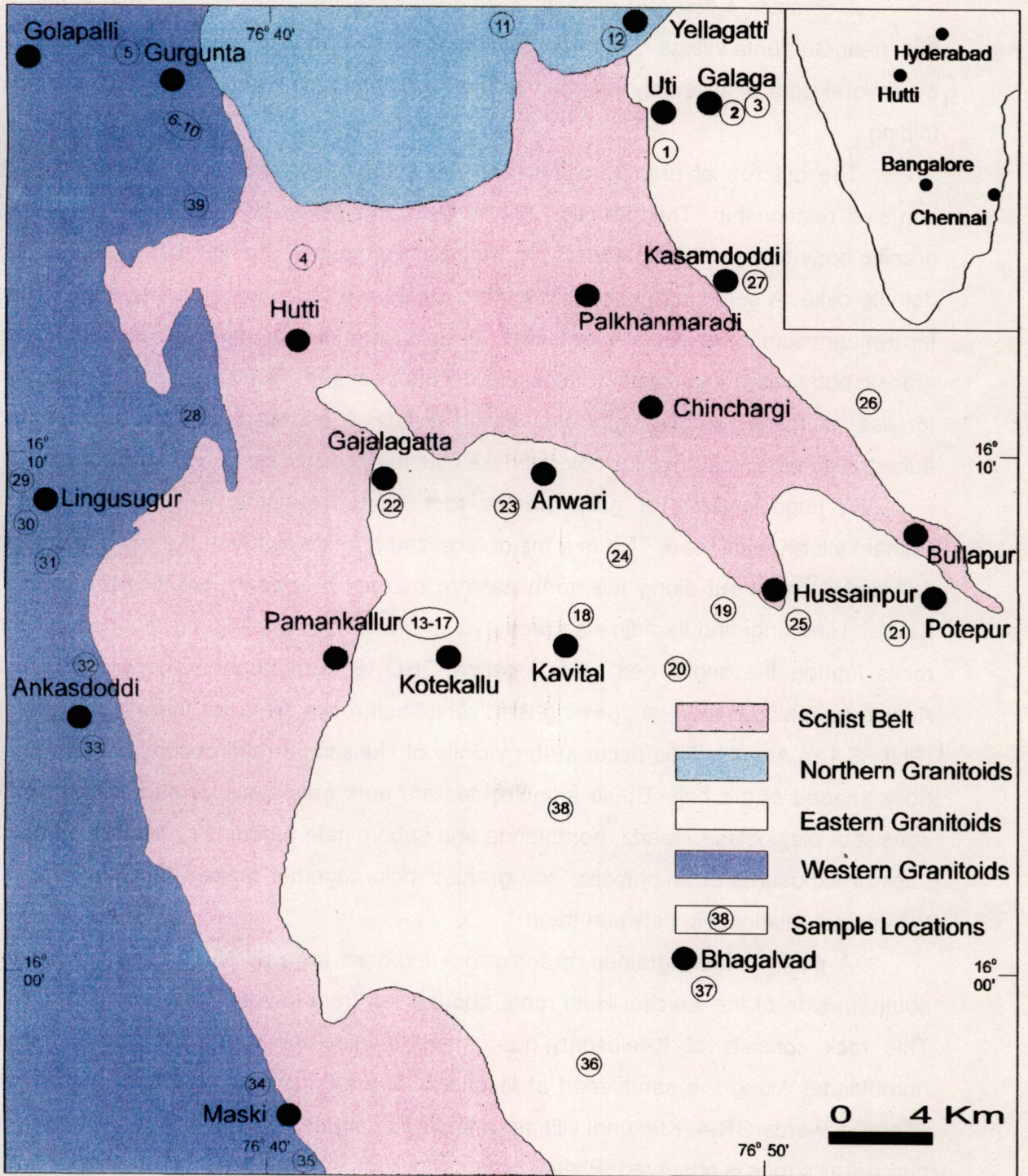
Fig. 3.1 Simplified geological map of the study area (modified after Srikantia, 1995).

A complex outcrop of granitic rocks occurs towards northwestern part of the schist belt, near Gurgunta village. The main granitic body is a grey coloured foliated gneiss and cut by several sets of diversely oriented aplitic and pegmatitic veins, which show ptygmatic folding.

The outcrop of granitic pluton and the schist belt rock near Pamankallur, shows intrusive relationship. The granitic rock intrudes the schist belt rocks. A large massive granitic body occurs at 2 km away from Pamankallur towards Kavital road and is cut by the dolerite dyke. A series of five samples with progressive decrease in quartz and increase in ferro-magnesian minerals are collected. A dark grey colour, medium to coarse-grained granitic body with megacrysts of feldspars occurs near Hire Guda village. This granitic rock (gneiss) is made up of plagioclase, bluish quartz, K-feldspars, biotite, hornblende and euhedral sphene. A 20 m thick dolerite dyke cuts the gneissic body.

A huge outcrop of grey granitic rock occurs towards west and north of the Pamankallur-Kavital road. This is a major localized granitic pluton in the eastern side of the belt and it crops out along the north eastern margin. It appears prominently as hill near Kavital, Hirehangi and its adjoining areas *viz.*, Potapur and Mudulgund. Tounges of granitic rocks intrude the schist belt, near location GRD-18 (Timmarpur Kadona village), along Anwari-Hussainpur road, suggesting that, schist belt rocks are older than the granitic rocks (Plate 3.1a). Amphibolites occur in the vicinity of Hussainpur and occupy the SE tip of the hook shaped of the belt. These amphibolites are dark grey-black, fine to medium grained, consist of plagioclase, quartz, hornblende and subordinate amounts of biotite and opaques. Lack of exposures of amphibolite and granitic rocks together makes it difficult to establish the contact relationship between them.

A pink, medium grained, granitic rock exposes towards NW of Bullapur, along the southern side of the Raichur-Hutti road, about a km from location GR-4 (Kurkundi village). This rock consists of K-feldspar, quartz and plagioclase with subordinate amount of hornblende. Along the same road at location GR-5 (about 500m away from Kasamdoddi village) towards GR-4 (Kurkundi village) a sheared contact between the schist belt rock and pink granitic rock is observed (Plate 3.1b).

Two different varieties outcrop of granitic rocks occur towards west of the Lingsugur town. One variety is light pink coloured, medium to coarse grained, and consists of plagioclase, K-feldspars, quartz with very less amount of hornblende and biotite. The rock is

not foliated and free from xenoliths (Plate 3.1c). The other variety is more dark coloured, weakly foliated, and contains abundant xenoliths of metabasaltic rocks (Plate 3.1d). It consists of plagioclase, K-feldspars, quartz, hornblende, biotite and subordinate amounts of sphene and opaques. At some places the light coloured variety contains the xenoliths of dark colour one, whereas, at other places the dark colour rock acts as a host for the xenoliths of the light colour variety. The contact relationship between them is ambiguous. Away from the belt, the light grey granitic rock becomes more prominent.

There are two types of granitic rocks in Maski area,. One (GRD-25) is dark coloured, and contains megacryst of plagioclase and K-feldspars in a fine-grained matrix. The other one (GRD-24) is lighter in colour, coarse grained, and consists of plagioclase, K-feldspars, quartz, hornblende, biotite and sphene. It contains more K-feldspar than the former. Away from the Maski village, the coarser variety is more common. Meso-scale sinistral shear zones cut these granitic rocks. Displacement of an aplitic vein along a fault plane is also observed (Plate 3.2a). At some places these rocks show S-C fabric as a result of minor shear zones (Plate 3.2b), as seen on the hill top of Maski Bull Temple. These features indicate that the Maski granitoids must have undergone considerable deformation.

3.2 PETROGRAPHY

Detailed petrographic work is a necessary step in classification, an aid to on-going field investigation, a prerequisite for geochemical and geochronological studies. As a first step, the constituent minerals must be identified and their modal proportions estimated because it will be important in mundane nomenclature and the petrogenesis. The texture of a magmatic granitiod rock is a function of the bulk composition of the magma (from which the minerals crystallize) and the relationship between temperature, pressure and time (the cooling rate). The degree of undercooling or cooling below the liquidus determines both the nucleation and growth rate of the minerals, and in turn governs the final textures. Textural criteria such as grain sizes, grain shapes, inclusion relationships, intergrowths and corona relationships are useful in determining the sequences of crystallization of minerals in igneous rocks (Clarke, 1992). But the inferences based on these criteria are not always unique (Flood and Vernon, 1988). For example, fine and coarse grain sizes of the crystals suggest the rapid and slow rate of crystallization, respectively, but relative grain size in a

rock says nothing about the order of crystallization; moreover, the large crystals are not necessary the ones that crystallized earliest (Clarke, 1992).

To carry out petrographic study of the rocks under investigation, the granitoids have been divided into eight groups in accordance with their geographic locations.

3.2.1 Kotekallu Granitoids

These rocks are fine to medium grained, light grey, holocrystalline and equigranular. Quartz (18-25 vol.%), plagioclase (40-55 vol.%), orthoclase (5-6 vol.%), microcline (10-12 vol.%) and the ferro-magnesian minerals which include biotite (5-7 vol.%) and hornblende (3-5 vol.%) constitute the essential minerals, and very fine-grained apatite, zircon and epidote are the accessory minerals. Alteration of alkali-feldspars to sericites and plagioclase to saussurites are very common. Most of the hornblendes are altered to chlorites and alteration of calcic-plagioclase to epidote is common.

3.2.2 Kavital Granodiorites

These rocks are foliated, grey in colour, medium to coarse grained with or without megacryst of K-feldspars. The modal mineralogy (in vol.%) is: quartz (20-22%), plagioclase (35-42%), orthoclase (4-6%), microcline (10- 12%), perthite (5-7%), biotite (10-12%) and hornblende (7-8%). Sphene, apatite, zircon and epidote are the common accessories and make up for the rest of the modal volume percentage. The granodiorites show typical granitoid texture (Plate 3.2c). The mineral assemblage in enclave is similar to that of the enclosing rock, the formers are much more enriched in ferro-magnesian minerals and plagioclase than their host. These enclaves may represent fragments of an earlier more mafic intrusive phase or they are the autoliths that have formed by segregation of ferro-magnesian minerals from the host granodioritic magma.

3.2.3 Kasamdoddi Granites

The rocks are pink, medium to coarse grained and porphyritic. They contain phenocrysts of K-feldspar (1-2 cm) within a coarse matrix that is made up of quartz, oligoclase, orthoclase, microperthite, and a few minute flakes of biotite. Amongst the few accessories, sphene is prominent one. The modal mineralogy (in vol.%) of the rock is as

follows: quartz (30-35%), K-feldspar (35-40%), microperthite (10-12%), plagioclase (12-15%) and biotite (1-2%). The accessories constitute the rest of the modal percentage. The rock of Kasamdoddi area have negligible ferro-magnesian minerals and are characterized by typical hypidiomorphic texture. Graphic as well as exsolution texture are also observed in these rocks (Plate 3.2d).

3.2.4 Uti Granodiorites

These rocks are medium to coarse grained, showing typical granitoid texture. They mainly consist of quartz (20-25 vol.%), plagioclase (42-45 vol.%), microcline (12-15 vol.%), orthoclase (6-8 vol.%), biotite (5-7 vol.%) and hornblende (3-4 vol.%). Flakes of biotite and fibers of hornblende are intergrown with the quartz along the fringes of quartz grain. Feldspars are mostly subhedral and show alteration to sericites and saussurites. Biotites are brown to brownish green in colour, strongly pleochroic, and they contain many inclusions of the accessory minerals such as apatite, zircon and sphene. Hornblende is dark green and highly pleochroic. It too contains inclusions of accessory minerals such as sphene (Plate 3.3a). Sphenes are in close contact with magnetite, hornblende and plagioclase. Sphene coronas over magnetite (possibly titanomagnetite?) have been observed and might have formed either as epitaxial growth from the coexisting fluid or may represent a reaction rim (Plate 3.3b).

3.2.5 Gurgunta Granitoids

Five different phases of granitoids have been identified in this group on the basis of megascopic textural characteristics and cross-cutting relationship with each other. They are named as MZD-1, GRD-3, GRD-4, GRD-5 and GR-3 according to relative younging order. Petrography of these samples are described individually:

MZD-1: It is a medium to coarse grained rock. The alteration of plagioclase and mafic minerals (such as hornblende and biotite) is very much pronounced in these rocks. Plagioclases are highly epidotized, whereas, hornblends are altered to chlorites. Invariably the cores of all plagioclases is altered to sericites or sassurites (Plate 3.3c).

GRD-3: The rock is medium to coarse grained and less altered than the MZD-1 type. Quartz grains are anhedral in shape and occupy the intergranular spaces. Mafic mineral concentration is lower than MZD-1.

GRD-4: This is a leucocratic to mesocratic, medium to coarse-grained granitoid, characterized by subhedral granular texture. Quartz grains are anhedral in shape, mostly occupying the interstices of the early formed crystals. Plagioclase is subhedral and at some places occurs as megacryst embedded in a fine grained matrix (Plate 3.3d). Many thin sections show poikilitic texture in which late forming crystals of microcline encloses quartz, K-feldspar and biotite (Plate.3.4a). The average mode (in vol.%) is approximately quartz (20-25%), plagioclase (38-45%), alkali-feldspars (18-22%), biotite (6-8%), hornblende (4-5%) and accessories constitute 2-3% of the mode.

GRD-5: This is fine to medium grained rock, shows inequigranular texture. It mainly consists of quartz (25-30 vol.%), plagioclase (40-42 vol.%), microcline (12-15 vol.%), orthoclase (5-8 vol.%), biotite (4-7 vol.%) and hornblende (3-4 vol.%). It exhibits the effect of mylonitization, manifested by the appearance of augen shaped feldspars surrounded by stretched biotite grains (Plate 3.4b).

GR-3: This is a fine grained rock, showing typical aplitic texture. The rock contains abundant big plagioclase as xenocrysts floating in a fine grained matrix of quartz and feldspars. These xenocrysts might have come from the granodioritic or monzodioritic rocks that are cut by this aplite.

3.2.6 Yellagatti Granitoids

These are pink, medium to coarse grained granitoids. They show hypidiomorphic texture with megacryst of potash-feldspar. The average modal mineralogy (in vol.%) is quartz (18-22%), plagioclase (35-40%), alkali-feldspars (15-20%), biotite (5-8%), hornblende (2-3%) and rest of the mode is constituted by the accessory minerals; namely, sphene, zircon, apatite and opaques. Plagioclase crystals are mostly subhedral and show polysynthetic twinning (Plate 4c). Quartz appears with its anhedral form and occupies the interstices of the early-formed crystals and shows wavy extinction. K-feldspars and quartz contain abundant inclusions. Larger grains of microcline form the poikiloblast at some places and include the small crystals of quartz, K-feldspars, bitotite and opaques.

3.2.7 Lingsugur Granitoids

These are light to dark grey coloured and medium to coarse grained rocks. The rocks show subhedral granular texture with plagioclase as megacryst at some places. The

24

average mode (in vol.%) of the rocks is: quartz (15-20%), plagioclase (40-45%), alkali-feldspars (16-21%), hornblende (10-12%), biotite (3-4%) and the accessories (sphene, zircon, apatite and opaques) constitute the rest of the mode. Amongst the ferro-magnesian minerals biotite is the predominant. They are flaky, subhedral, lath shaped and strongly pleochroic (pale yellow to dark green). Hornblendes are light green to dark green and show strong pleochroism in these colours, and they are mostly altered. Sphene is mostly euhedral (Plate 3.4d), occurs as composite grains that have developed due to epitaxial growth or overgrowth. The composite grains of sphene are in optical continuity.

3.2.8 Maski Granitoids

There are two types of granitoid rocks occurring in Maski area; one is fine to medium grained, dark grey in colour, and other type is light grey, medium to coarse grained. Both the rock types show hypidiomorphic texture. Finer grains of quartz and alkali-feldspars surround megacrysts of plagioclase. Inclusions of biotite, epidote in plagioclase is very common. The alteration of plagioclase and alkali-feldspars is limited to minor extents. The average mode (in vol.%) of the rocks is approximately quartz (20-22%), Plagioclase (40-45%), alkali-feldspars (15-20%), hornblende (10-12%), biotite (5-6%) and sphene, zircon, apatite, epidote and opaques constitute the rest of the mode. The rock shows myrmektie texture (Plate 3.5a). Subhedral to euhedral apatites across the mylonitized zone can be seen (Plate 3.5b). Hornblendes are mostly altered either partially or completely. Epidotization of plagioclases is also commonly observed (Plate 3.5c). The granitoids are often mylonitized with the manifestation of grain size reduction of quartz and formation of quartz ribbons (Plate 3.5d).

Plate 3.1

a   Tounge of granitic rocks intrude the schist belt (at Timmarpur Kadona village) suggesting that the schist belt is older than the granitic rocks.

b   A sheared contact between the schist belt and granite (near Kasamdoddi village).

c   A light coloured granitoid free from xenolith (west of Lingusugur).

d   A dark coloured, weakly foliated granitoid with abundant xenolith (west of Lingusugur).

Plate 3.1
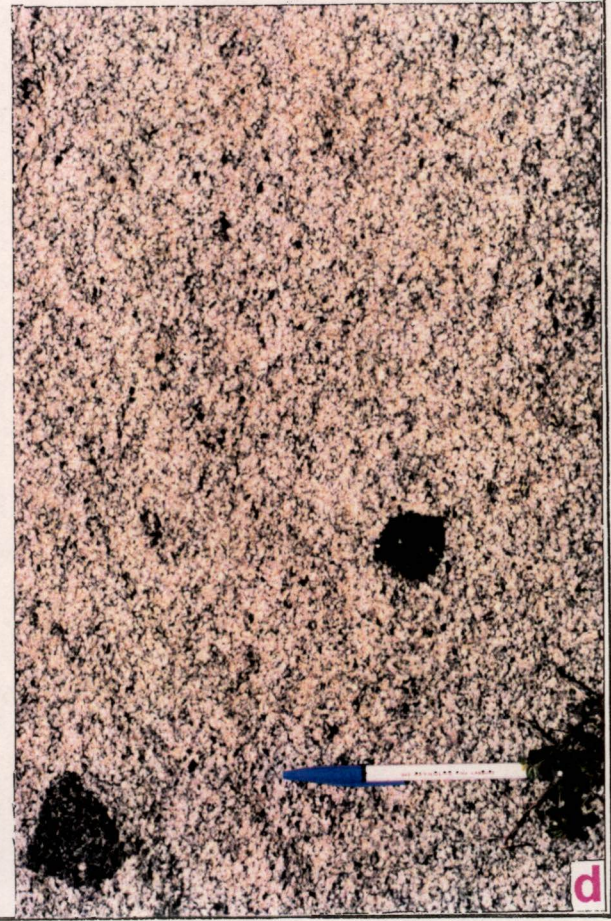
Plate 3.2

a   Displacement of an aplitic vein along a fault plane (near Maski).

b   Maski granitoid shows S-C fabric as a result of minor shear zone.

c   Kavital granodiorites show typical granitod texture (2.5X1.25X2.25). Crossed polars.

d   Graphic texture in Kasamdoddi granite (10X1.25X2.25). Crossed polars.
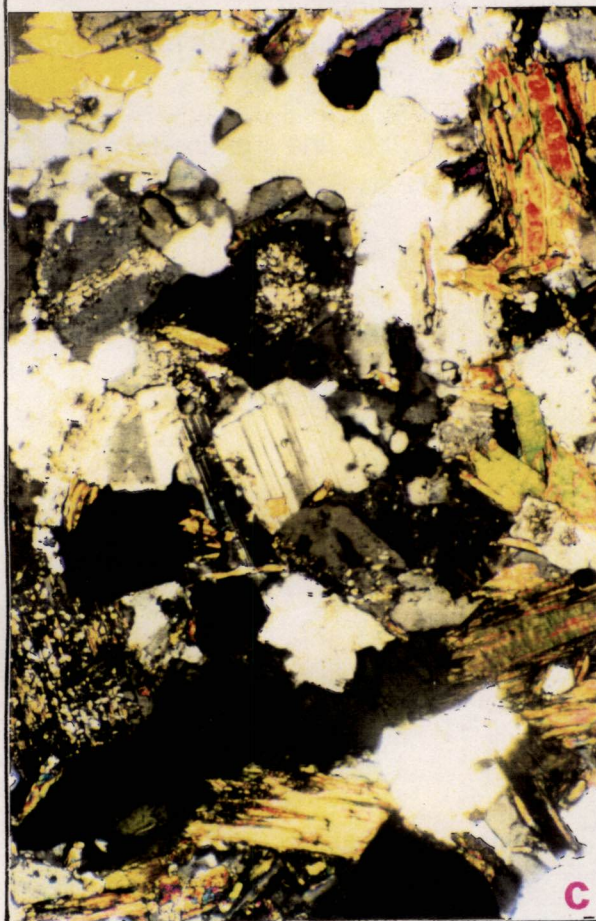
Plate 3.3

a   Hornblende contains accessory minerals such as sphene, zircon (10X1.25X2.25). Crossed polars.

b   Sphene coronas over magnetite, hornblede and plagioclase (10X1.25X2.25). Plane polars.

c   Core of plagioclase is altered to sericites and/or saussurites (10X1.25X2.25). Crossed polars.

d   Subhedral plagioclase phenocrysts embedded in fine grained matrix (10X1.25X10). Crossed polars.
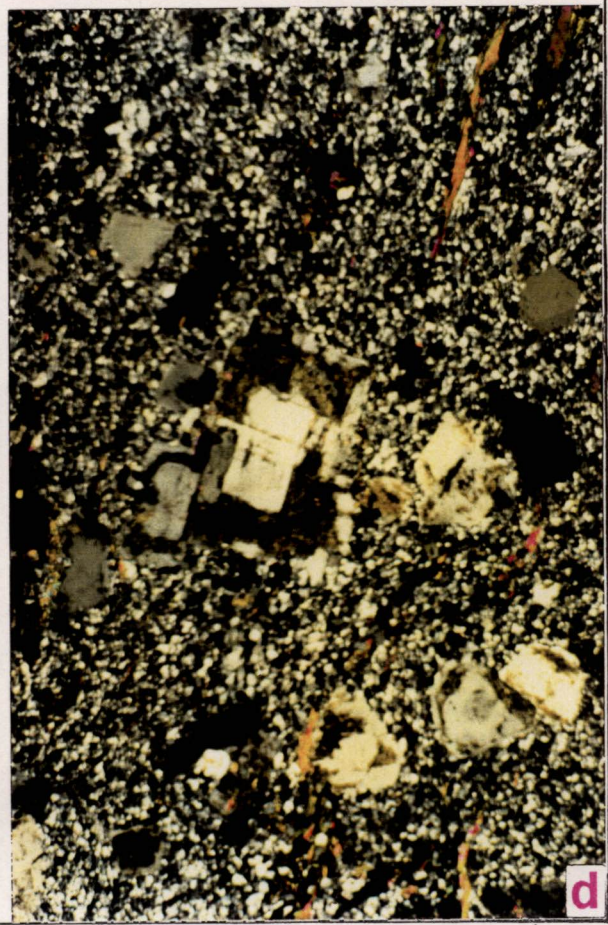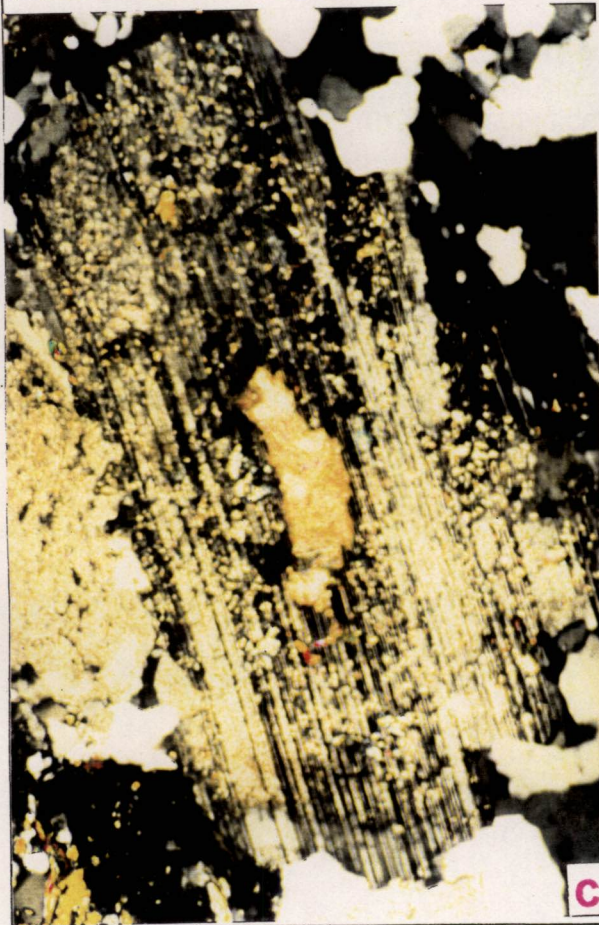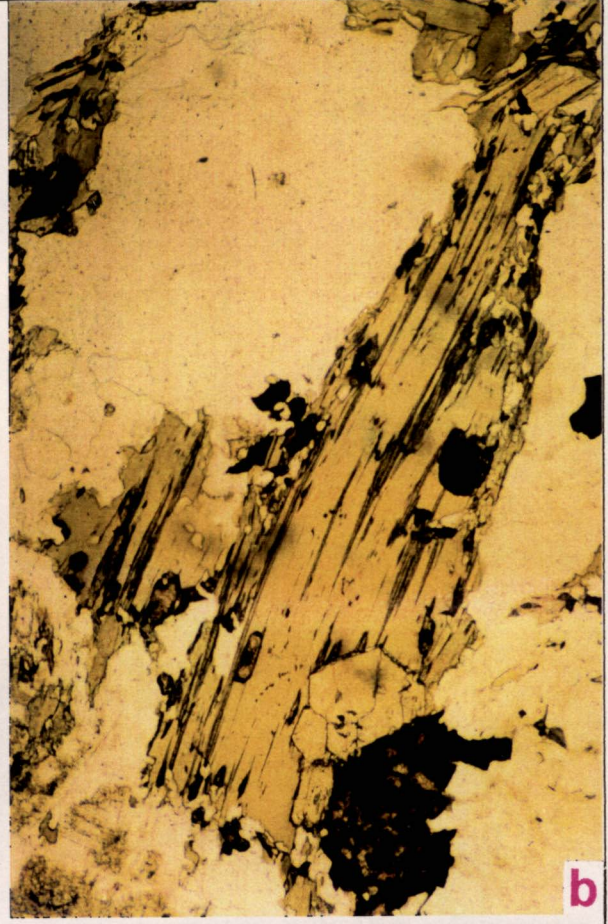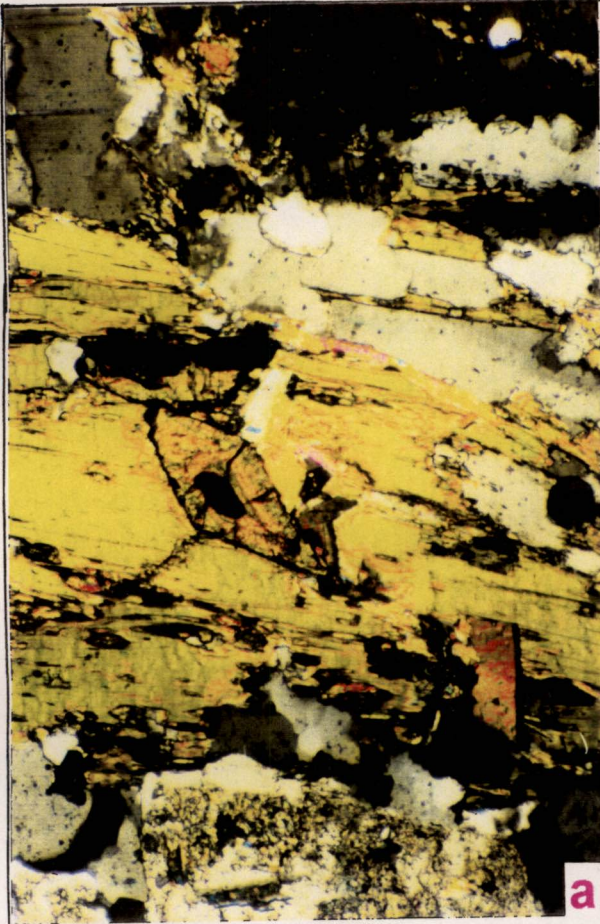
Plate 3.4

a   Poikilitic texture. Microcline encloses quartz, K-feldspar and biotite (10X1.25X10). Crossed polars.

b   Augen structure in granitoid (10X1.25X2.25). Crossed polars.

c   Plagioclase shows polysyntheitc twinning (10X1.25X2.25). Crossed polars.

d   Sphene with its typical wedge shaped habit (10X1.25X10). Crossed polars.
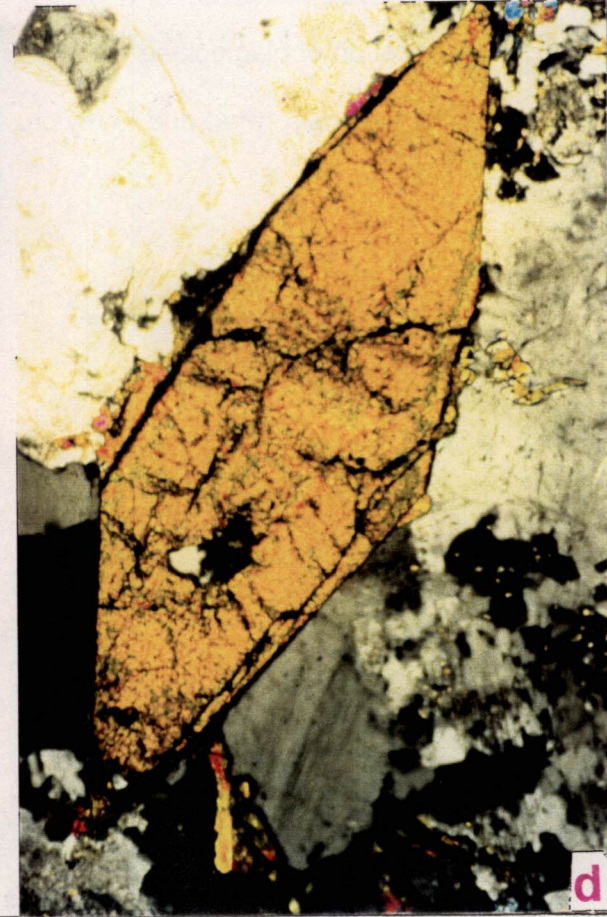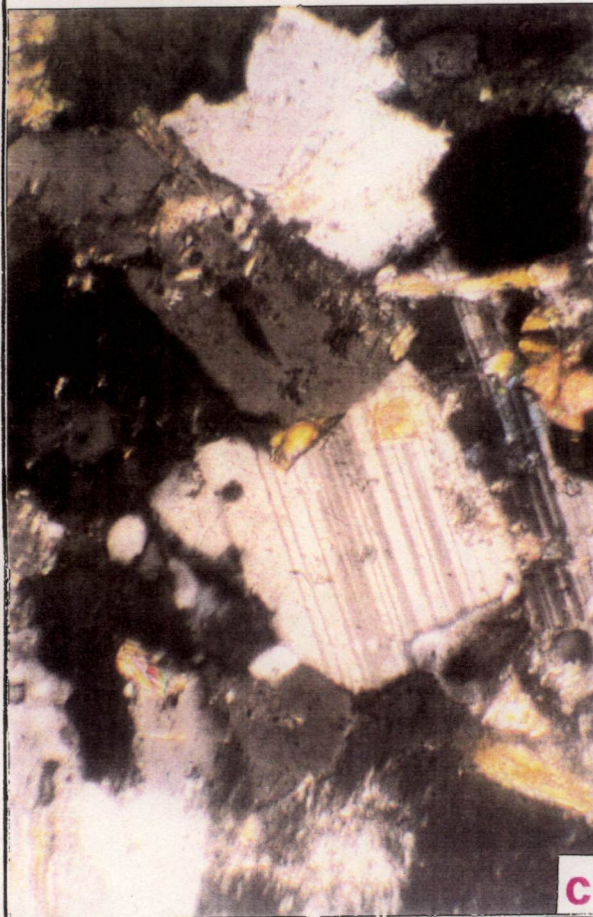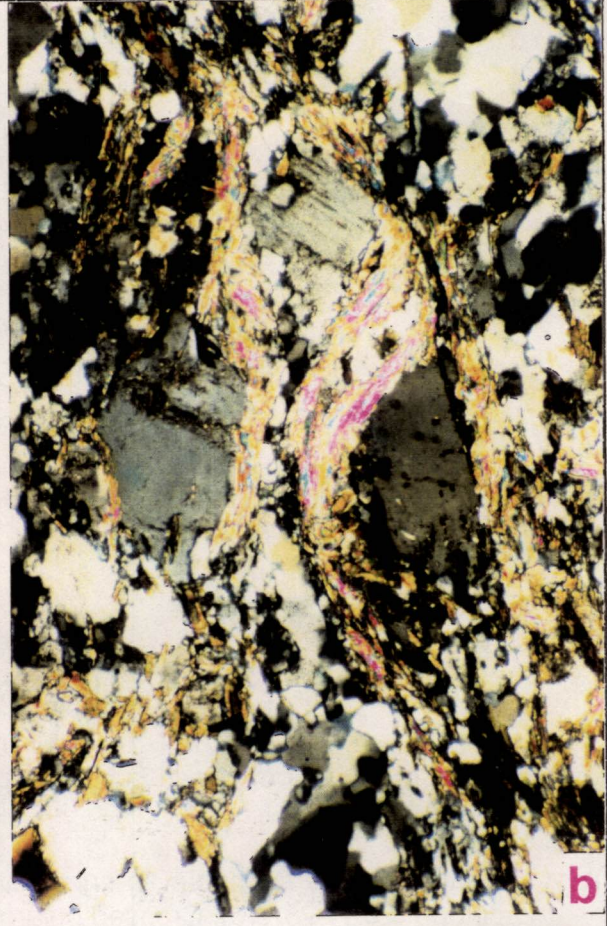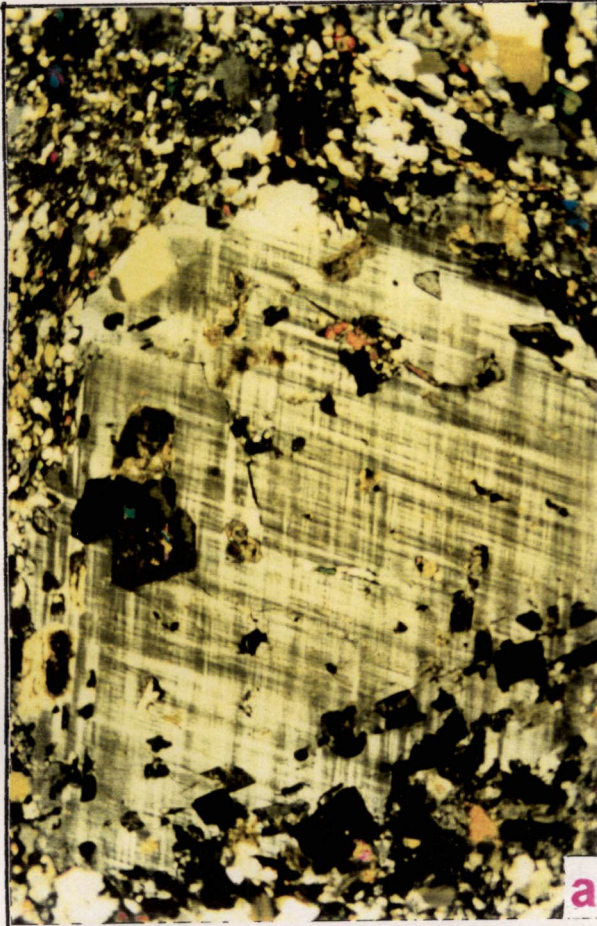
Plate 3.5

a   Widespread myrmekitisation of quartz and plagioclase intergrowth (10X1.25X10). Crossed polars.

b   Apatite with its subhedral to euhedral shape showing first order grey interfernce colour (20X1.25X10). Crossed polars.

c   Epidotization of plagioclase (2.5X1.25X10). Crossed polars.

d   Quartz ribbons formed due to mylotization (10X1.25X10). Crossed polars.

Plate 3.5
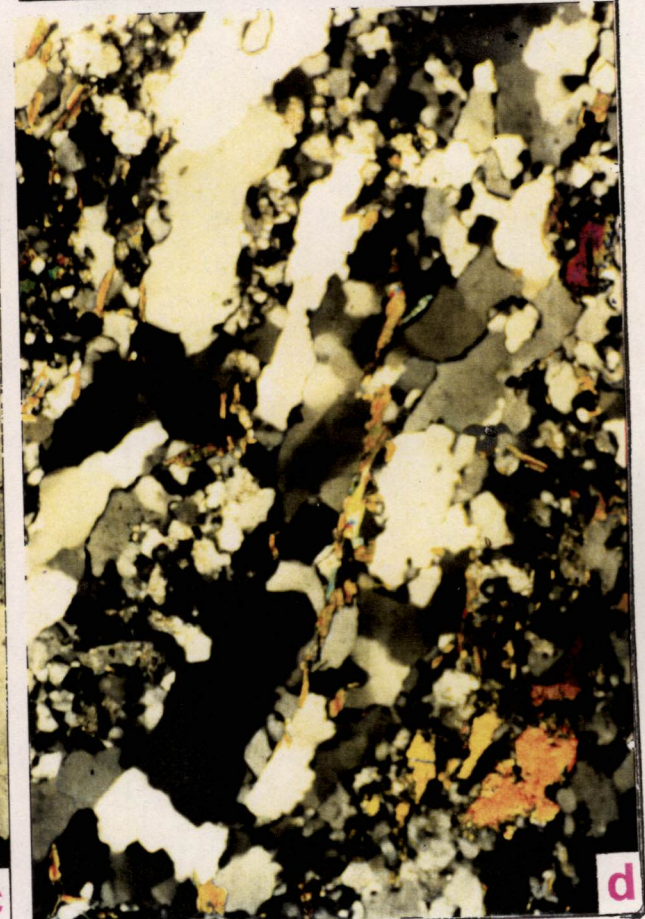
CHAPTER 4

GEOCHEMISTRY

4.1 ANALYTICAL PROCEDURES

4.1.1 Sample Processing

Approximately 5 Kg of the fresh samples have been taken for sample processing. The samples are washed with double distilled water to remove dust and other impurities, which might have been attached with the samples while collecting them in the field. After drying the samples they are broken into small chips of about 0.5 to 1.0 cm size. About 500 gm of the chipped samples are taken after coning and quartering for crushing. The steel mortar and pestle have been used for crushing the rocks up to −60 to −80 mesh and then again coning and quartering is done to select 250 gm of the crushed samples for powdering using a mechanical steel mortar, followed by an agate mortar to −200 mesh size. Geochemical analysis involves many steps from powdering to dissolution and finally analysis. For the purpose of geochemical modeling one needs to determine the concentration of elements with great accuracy and precision. To fulfill this requirement an utmost care has been taken at every step to avoid any kind of cross contamination.

4.1.2 Sample Dissolutions

There are several standard sample dissolution procedures for the geochemical analysis of the rocks in vogue. The procedure followed here is the modified version of Shapiro and Brannock (1962). Two types of solution are prepared, one is for determining the silica only and other one is for determining the major, trace and rare earth elements. The

former is called as "A" solution where as the latter as "B" solution. To dissolve the rocks completely, acid digestion followed by lithium tetraborate fusion method has been adopted.

"A" SOLUTION

To prepare "A" solution nickel crucible is used to fuse the rock powder. The crucibles are cleaned by 1:1 HCl and washed with double distilled water. Approximately 10 ml of 15% NaOH solution is taken in nickel crucible and then dried over hot plate. 0.05 gm of −200 mesh rock powder is taken in the same crucible and fused under low flame using Meker burner for about 15 to 20 minutes. The melt is swirled repeatedly to mix well with flux and to make it more homogeneous. Then the crucible is allowed to cool. After attaining the room temperature approximately 50 ml of triple distilled water is added and the crucible is covered with lid and left for overnight. After this, the contents of the crucible are transferred to a 500 ml beaker containing 300 ml of triple distilled water and 10 ml concentrated HCl (~12N). During transferring the contents from the crucible, care is taken so that the solution should fall directly to the acid water in the glass beaker without touching its wall. If the solution is cloudy, it is heated till the solution becomes clear, and then left to cool down to room temperature. The solution is then transferred to a one litre volumetric flask and triple distilled water is added to make up to volume. The solution is mixed thoroughly by shaking and allowed to stand for at least 5 hours to homogenize by itself. After this, approximately 100 ml of this solution is transferred to a plastic bottle and stored for analysis.

To determine silica by using this "A" solution, following reagents are prepared:

Ammonium Molybdate Solution: 7.5 gm of reagent grade ammonium molybdate [$(NH)_4$ $Mo_7O_{24}. 4H_2O$] is dissolved in 75 ml of triple distilled water in a 100 ml volumetric flask. 10 ml of 1:1 H_2SO_4 is added to this solution and mixed thoroughly. After this triple distilled water is added to make up to volume. The solution is then transferred to a plastic bottle.

Tartaric Acid (8.0%): Exactly 40 gm of reagent grade tartaric acid is taken in a 500 ml volumetric flask and dissolved with triple distilled water. Water is added to make up to the volume. The solution is then transferred to a plastic bottle and kept for silica analysis.

Reducing Solution: 0.5 gm of reagent grade sodium sulfite is dissolved in 10 ml of triple distilled water and subsequently 0.15 gm of 1-amino-2-napthol-4-sulfonic acid is added. The solution is stirred continuously till it is dissolved completely. After this, 9.0 gm of reagent

grade sodium bisulfate is dissolved in 90 ml of triple distilled water and this solution is mixed thoroughly with the first solution. Then this mixed solution is stored in a plastic bottle.

10 ml of each sample solution "A" is pipetted out and transferred to a 100 ml volumetric flask. 1.0 ml of ammonium molybdate solution (7.5%) is added to this and stirred for about 5 minutes. Then the solution is allowed for at least 10 minutes to homogenize by itself. Then 5.0 ml of tartaric acid solution is added and mixed thoroughly. Immediately after this 1.0 ml of reducing solution is added and swirled continuously for about 5 minutes. The volume is then made up to 100 ml by adding triple distilled water and the solution is allowed to stand for 30 minutes. After calibrating the spectrophotometer with blank and standard solutions, the absorbance of each sample is determined at 650 nm.

"B" SOLUTION

"B" solutions are prepared by acid digestion and subsequent alkali fusion method. 0.5 gm of –200 mesh size rock powder is taken in a 75 ml cleaned teflon beaker and to this 10 ml HF, 5 ml HNO_3 and 1 ml $HClO_4$ are added. It is covered and heated for about 12 hours on hot plate at a temperature of about 120^0 C for closed digestion. After 12 hours, the lid is removed and the solution is allowed to incipient dryness. In the next step, 5 ml HF and 10 ml HNO_3 are added, and evaporated to incipient dryness. In the final step, 15 ml concentrated HNO_3 is added, and evaporated off completely. When fumes stopped coming, 30 ml of 2N HCl is added to dissolve the contents in the teflon beaker, and heated gently to get a clear solution. Then the solution is transferred to a glass beaker.

The granitic rocks invariably contain abundant refractory minerals like rutile, sphene, apatite, zircon, monazite that may not undergo complete dissolution under acid attack. To avoid incomplete dissolution the solution prepared by acid attack is filtered using Whatman # 42 ashless filter paper. The filtrate is then transferred to a 100 ml volumetric flask. The filter paper is dried in oven at 80^0 C for about 2 hours. After this the dried filter paper with refractory minerals (if any) is taken in a platinum crucible and is then heated in a muffle furnace at 600^0 C to 800^0 C for about 10 minutes to burn the ashless filter paper. After burning there is white residue with refractory minerals left and to this 0.1 gm lithium tetraborate powder is added and mixed thoroughly. Then the platinum crucible is covered with lid, and is again put in the muffle furnace for fusion at 1050^0 C for 30 minutes. After this

with lid, and is again put in the muffle furnace for fusion at 1050^0 C for 30 minutes. After this 15 ml of 6N HCl is added to this fused material to dissolve this and heated gently to obtain clear solution. This solution is then added to the earlier solution and is made up to volume.

4.1.3 REE separation and pre-concentration for quantitative REE analysis

REEs concentration in rocks, particularly in granitic rocks is too low for detection and are analysed using ICP-AES. They generally occur in the range of few tens of ppm to ppb levels. There are several standard procedures suggested by various workers (Walsh et al., 1981; Crock et al., 1984; Satyanarayan et al., 1989; Rathi et al., 1991; Zachariah, 1992; Sahoo and Balakrishnan, 1994) for sample digestion and preconcentration of REEs. But, depending upon the laboratory conditions, type of the instrument, and above all nature of samples, one has to adopt a suitable procedure. Here, I have followed the procedure outlined by Sahoo and Balakrishnan (1994) with some minor modifications.

Particularly in granitic rocks more than 80% of the REEs reside in accessory minerals (Gromet and Silver, 1983). In general, the accessory minerals like sphene, zircon, monazite, rutile are refractory in nature. Therefore, it is important to bring these accessory minerals into solution by proper dissolution procedure in order to get the actual abundance of REEs of the rock concerned. The dissolution technique is same as described in section 4.1.2 for the preparation of "B" solution.

The acid digestion procedure has many advantages over other suggested methods. Hydrofluric acid readily dissolves silica to form $(SiF_6)^{-2}$ ions in acid solution. At higher temperature with the addition of perchloric acid HF forms silicon tetrafluoride which is a volatile substance and thus, silica is removed from the solution. The solution free from silica is more stable than the silica bearing solutions as the latter, tends to hydrolyze and precipitate on long standing. One of the advantages of this procedure is that the interference between silicon and fluorine with some photometric determination can be avoided. The undissolved refractory minerals are brought into solution by filtering, fluxing with lithium tetraborate, and fusing at 1050^0 C. Thus, minimum salt load is added to the cation exchange resin column, and at the same time ensuring complete digestion. Further, removal of Si from the solution is essential in high Si samples, as it coagulates and blocks the passage of solution in the cation exchange resin columns.

The rock digestion followed by alkali fusion procedure has also been tried to dissolve the rock samples. 0.5 gm of rock powder is mixed up with 2.0 gm of flux (Na_2O_2 and NaOH) in the ratio 1:4, and the mixture is fused on Meker burner. The main disadvantage of this method is the high salt content in the resultant solution. Solution with high salt contents is responsible for clogging of nebulizer-burner apertures in Atomic Emission Spectrometer, high background signals, and scattered light effects in optical emission measurements (Potts, 1987).

REEs are generally separated as a group from the matrix to avoid the spectral interference from the matrix elements during analysis using ICP-AES. Amongst the matrix elements Fe cannot be removed in HNO_3 column (Fe may interfere with Er), whereas Ca and Sr cannot be separated completely in HCl column. Therefore, for effective separation of REEs as a group from the matrix elements two columns procedure is followed.

The separation of REEs as a group is done using cation exchange resin (Biorad AG 50 X-8, 100-200 mesh size) in quartz columns (24 cm long and 1 cm inner diameter). The columns are calibrated using multi-element solution (in HNO_3 medium) containing matrix elements (Ca, Mg, Fe, Al, Na, K, Sr, Ba and Zr) and rare earth elements. 50 ml of this multi-element solution is loaded into the HNO_3 cation exchange resin column. In order to elute the matrix elements 1.75N HNO_3 is passed through column at 10 ml intervals, the cuts are collected and subsequently analyzed using ICP-AES in order to know the optimum requirement of acid to separate the matrix elements effectively without losing any REEs. From the analytical data, it is suggested that 100 ml of 1.75N HNO_3 is enough to separate all the matrix elements except Fe from the REEs and 130 ml of 6N HNO_3 is required to elute all REEs effectively (Fig. 4.1 & 4.2).

A similar type column calibration exercise is carried out for HCl column also. It is found that 70 ml of 1.75N HCl is required to remove Fe and other matrix elements and REEs are eluted by passing 225 ml of 6N HCl (Fig. 4.1 & 4.2).

The HNO_3 and HCL acid cation exchange columns are periodically recalibrated and the volumes of 1.75N and 6N acids required to elute matrix elements and REE, respectively, are accordingly adjusted.

The "B" solution (as described in previous section) which is kept in a plastic bottle is transferred to 250 ml teflon beaker and evaporated to incipient dryness. 20 ml of 2N HNO_3 and 30 ml of quartz distilled water are added to dissolve the content in teflon beaker and the
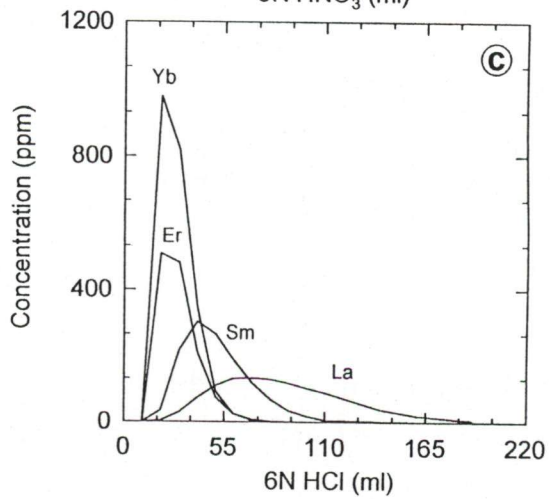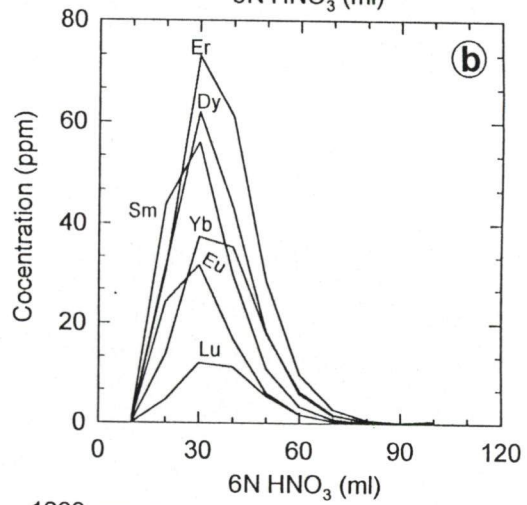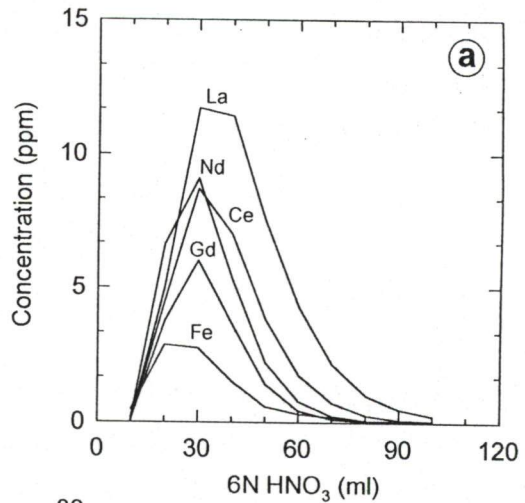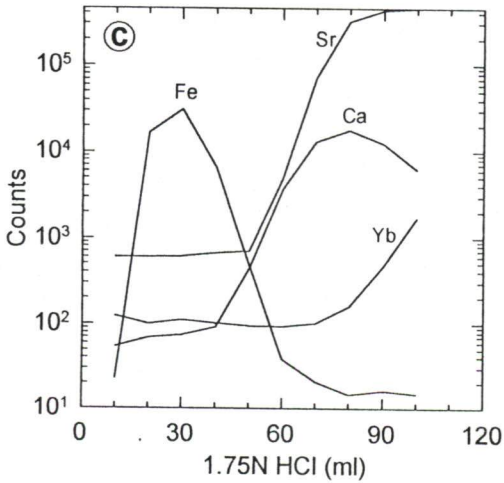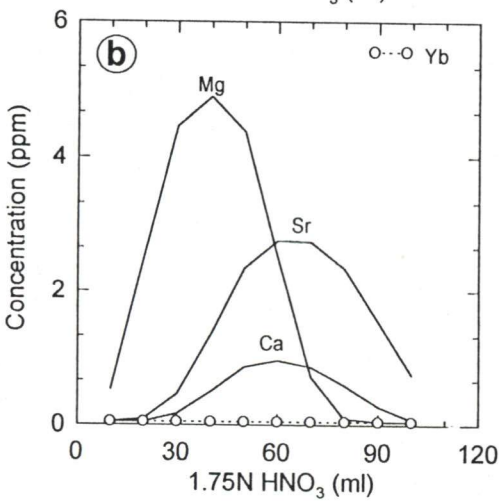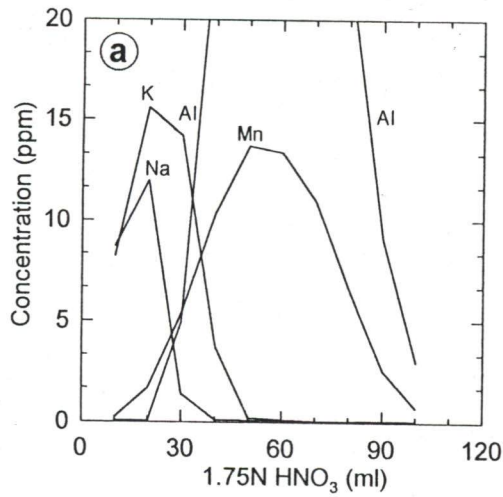
Fig. 4.1 Elution patterns for matrix elements at 1.75N HNO₃ and 1.75N HCl.

Fig. 4.2 REE elution patterns at 6N HNO₃ and 6N HCl.

solution is loaded in HNO_3 resin column. Most of the matrix elements except Fe are removed by passing 100 ml of 1.75N HNO_3 and the solution collected at the bottom of the column is discarded. Rest of the matrix elements (mostly Fe) and REEs are eluted by passing 120 ml of 6N HCl.

The eluent is then evaporated to complete dryness and redissolved with 30 ml of 1N HCl. This 30 ml solution is then loaded into HCl column. Fe and other remaining matrix elements if any, after the elution through HNO_3 column, are removed by passing 70 ml of 1.75N HCl and the successive 225 ml eluent of 6N HCl is collected and dried up. Before doing analysis the dried up material is dissolved in 10 ml 2N HNO_3; here the dilution factor is 20.

4.2 ANALYSES OF SAMPLES

Major elements (except SiO_2, K_2O and Na_2O) and most of the trace elements are analyzed using ICP-AES (LABTAM-8440). Before carrying out any analysis the instrument is calibrated using USGS rock standards *viz.*, STM1, RGM1 and MB-H (an international standard developed by Wadia Institute of Himalayan Geology, Dehradun, India by Rathi, 1994) for major elements and for trace elements calibration, Spex ultra pure salt solution of the concerned element is prepared and used. To check the accuracy and precision of the analysis, same samples are run as unknown repeatedly. Silica is determined using spectrophotometer, whereas Na_2O and K_2O are analyzed by flamephotometer. Some of the trace elements *viz.*, Rb, Nb, Y, U, Th and Ga of a few selected samples are analyzed by XRF at Wadia Institute of Himalayan Geology, Dehradun.

For REE analysis, the instrument is calibrated against multi-element standard solution prepared from high purity REE salts (procured from Johnson & Matthey and Spex Inc., USA). To check the instrumental performance international rock standard MB-H (on which REE values are available) is run as unknown.

The replicate analysis of various samples indicates the precision of the analysis (Table. 4.1). The accuracy of the major and trace element data are ± 10% and ± 5%, respectively.

Replicate analysis of the samples for major and trace element abundance. R refers to replicate analysis.

Samples	QMD-1	QMD-1R	GRD-7	GRD-7R	GRD-17	GRD-17R	GR-5	GR-5R
SiO_2	62.71	61.09	65.69	67.19	67.14	68.94	74.33	72.73
TiO_2	0.6	0.62	0.46	0.46	0.44	0.46	0.16	0.17
Al_2O_3	14.68	14.21	14.68	14.47	14.49	15.01	13.66	13.98
FeO	5.35	5.35	4.84	4.89	3.96	4.01	1.51	1.5
MnO	0.09	0.09	0.08	0.09	0.06	0.05	0.02	0.02
MgO	5.85	5.81	2.53	2.51	2.1	2.13	0.3	0.29
CaO	5.57	5.48	3.91	3.89	3.34	3.36	1	1.05
Na_2O	3.11	3.09	3.54	3.51	4.32	4.34	3.64	3.61
K_2O	2.49	2.47	3.36	3.38	2.2	2.22	5.1	4.98
P_2O_5	0.32	0.33	0.19	0.2	0.18	0.19	0.05	0.05
TOTAL	100.81	98.54	99.28	100.59	98.23	100.71	99.77	98.38
Rb	59	56	120	129	79	81	199	196
Ba	968	959	525	550	577	583	547	552
Sr	562	558	474	467	509	513	167	171
Zr	185	190	196	204	167	163	195	202
Y	15	14	36	40	12	9	8	9

Replicate analysis of the samples for REE abundance. R refers to replicate analysis.

Sample	QMD-1	QMD-1R	GRD-7	GRD-7R	GRD-27	GRD-27R	GR-4	GR-4R
Ce	84	84.07	47.3	47.31	45.4	45.3	46.3	46.37
Nd	39.9	40.02	24.1	24.12	20.3	20.27	18.7	18.73
Sm	8.7	8.51	6.8	6.82	4.71	4.69	4.23	4.28
Eu	1.81	1.88	1.66	1.69	0.9	1.12	0.77	0.71
Gd	4.96	4.93	6.8	6.96	2.52	2.53	2.41	2.46
Dy	3.12	3.19	6.1	6.13	1.52	1.51	1.77	1.8
Er	1.75	1.81	4	4.15	0.86	0.93	1.05	1.1
Yb	1.52	1.51	4.45	4.46	0.74	0.76	0.97	0.95

Table 4.1 Replicate analysis of the samples for major and trace element including REE abundance.

4.3 CLASSIFICATION

There are several classification schemes based on measurable physical and chemical parameters such as colour, mineral assemblage, modal abundance, grain-size, specific gravity, seismic velocity, major-trace-isotopic chemical composition, degree and style of alteration, size and shape of the pluton, abundance of pegmatite (Clarke, 1992), depth of emplacement according to field relations (Read, 1948; Buddington, 1959) and even

observed local, regional or global tectonic environment (Marmo,1971; Martin and Piwinskii,1972) etc. These classification schemes may have considerable utility for specific purposes.

It seems that the classification scheme based on modal proportion of QAP (of Lebas and Striekisen, 1991) is simple but it is difficult to practice. The scheme involves tedious slabbing, messy staining and point-counting. Moreover, there exits the possibility of human error.

To avoid the slabbing, staining and point-counting the rocks are simply powdered, and analyzed chemically. Then the chemical data can be reconstituted in terms of CIPW normative mineralogy. The amounts of quartz and feldspars can be plotted in QAP to assign a name of the rock. But the problem arises here because of the fact that the normative mineralogy does not always truly reflect the modal abundance of minerals. Furthermore, this classification scheme is based on the three constituents *viz.,* quartz, plagioclase and alkali-feldspars, whereas, there is much more to granitoid rocks than just quartz and feldspars.

In QAP plot using normative mineralogy the granitoid rocks of the Hutti schist belt fall in three groups *viz.,* granite, granodiorite and quartz monzodiorite (Fig. 4.3a). Attempt is made to classify the granitoid rocks on the basis of $CaO-Na_2O-K_2O$ wt.% using Condie and Hunter's (1976) and Glikson's (1979) triangular diagrams. For reference, two samples of monzodiorite and three samples of granodiorite of Stern and Hanson (1991) have been plotted along with the granitoid rocks arround the Hutti schist belt. But these two classification schemes show inconsistent results. In Condie and Hunter's (1976) triangular plot monzodiorite along with three granodiorite samples are plotted in quartz monzodiorite field (Fig. 4.3b), whereas, in Glikson's (1979) triangular diagram the plots for monzodiorites and two granodiorites fall in adamellite field (Fig. 4.3c). Therefore, a rock may have different name depending upon which triangular plot one is using to define the rock.

An attempt has been made to classify the granitoid rocks surrounding the Hutti schist belt by using K_2O and SiO_2 variation diagram. To verify the reliability of the diagram, the same samples of Stern and Hanson (1991) have also been plotted. The plots of granitoid rocks fall in two fields *viz.,* dacite-rhyolite and andesite. A limitation of this classification scheme is that there is no distinction between the rhyolite and dacite. From the figure 4.4, it is clear that the rocks which are ≥ 63 wt.% of SiO_2 plot in dacite-rhyolite field irrespective of K_2O wt.%.
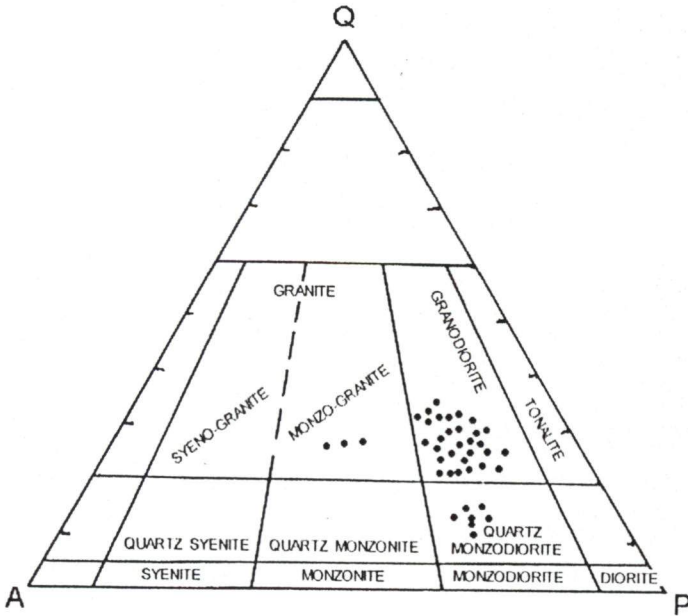
Fig. 4.3 a) The normative data of the granitoid rocks surrounding the Hutti schist belt
as plotted in QAP modal diagram. The granitoid rocks lie in the fields of
granite, granodiorite and quartz monzodiorite (the fields are after, Streckeisen,
1976).
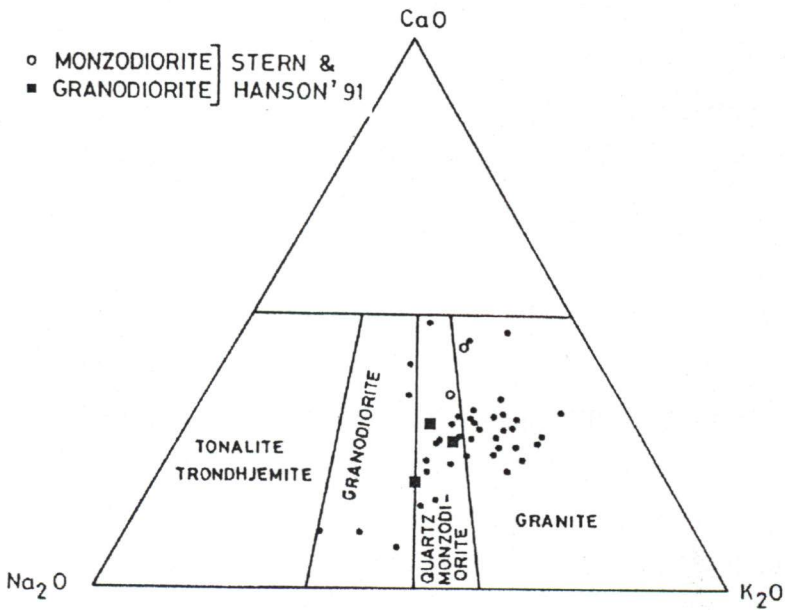
Fig. 4.3 b) The CaO-Na$_2$O-K$_2$O ternary diagram (after Condie and Hunter, 1976) for the
granitoid rocks around the Hutti schist belt. The rocks lie in the fields of
granite, granodiorite and quartz monzodiorite. Three granodiorite samples and
two monzodiorite samples of Stern and Hanson (1991) are also plotted for
comparison.
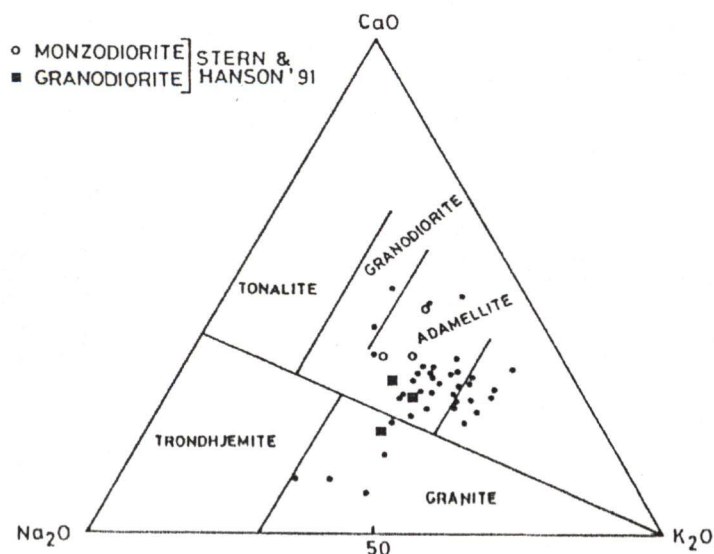
Fig. 4.3 c) The CaO-Na₂O-K₂O ternary diagram (after Glikson, 1979) for the granitoid rocks around the Hutti schist belt. Majority of the granitoid rocks plot in the granite field. Three granodiorite samples and three monzodiorite samples of Stern and Hanson (1991) are also plotted for coparison

It is found that the best way of classifying these granitoid rocks is by using chemical data involving total alkali (K₂O+Na₂O) and SiO₂ variation diagram (TAS diagram) on Lebas and Striekisen (1991), recommended by IUGS for volcanic rocks. In this diagram the granitoid rocks surrounding the Hutti schist belt are plotted in four distinct fields. The rocks plot in rhyolite, dacite, andesite and trachyandesite field, will be called as granite, granodiorite, quartz monzodiorite and monzodiorite, respectively (Fig. 4.5). From the figure 4.5, it is evident that there are two types of granite; one is high alkali granite and other one is low alkali granite. Interestingly, these two types of granites are confined to two distinct geographic locations. The high alkali granite occurs in the northeastern side of the belt (called as Eastern granites), whereas, the low alkali granites occurs on the north and northwestern side of the belt (called as Western granites). The quartz monzodiorite occur on the western side of the belt specifically on the western part of the Lingsugur, whereas, the monzodiorites occur as pockets in the east and northwest of the belt. Amongst the granitoid rocks, the granodiorites are most widespread as they occur throughout the study area from north to south and from east to west.
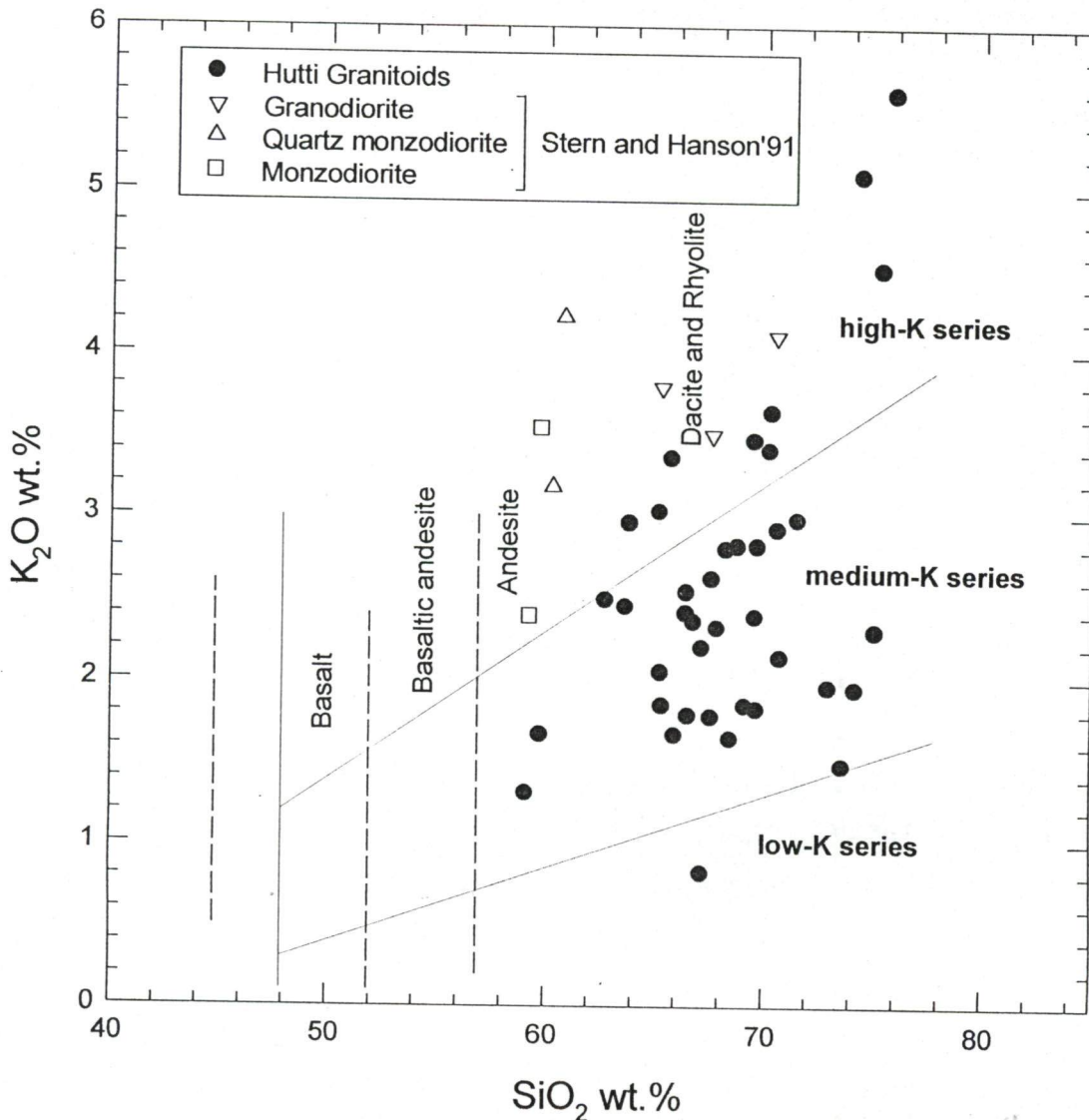
Fig. 4.4 K_2O versus SiO_2 classification scheme for subduction zone magmas (after Le Bas and Streckeisen, 1991). SiO_2 contents of 53 wt.%, 57wt.% and 63 wt.% separate basalt, basaltic andesite, andesite and dacite and rhyolite compositions. Note that high–K is not synonymous with potassic. Majority of the granitoid rocks of the study area plot in the medium-K series. For comparison three granodiorite, two quartz monzodiorite and two monzodiorite samples of Stern and Hanson (1991) are also plotted.

One of the important uses of (K_2O+Na_2O) versus SiO_2 plot (Fig. 4.5) is that it indicates the tectonic setting in which the rocks might have come into existence during Archean. By using this 'TAS' (Le Bas and Striekisen, 1991) Classification diagram one can compare the Phanerozoic volcanic rocks erupted in different tectonic setting to that of Archean plutonic rocks.
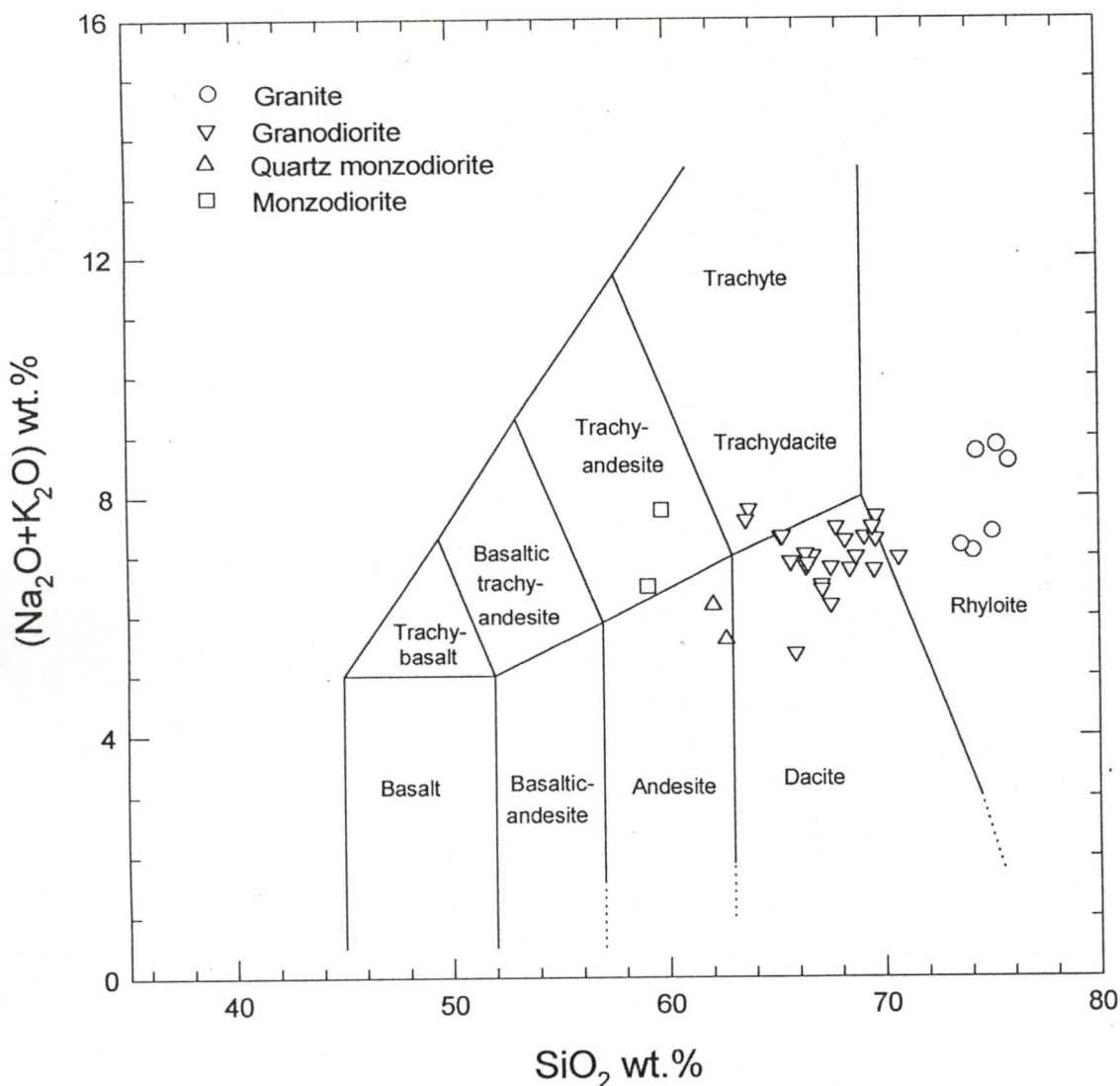
Fig. 4.5 Chemical classification and nomenclatute of volcanic rocks using the total alkali versus silica (TAS) diagram (after Le Bas and Streckeisen, 1991). Symbols indicate different rock types.

4.4 RESULTS

4.4.1 Granites

Depending upon total alkali content granites of Hutti schist belt can be classified into two groups: high alkali granites (Eastern granites) and low alkali granites (Western granites). Overall these granites have a narrow range of silica content (73.6 to 75.84 wt.%), and

except in one sample (GR-1 of Galaga village) there is not much difference in TiO_2, Al_2O_3, FeO and MgO. The CaO content in these granites ranges from 0.75 to 2.8 wt.%. The low alkali granites have high amount of CaO content than that in the high alkali granites (Table. 4.2).

Major element oxides data in wt.%						
	2	4	10	26	27	39
Samples	GR-1	GR-2	GR-3	GR-4	GR-5	GR-6
SiO_2	75.3	74.17	73.6	75.84	74.33	75.07
TiO_2	0.06	0.19	0.37	0.24	0.16	0.31
Al_2O_3	13.44	14.31	12.98	12.88	13.66	13.1
Fe_2O_3	0.12	0.18	0.38	0.2	0.23	0.35
FeO	0.68	1.01	2.13	1.12	1.28	1.96
MnO	0.02	0.02	0.03	0.02	0.02	0.03
MgO	0.13	0.45	0.71	0.35	0.3	0.59
CaO	0.75	2.1	2.7	1.02	1	2.03
Na_2O	4.33	5.12	5.69	2.98	3.64	5.09
K_2O	4.52	1.95	1.48	5.6	5.1	2.3
P_2O_5	0.03	0.1	0.1	0.09	0.05	0.03
TOTAL	99.38	99.6	100.17	100.34	99.77	100.86
Trace element data in ppm.						
Ba	296	311	784	482	547	322
Cr	9			35	6	
Ni	10		22.8	13	9	
Rb	206	212		252	199	216
Sr	129	105	924	226	167	121
V			33.8			
Zr	83	115	428	184	195	93
Th	16.9			54.9	67.9	
U	6.9			12.1	9.2	
Ga	20			18	17	
Nb	6			10	2	
Y	5	6		12	8	7
Zn	18		55.6	28	32	
Cu	3			6	9	
Mg#	0.223	0.402	0.334	0.32	0.259	
zrT	833		1041	914	921	
apT	845		939	950	880	
REE data in ppm.						
Ce	20.4	36		46.3	38.5	13.8
Nd	10.45	13.7		18.7	17.1	6.25
Sm	2.32	1.92		4.23	2.54	1.13
Eu	0.05	0.35		0.77	0.24	0.25
Gd	1.32	1.83		2.41	1.66	1
Dy	1	1.24		1.77	1.01	0.97
Er	0.66	0.63		1.05	0.49	0.46
Yb	0.58	0.39		0.97	0.45	0.31

Table 4.2 Major and trace element including REE data of granites around the Hutti schist belt (zrT & apT are zircon & apatite saturation temperature, respectively).

The abundance of Ba in both the granites is high (varies from 296 to 784 ppm), while Sr content is invariably low except for sample GR-3 which contains 924 ppm Sr. Zr concentration is moderate and varies from 83 to 428 ppm.

Low alkali granites contain higher amount of Ba, Sr and Zr; and less enriched in LREE as compared to high alkali granites. Both the granites exhibit strongly fractionated chondrite normalized REE patterns with negative Eu anomaly (Fig. 4.6). The high alkali granites show a stronger Eu anomaly as compared to low alkali granites. The Ce_N/Yb_N ratio varies from 21.58 to 23.62 except for samples GR-1 and GR-6. The chondrite normalized REE pattern of GR-1 shows strong negative Eu anomaly (Eu/Eu*=0.08), where as GR-6 is an aplite vein showing less fractionated chondrite normalized REE pattern with slight negative Eu anomaly (Eu/Eu*=0.72).
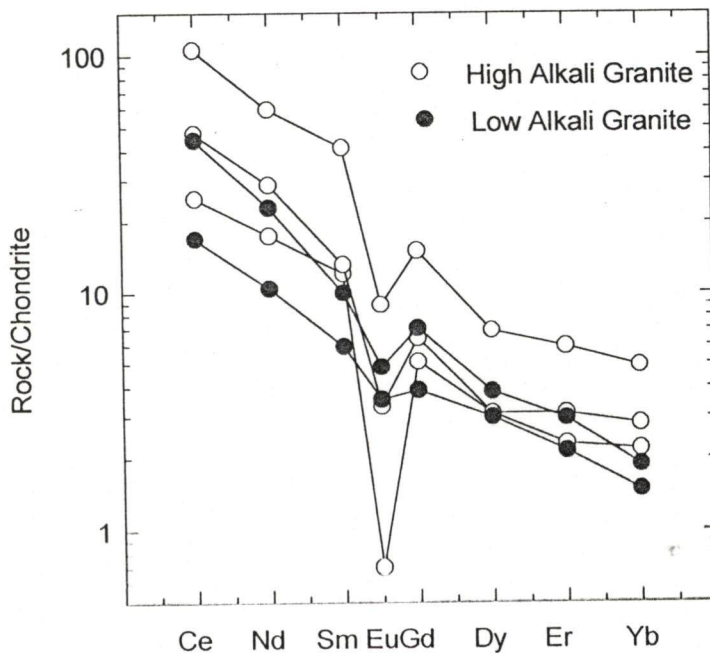
Fig. 4.6 Chondrite normalized REE patterns of granites. In general, the high alkali granites have higher REE abundance, and more prominent negative Eu anomaly than the low alkali granites.

G10,199.

4.4.2 Granodiorites

These are the most predominant rock type amongst the granitoids around the Hutti schist belt. They are silica saturated to oversaturated rocks containing high amount of silica (varies from 65.25 to 72.49 wt.%). The granodiorites have a range of TiO_2 content from 0.17 to 0.69 wt.%. They have a wide range of Al_2O_3 content (varies from 13.71 to 17.1 wt.%) with moderate amount of CaO content (> 2.25 wt.%). Amongst the alkalies Na_2O content is invariably higher than the K_2O content (Table 4.3). Majority of the rock samples has greater than 2.0 wt.% FeO(T) whereas, MgO content varies from 0.38 to 2.53 wt.%. In the IUGS recommended K_2O versus SiO_2 diagram, most of these rock samples plot in medium K–series dacite and rhyolite field (Fig. 4.4). The rocks are meta-aluminous in nature and define calc-alkaline trend (Fig. 4.7).
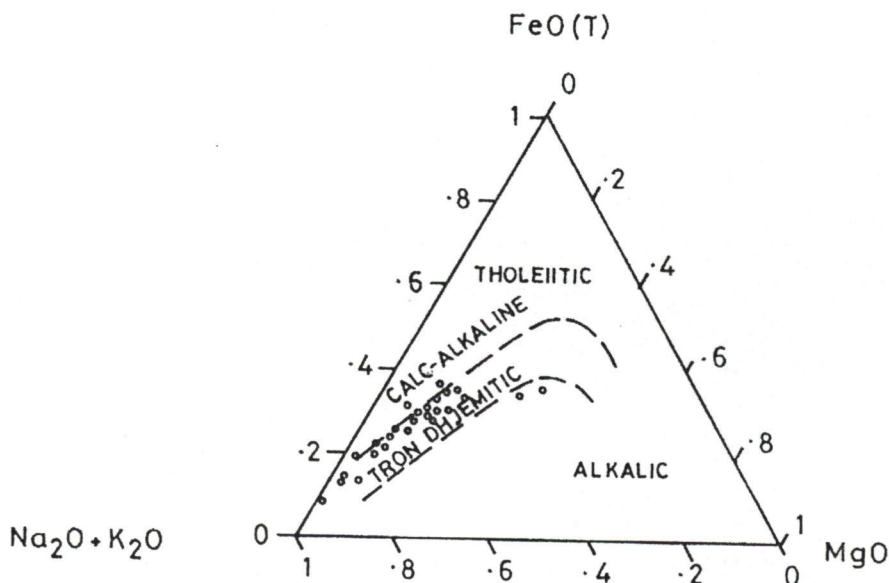
Fig. 4.7 The granitoid rocks show alkali to calc-alkaline character in AFM diagram (after Barker and Arth, 1976).

The granodiorites have higher concentration of Ba and Sr as compare to Zr concentration. Ba content varies from 454 to 918 ppm except for samples GRD-22 and GRD-23 that contain 2004 ppm and 1413 ppm, respectively. Majority of these rocks contain more than 450 ppm of Sr. One of the samples (sample no. GRD-18) contain very low abundance of Sr (167 ppm). They have narrow range of Zr concentration and it varies from

Major element oxides data in wt.%									
	1	5	7	8	9	11	12	13	14
Samples	GRD-1	GRD-2	GRD-3	GRD-4	GRD-5	GRD-6	GRD-7	GRD-8	GRD-9
SiO_2	69.12	63.78	70.19	70.26	67.56	65.91	65.69	67.56	65.25
TiO_2	0.24	0.46	0.17	0.17	0.34	0.64	0.46	0.5	0.46
Al_2O_3	14.84	15.82	15.98	16.12	16.28	15.01	14.68	15.8	17.1
Fe_2O_3	0.35	0.71	0.29	0.29	0.48	0.71	0.73	0.54	0.62
FeO	1.98	4	1.64	1.62	2.7	4.02	4.11	3.03	3.48
MnO	0.04	0.07	0.02	0.02	0.03	0.09	0.08	0.04	0.04
MgO	0.68	1.8	0.28	0.38	0.7	1.84	2.53	1.35	1.62
CaO	2.73	3.68	3.06	2.05	2.95	4.76	3.91	3.08	3.56
Na_2O	5.47	4.82	4.48	4.2	4.41	3.7	3.54	4.19	5.27
K_2O	1.85	2.96	3.41	3.64	1.78	1.67	3.36	2.62	2.05
P_2O_5	0.1	0.28	0.02	0.03	0.04	0.18	0.19	0.24	0.21
TOTAL	97.4	98.38	99.54	98.78	97.27	98.53	99.28	98.95	99.66
Trace element data in ppm.									
Ba	605	933	918	814	454		525	708	
Cr	25	38					35		
Ni	17	19		12.4	13.4		18	20.4	
Rb	57	72					120		
Sr	619	965	474	528	572		474	928	1030
V			12	11.2	27.6			51.2	66
Zr	141	229	724	468	526		196	488	104
Th	3.6	9.7					23.1		
U	0.8	4.1					6.6		
Ga	25	25					22		
Nb	2	11					11		
Y	8	29					36		
Zn	51	90	49.2		59.2		73	83.4	
Cu	10	44			14.8		41	25	
Mg#	0.342	0.405	0.206	0.26	0.281	0.409	0.482	0.403	0.413
zrT	885	938	1085	1026	1041		920	1031	854
apT	895	953	763	796	792		928	975	935
REE data in ppm.									
Ce	34.2	72		64			47.3	71	87
Nd	12.1	35.5		19.6			24.1	30.3	35.6
Sm	3.2	9.1		2.89			6.8	5.1	6.3
Eu	0.9	2.15		0.61			1.66	1.16	1.4
Gd	2.56	7.5		1.94			6.8	3.04	3.62
Dy	1.5	5.4		1.22			6.1	1.72	1.98
Er	0.77	3.05		0.57			3.98	0.94	1.08
Yb	0.83	2.96		0.22			4.45	0.54	0.62

Table 4.3 Major and trace element including REE data of granodiorites around the Hutti schist belt (zrT & apT are zircon & apatite saturation temperature, respectively, table contd...).

Major element oxides data in wt.%

Samples	15 GRD-10	16 GRD-11	18 GRD-12	19 GRD-13	20 GRD-14	21 GRD-15	22 GRD-16	23 GRD-17	24 GRD-18	25 GRD-19
SiO_2	65.31	67.16	66.39	68.23	68.45	72.94	67.82	67.14	69.49	66.74
TiO_2	0.69	0.64	0.41	0.42	0.27	0.24	0.27	0.44	0.34	0.42
Al_2O_3	16.9	16.1	14.91	16.6	14.78	16.7	15.16	14.49	13.71	14.64
Fe_2O_3	0.56	0.57	0.59	0.43	0.42	0.32	0.41	0.59	0.55	0.6
FeO	3.15	3.2	3.34	2.43	2.38	1.78	2.35	3.37	3.09	3.41
MnO	0.03	0.03	0.06	0.03	0.05	0.32	0.04	0.06	0.06	0.06
MgO	1.58	1.49	1.92	1.16	1.05	0.69	0.88	2.1	1.88	2.18
CaO	3.2	3.16	3.28	2.8	3.04	2.8	2.98	3.34	1.31	3.38
Na_2O	5.48	5.63	4.62	4.47	5.14	4.92	5.16	4.32	4.02	4.64
K_2O	1.85	0.82	2.41	2.8	1.67	1.96	2.32	2.2	3.47	2.36
P_2O_5	0.26	0.27	0.19	0.1	0.07	0.17	0.12	0.18	0.12	0.17
TOTAL	99.01	99.07	98.12	99.47	97.32	102.84	97.51	98.23	98.04	98.6

Trace element data in ppm.

	GRD-10	GRD-11	GRD-12	GRD-13	GRD-14	GRD-15	GRD-16	GRD-17	GRD-18	GRD-19
Ba		718	693		483	642	606	577	675	694
Cr			91		32		23	53	77	71
Ni		24.2	33		20	18	22	31	34	37
Rb			78		59		79	79	94	114
Sr		940	604	620	646	874	577	509	167	538
V		53.6		52		25.8				
Zr		504	143	80	130	690	131	167	155	173
Th			8.4		9.9		8.6	15.1	37.4	21
U			3		0.9		2.6	4.4	7	5.5
Ga			22		22		22	21	18	20
Nb			6		5		4	6	8	6
Y			13		9		8	12	14	13
Zn		51.2	70		52	51.2	46	72	40	62
Cu		16.4	19		24		17	23	26	22
Mg#	0.432	0.413	0.466	0.419	0.4	0.37	0.362	0.486	0.479	0.492
zrT		1035	1059	829	877	1078	878	903	896	907
apT		985	935	886	853	989	900	937	918	927

REE data in ppm.

	GRD-10	GRD-11	GRD-12	GRD-13	GRD-14	GRD-15	GRD-16	GRD-17	GRD-18	GRD-19
Ce			60	53	53	62	48.2	53	57	72
Nd			24.1	21.3	18.2	18	18.3	25.7	21.8	30.5
Sm			4.22	3.27	2.59	2.3	4.16	5.7	4.8	6.4
Eu			1.03	0.79	0.82	0.64	1.11	1.06	0.8	1.15
Gd			3.05	2.35	1.99	1.65	3.01	3.14	2.4	3.35
Dy			2.06	1.54	1.37	1.1	1.73	2.11	1.97	2.1
Er			1.07	0.9	0.75	0.58	0.93	1.3	1.05	1.25
Yb			0.73	0.68	0.46	0.38	0.98	1.17	1.04	1.1

Table 4.3 contd...

Major element oxides data in wt.%

Samples	28 GRD-20	29 GRD-21	32 GRD-22	33 GRD-23	34 GRD-24	35 GRD-25	36 GRD-26	37 GRD-27	38 GRD-28
SiO_2	66.52	69.66	70.57	66.42	69.57	71.49	69.63	70.72	63.62
TiO_2	0.35	0.18	0.26	0.38	0.3	0.23	0.21	0.24	0.41
Al_2O_3	17	14.68	14.18	15.06	14.47	13.97	14.9	14.18	16.61
Fe_2O_3	0.64	0.34	0.36	0.57	0.4	0.33	0.3	0.34	0.59
FeO	3.62	1.92	2.02	3.22	2.25	1.87	1.69	1.95	3.32
MnO	0.04	0.05	0.03	0.07	0.04	0.04	0.03	0.04	0.06
MgO	1.67	0.75	0.72	1.43	0.74	0.57	0.54	0.73	1.36
CaO	3.91	2.65	2.6	3.13	2.68	2.25	2.4	2.39	3.32
Na_2O	5.08	4.85	3.91	4.28	4.39	4.29	5.46	4.84	5.15
K_2O	1.79	2.82	2.92	2.54	2.39	2.98	1.83	2.14	2.45
P_2O_5	1.1	0.11	0.12	0.23	0.11	0.1	0.09	0.11	0.18
TOTAL	101.72	98.01	97.69	97.33	97.34	98.12	97.08	97.68	97.07

Trace element data in ppm.

Ba	918	868	2004	1413	568	885	856	659	812
Cr		39	21	19	19	5	73	43	29
Ni	42.5	22	12	14	12	10	21	17	20
Rb		89	58	70	88	92	39	53	103
Sr	954	691	693	744	285	363	638	559	664
V	118								
Zr	1280	145	181	211	157	150	144	142	162
Th		10	10.7	17.2	10.3	13.2	2.7	7.9	10.3
U		2.5	1.8	3.2	3.2	3	0.2	1.2	3.6
Ga		19	17	19	19	18	22	22	2.5
Nb		6	6	8	9	8	4	6	8
Y		11	13	17	12	13	9	11	12
Zn	51.2	38	40	65	55	44	51	56	66
Cu		6		21	12		7		16
Mg#	0.412	0.35	0.402	0.402	0.332	0.315	0.326	0.362	0.383
zrT	1171	888	912	929	897	892	888	886	900
apT	1179	910	924	958	909	919	890	910	898

REE data in ppm.

Ce	21.73	48.5	64	123	46.3	52	29	45.4	62
Nd	11.26	19	25	51	18.7	21.8	13.1	20.3	26.6
Sm	2.52	4.07	5.3	10	4.23	4.75	3.15	4.71	5.9
Eu	0.65	0.8	1.1	2.12	0.77	0.89	0.61	0.9	1.1
Gd	1.22	2.09	2.6	6.1	2.41	2.55	1.6	2.52	3.42
Dy	1.38	1.37	1.66	3.3	1.77	1.71	0.99	1.52	2.36
Er	0.66	0.88	0.98	1.49	1.05	1.01	0.58	0.86	1.35
Yb	0.35	0.86	0.79	0.96	0.97	0.93	0.51	0.74	1.13

Table 4.3 concluded.

131 to 211 ppm. However, a few rock samples have a high abundance of Zr (468 to 690 ppm), the exception is GRD-20 which contains exceptionally high amount of Zr (1280 ppm). The abundance of Cr, Ni, Zn and Cu are invariably low. Cr content is less than 92 ppm but in most of the rocks it varies between 19 to 40 ppm, whereas, Ni abundance ranges from 10 to 42.5 ppm. In general, Mg# of these rocks is greater than 0.4 but a few selected samples, mainly from the western part of the belt (Gurgunta outcrop), have Mg# less than 0.3. One of the samples, GRD-21, from Lingsugur area, shows extremely low Mg# (0.14). The major element oxides and trace elements data with the Mg# of the Hutti granodiorites are comparable to that of the granodiorites of the Roaring River Complex, Superior Province, Canada, as reported by Stern and Hanson (1991). On an average the granodiorites of the Hutti·granodiorites have a lower ranges of Ba and Sr and higher abundance of LREE as compared to that of the Roaring River Complex granodiorites. However, the concentration of HREE of the Hutti granodiorites is lower than that of the Roaring River Complex granodiorites.

Total REE content of these rocks vary in between 50 to 113 ppm except for samples GRD-10 and GRD-23 (both are from western side of the belt). Majority of the samples has REE concentration well within the ranges of 80 to 100 ppm (Table 4.3). The total REE abundance of the sample GRD-20 is very low (ΣREE = 39.77 ppm) as compared to the other samples, whereas the sample GRD-23 contains very high amount of REEs (ΣREE = 197.97 ppm). In general, the rocks have LREE enriched highly fractionated rare earth element patterns (Ce_N/Yb_N = 10.54 to 41.33), except for samples GRD-20 and GRD-7 which are characterized by LREE enriched less fractionated REE patterns (Ce_N/Yb_N = 2.43 to 2.72). In majority of these rocks, Er_N/Yb_N varies from 0.71 to 1.14 indicating a flat to slightly fractionated HREE patterns (Fig. 4.8). In general, the chondrite normalized REE patterns of these rocks are generally smooth with slight negative Eu anomaly (Eu/Eu* = 0.64 to 0.96).

4.4.3 Quartz Monzodiorites

These rocks have SiO_2 content of the order of 62 wt.%. The abundance of major element oxides and trace elements are comparable with that of ADAK type andesites (Yogodzinski et al., 1995) except in SiO_2 content which is slightly higher than that of latter (Table 4.4). As compared to granodiorites their Ba content is higher, and their Mg# is much higher than that of any other rock type in the study area. The rocks are plotted in medium K-
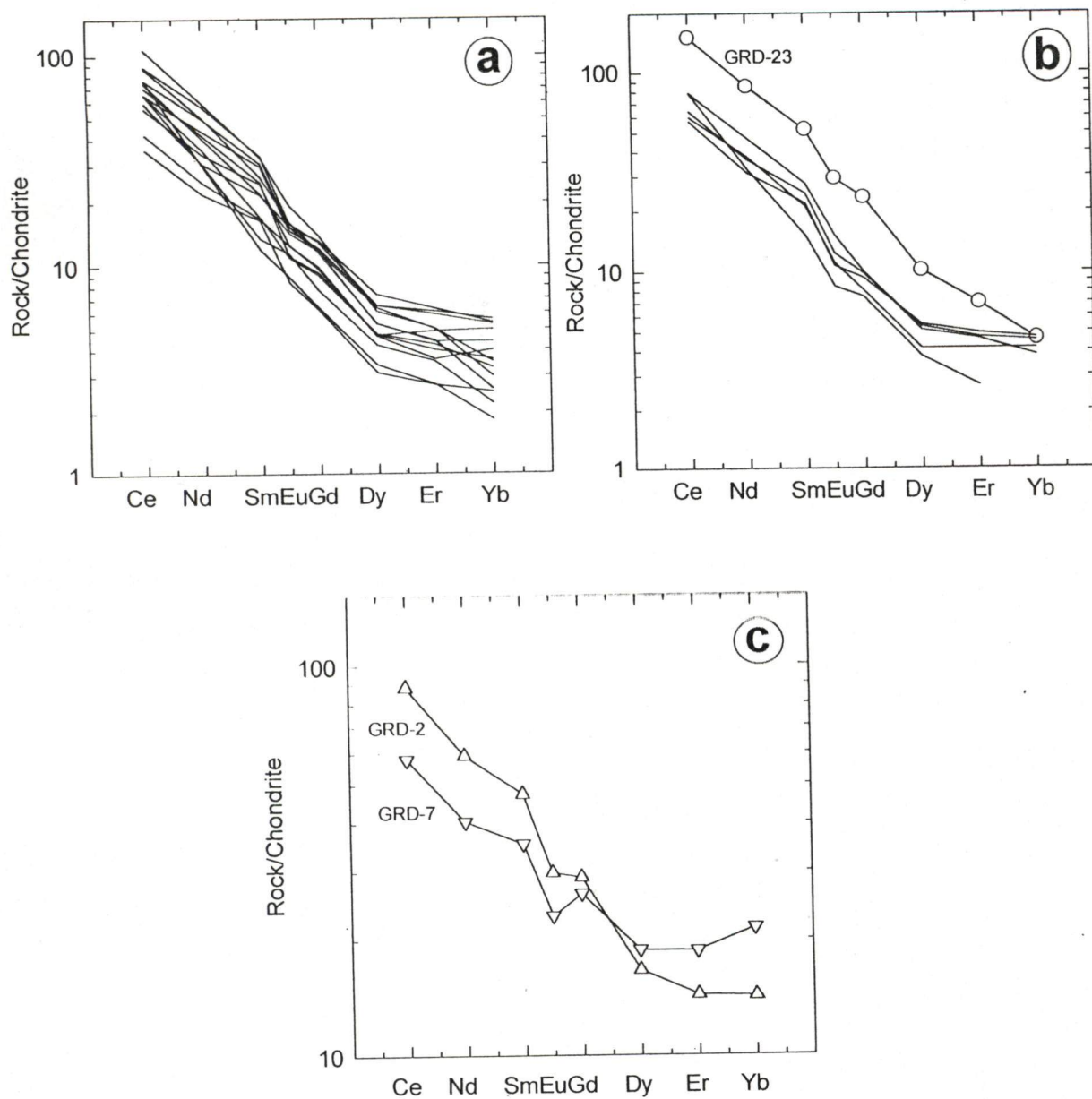
Fig. 4.8 Chondrite normalized REE patterns of: a) Eastern (Kavital) granodiorites. b) Western granodiorites. c) Northern granodiorites. Note that the Western and Northern granodiorites have less fractionated REE patterns as compared to Eastern granodiorites and one of the Western granodiorite samples, GRD-23 has the highest REE abundance.

series field in K_2O versus SiO_2 diagram of IUGS (Fig. 4.4). They have higher content of MgO (5.85 wt.%) and CaO (5.57 wt.%), whereas, Na_2O and K_2O concentration are lower than that of the granodiorites.

Total REE content is of the order of 145.76 ppm. The rocks show LREE enriched (Ce_N/Yb_N = 14.14) and HREE depleted (Er_N/Yb_N=0.89) chondrite normalized REE patterns with slight negative Eu anomaly (Fig. 4.9). In general, quartz monzodiorites are very much comparable to ADAK type andesites in their LREE content, except that, the former has higher abundance of HREE.
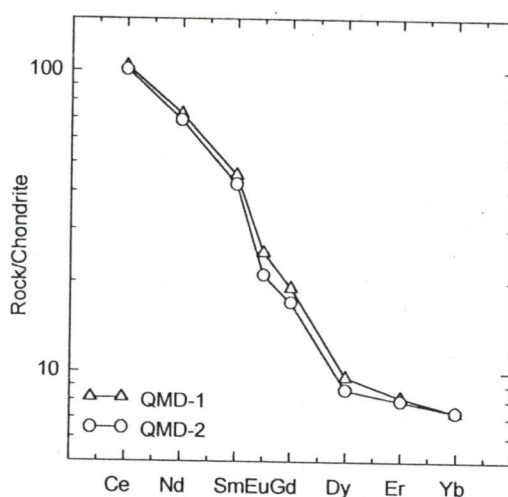
Fig. 4.9 Chondrite normalized REE patterns of quartz monzodiorites.

4.4.4 Monzodiorite

Monzodiorites have a restricted range of SiO_2 (59.09 to 59.74 wt.%). The TiO_2 content ranges from 0.15 to 0.64 wt.%. The rocks contain very high amount of Al_2O_3 (19.1 to 20.69 wt.%) as compared to other rock type of the study area. The major element oxides of the two monzodiorite samples are comparable except for CaO and TiO_2. The monzodiorite of the western side (MZD-1) has much higher CaO (6.19 wt.%) and lower TiO_2 (0.15 wt.%) content than the monzodiorite (MZD-2) of the eastern side (Table. 4.4). The abundance of trace element are very much similar between these two samples, but they differ in their Mg#. The eastern side sample (MZD-2) has Mg# 0.44, whereas, Mg# of the sample MZD-1 is 0.36.

Major element oxides data in wt.%				
	30	31	6	17
Samples	QMD-1	QMD-2	MZD-1	MZD-2
SiO_2	62.71	62.1	59.09	59.74
TiO_2	0.6	0.57	0.15	0.64
Al_2O_3	14.68	14.06	20.69	19.1
Fe_2O_3	0.96	0.86	0.69	0.84
FeO	4.43	4.87	3.91	4.76
MnO	0.09	0.08	0.04	0.06
MgO	5.85	4.77	1.44	2.46
CaO	5.57	4.39	6.19	3.17
Na_2O	3.11	3.15	5.19	6.1
K_2O	2.49	3.03	1.31	1.67
P_2O_5	0.32	0.3	0.15	0.28
TOTAL	100.81	98.18	98.94	98.82
Trace element data in ppm.				
Ba	968	1046	346	668
Cr	175	115		
Ni	75	58		
Rb	59	83		
Sr	562	496	980	1050
V			71	94
Zr	185	208	112	93
Th	10	12.7		
U	3.7	5		
Ga	17	17		
Nb	9	10		
Y	15	18		
Zn	82	76		
Cu	39	38		
Mg#	0.659	0.597	0.358	0.439
zrT	913	927		844
apT	957	977		904
REE data in ppm.				
Ce	84	82	26.8	94
Nd	39.9	37.6	13.6	40.8
Sm	8.7	8.1	2.71	7.5
Eu	1.81	1.52	0.89	1.75
Gd	4.96	4.42	2.94	4.33
Dy	3.12	2.82	2.31	2.29
Er	1.75	1.7	1.26	1.21
Yb	1.52	1.52	0.97	0.65

Table 4.4 Major and trace element including REE data of quartz monzodiorites and monzodiorites around the Hutti schist belt (zrT & apT are zircon & apatite saturation temperature, respectively).

The monzodiorites of eastern and western side of the schist belt differ in their REE content as well as in their chondrite normalized REE patterns. The total REE content of eastern side monzodiorite is much higher (ΣREE = 152.528 ppm) than that of western side monzodiorite (ΣREE = 51.48ppm). The chondrite normalized REE pattern of MZD-2 is highly fractionated (LREE enriched, Ce_N/Yb_N = 36.99), and HREE depleted (Er_N/Yb_N = 0.55) with no negative Eu anomaly (Fig. 4.10). Whereas, the chondrite normalized REE pattern of western side monzodiorite is less fractionated (Ce_N/Yb_N = 7.07) with no Eu anomaly (Eu/Eu* = 0.97) and slightly fractionated HREE (Er_N/Yb_N = 0.79). The chondrite normalized REE pattern of this western monzodiorite (MZD-1) is nearly flat and less fractionated than its eastern counter part (Fig. 4.10).
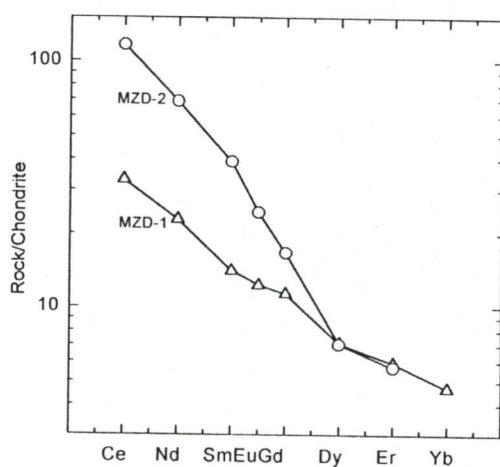
Fig. 4.10 Chondrite normalized REE patterns of monzodiorites. Note that monzodiorite (MZD-2) occurring to east of the Hutti schist belt has higher REE abundance, and more fractionated chondrite normalized REE pattern than the monzodiorite (MZD-1) occurring to west of the belt.

CHAPTER 5

PETROGENESIS

The petrogenetic studies using geochemical approach are an important tool to reveal the evolutionary history of the Archean continental crust. Multiple deformation and metamorphism obscure the original texture and mineralogy of the Archean rocks. On the basis of geochemical modeling it is possible to place constraints on various hypotheses that outline the source characteristics, the igneous processes by which the rocks might have formed, as well as the tectonic settings in which they have been emplaced.

Petrogenetic modeling of granitic rocks using major and trace elements is very complex and therefore less definitive. This is because, the magmas parental to granitic rocks could be formed from a variety of sources such as mantle, basalts, sedimentary and pre-existing granitic rocks and their source could be heterogeneous on a larger scale (Hanson, 1980). Furthermore, the quantitative modeling is difficult due to inadequate knowledge of mineral-melt distribution coefficients (K_d) of many trace elements, which vary considerably in the granitic systems. K_d values depend not only on temperature, pressure, fO_2 conditions of melting and crystallization but also on the nature and extent of fluids involved during melting and crystallization processes (Mahmood and Hildreth, 1983; Green and Pearson, 1983; Nash and Crecraft, 1985).

The geochemical modeling is usually carried out using least mobile trace elements, such as, rare earth elements (REEs). The REEs are relatively less mobile even under granulite grade of metamorphism (Balakrishnan and Rajamani, 1987). Therefore, only the less mobile elements like REEs are used for the petrogenetic studies.

5.1 MAGMATIC PROCESSES

There are several magmatic processes such as, fractional crystallization, partial melting, mixing, assimilation etc., which are responsible for diversification of magma. For example, when a body of magma leaving its source is potentially subjected to magmatic differentiation or assimilation it changes its overall bulk chemical composition before it finally solidifies. Out of several magmatic processes, fractional crystallization and partial melting are the most important, and these processes can be quantified using trace element modeling. The process of melting, in many ways, is the reverse of solidification; the compositions of liquids vary as melting advances as much as they do with crystallization. If a melt is extracted at an early stage of partial melting, it will be richer in low-temperature components, whereas more advanced melting produces liquids with larger proportions of refractory components. A series of liquids can be produced that resembles the compositions of liquids evolving by crystal fractionation, but their order of appearance in the magmatic sequence is reversed. Despite the broad similarities, details of the two processes may differ in several important ways. The relative concentrations of certain trace elements in liquids produced by melting differ from those liquids that are evolved during crystal fractionation. Furthermore, the compositions and proportions of liquids may differ, depending on how melting takes place.

Trace elements are frequently used to quantify magmatic processes using inverse or forward modeling techniques. They are also often used as qualitative discriminants between magma types, particularly between magmas erupted in different tectonic settings.

The behaviour of trace elements during partial melting processes is usually described by equilibrium batch melting or integrated fractional (Rayleigh) melting equations (Shaw, 1965). These equations are based on static melting model and can be formulated for either modal or nonmodal melting depending on whether the solid phases melt in the proportion in which they are present in the source or in different proportions.

The modal batch and fractional melting equations are:

$C_l = Cs/(F+D-FD)$ and

$C_l = [Cs/F]\,[1-(1-F)^{1/D}]$

For nonmodal melting,

$C_l = Cs/[D+F(1-P)]$ and

$C_l = [Cs/F]\,[1-(1-PF/D)^{1/P}]$

where C_l and Cs are the element concentrations in the partial melt and source material, F is the degree of melting or the mass fraction of the partial melt relative to the initial solid mass, D is the bulk partition coefficient given by

$$D \equiv \Sigma X\alpha D\alpha \qquad \Sigma X\alpha = 1$$

Where $X\alpha$ are the phase fractions in the source and $D\alpha$ are their respective solid-melt partition coefficients, and P is the equivalent coefficient calculated using the phase fractions which enter the melt $(P\alpha)$:

$$P \equiv \Sigma P\alpha D\alpha \qquad \Sigma P\alpha = 1$$

Trace element behaviour in magmatic systems under going crystal fractionation can be described by the equilibrium and fractional (Rayleigh) crystallization equations, depending on whether the crystallization solid phases remain in equilibrium with the evolving melt or become chemically and or physically isolated from it. These equations are, respectively,

$$C_l = C_0/(F+D-FD) \text{ and}$$

$$C_l = C_0 F^{(D-1)}$$

where C_l and C_0 are the element concentrations in the evolving and parent melts, D is a bulk partition coefficient, based on the crystallizing or fractionating phase assemblage, and F is the mass fraction of the original melt remaining.

A comparison of the trace element behaviour produced by varying extent of partial melting and fractional crystallization for D values ranging from compatible (D > 1) to highly incompatible (D << 1) are shown in figure 5.1. The relative enrichment or depletion of a particular element depends on D value. For example, at D = 0.1 the melt is enriched in incompatible trace elements at low extent of melting but as melting proceeds the concentration of the incompatible trace element decreases and, at higher extents of melting the variation becomes negligible. In case of compatible element (D > 1), the variation in concentration is not much at low extents of melting (Fig. 5.1).

In case of perfect fractional crystallization, the variation of incompatible element's (D < 1) concentration is not much at low extents of crystallization but the depletion of the compatible element (D > 1) in the melt is noticeable (Fig. 5.1). As D approaches to zero, $C_l/C_0 = 1/F$, it is nothing but the equation of melting at same D. Therefore, at D = 0 it is not possible to distinguish between the melts formed by low extents of partial melting and high degrees of fractional crystallization.
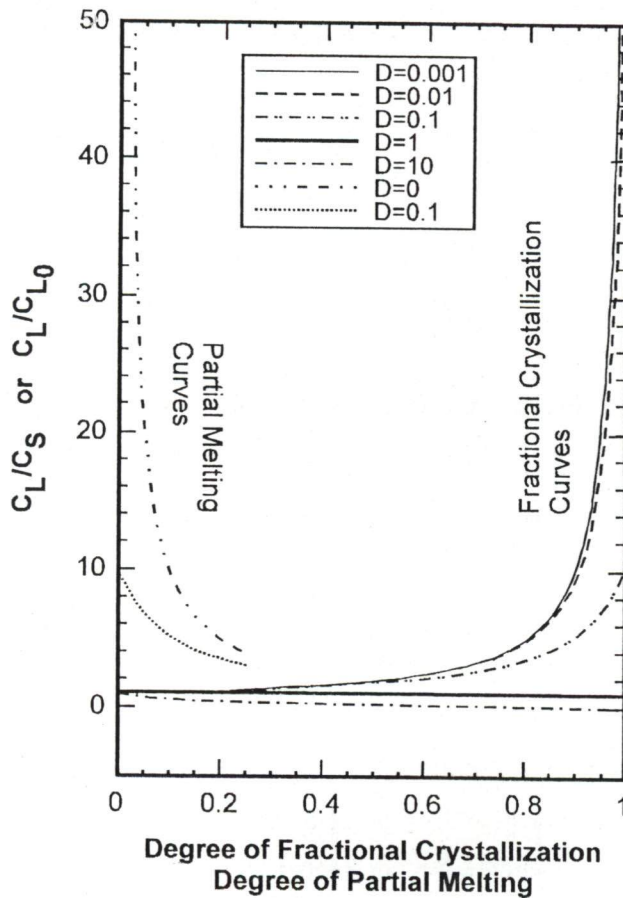
Fig. 5.1 Concentration variation of trace elements with differing bulk partition coefficients (D values) during partial melting and fractional crystallization. Concentrations are shown relative to the source region for partial melting and relative to the initial melt for fractional crystallization.

In summary, the values of bulk distribution coefficient, D may change during the course of differentiation, due to change in the crystallizing phase assemblage, magma composition and temperature.

5.2 QUARTZ MONZODIORITES

Quartz monzodiorites have relatively high SiO_2, Sr, Ba, alkali elements as well as LREE contents amongst the granitoid rocks of the study area. Their major element chemistry is quite comparable to that of intermediate rocks such as sanukitoids of Archean Superior Province (Stern at al., 1991) and high magnesian andesites of Aleutian arc

(Takahasi and Scarfe, 1985). As compared to the sanukitoids, these rocks have higher SiO_2 and lower MgO, CaO, Ba, Sr Ni and Cr content. This may indicate that their parental magmas are more evolved.

5.2.1 Fractional Crystallization

Fractional crystallization is one of the important mechanisms by which intermediate magmas could be produced from basic magmas on fractionation of mainly ferro-magnesian minerals. Quartz monzodiorites outcrop close to Hutti schist belt which consists of predominantly tholeiitic amphibolites. Therefore, magmas representing these quartz monzodiorites might have been derived by fractional crystallization of magmas similar to the tholeiitic amphibolites. This hypothesis is tested by considering one of the most common amphibolites (GH-10) of the Hutti schist belt as the parent magma. The SiO_2 content of quartz monzodiorites of the study area is of the order of 62 wt.%, whereas, the tholeiitic parent contains 48 wt.% SiO_2. To attain SiO_2 from 48 wt.% to 62 wt.% a high extent of fractional crystallization of silica undersaturated phases such as olivine, hornblende, biotite etc. is required.

Magma of andesitic to trachyandesitic composition can be derived by fractional crystallization of ferro-mangesian minerals and plagioclase from tholeiitic parent in both wet and dry conditions (Arth et al., 1978; Wilson et al., 1995). If olivine is considered as the only fractionally crystallizing phase then it will increase the silica content of the melt but simultaneously it will also decrease the MgO content. As a consequence there will be a decrease in Mg# (Mg/Mg+Fe cation mole%) in the residual magma. However, Mg# of quartz monzodiorites are 0.6 and 0.65 which are very much similar to the tholeiitic amphibolite parent. Hence, fractional crystallization of olivine, hornblende or biotite, or a combination of these minerals from tholeiitic magma cannot give rise to magmas similar in composition to quartz monzodiorites.

Assuming the tholeiitic amphibolite (GH-10) from the Hutti schist belt as the parent magma, and using Raleigh's fractional crystallization equation $C_l/C_0 = F^{(D-1)}$, the liquid composition is calculated for 5 to 70% fractional crystallization of clinopyroxene. It is observed that the residual melt by high degrees (up to 70%) of clinopyroxene fractionation leads to significant change in REE concentration as well as chondrite normalized REE pattern (Fig. 5.2a). The abundance of REE increase as the fractionation proceeds up to 30%

and then the abundance of HREE decrease in the residual melt with further extents of fractional crystallization. This is because of change in D values as the magma composition changes from basaltic to andesitic. It suggests that the fractional crystallization of clinopyroxene cannot give rise to required REE concentration of quartz monzodiorites.

Fractional crystallization of hornblende and plagioclase from a wet basic magma can give rise to melts of tonalitic composition (Arth et al., 1978; Kramers, 1988; Wilson, 1989). Fractional crystallization of hornblende increases the REE concentration in the residual melt and gives rise to chondrite normalized REE patterns that are parallel to that of the tholeiitic parent magma (Fig. 5.2b). Therefore, hornblende fractionation or fractional crystallization of hornblende and clinopyroxene in any proportion cannot give rise to the REE abundance of quartz monzodiorite.

5 to 70% fractional crystallization of plagioclase and hornblende in 6:4 ratio from a tholeiitic magma leads to an overall increase in REE concentration. The calculated chondrite normalized REE patterns for the residual magmas formed by different extents of fractional crystalliztion are different from that of quartz monzodiorites (Fig. 5.2c). Thus, the fractional crystallization of plagioclase and hornblende from a tholeiitic magma cannot give rise to melt having REE concentration similar to that of quartz monzodiorites.

If clinopyroxene and plagioclase in different proportions are considered as the dominating crystallizing phases then there is a decrease of SiO_2 content of the residual melt as the fractionally crystallizing phases contain higher amount of SiO_2 than that of the tholeiitic parent. Furthermore, if plagioclase is one of the fractional crystallizing phases then there will be depletion of Sr content in the melt. The average Sr content in the quartz monzodiorites is 550 ppm, whereas, in the tholeiitic parent the Sr content is of the order of 250 ppm. As the plagioclase fractionation further lowers the Sr content of the melt the fractionation of plagioclase from the melt cannot be a plausible mechanism.

The above arguments imply that fractional crystallization of possible liquidus minerals from a parent magma similar in composition to that of tholeiitic amphibolites of the Hutti schist belt cannot give rise to intermediate residual magma similar in composition to that of quartz monzodiorite.
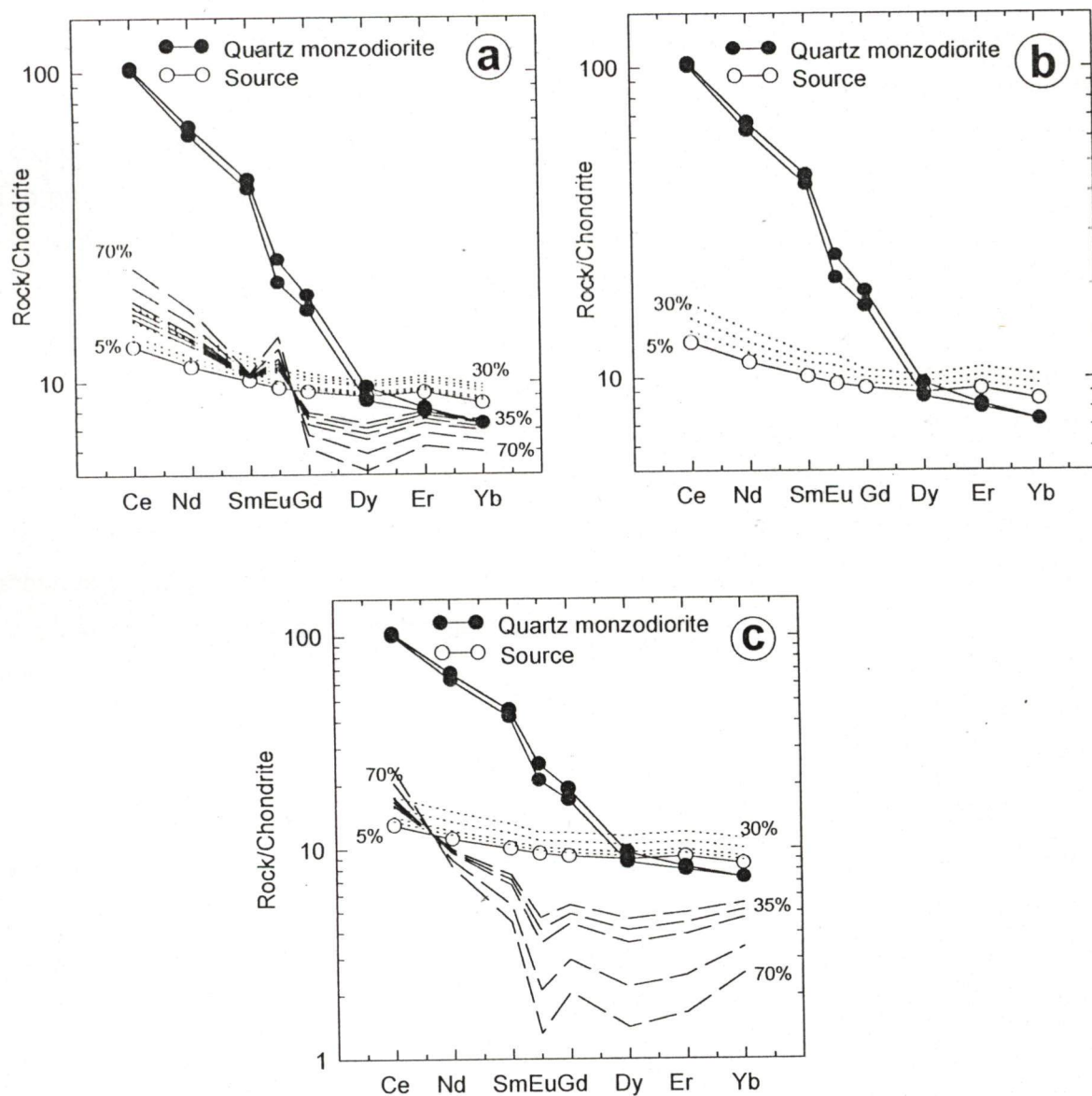
Fig. 5.2 Calculated chondrite normalized REE patterns for fractional crystallization from a tholeiitic source, GH-10 (dotted lines represent 5 to 30% and dashed lines represent 35 to 70% fractional crystallization). a) For 5 to 70% fractional crystallization of clinopyroxene. b) For 5 to 30% fractional crystallization of hornblende. c) For 5 to 70% fractional crystallization of plagioclase and hornblende in 60:40 ratio. Note that the chondrite normalized REE patterns of quartz monzodiorites are quite different from that of the calculated patterns.

5.2.2 Partial Melting

Experimental studies by Condie (1986), Martin, (1987) Rapp et al. (1991), Rapp and Watson (1995) show that low degree of partial melting of basalt can give rise to intermediate to high silica felsic melts. The composition of the melt is a function of original source rock composition, extent of melting and residual phases. The residual mineralogy during or after the melting depends upon the temperature, pressure, volatile content and the bulk composition of the source. For example, garnet is stable in dehydration melting condition at high pressure (1.6-2.2 GPa) but it is unstable at even 0.7 Gpa in hydrous condition of melting. Amphibole is the dominant residual phase during low degrees of partial melting of basalts in hydrous conditions. Low pressure (0.1-0.7 GPa) melting (both hydrous and anhydrous) experiment of basalt by Beard and Lofgren (1991) show that plagioclase is unstable during hydrous melting condition and it's break down causes an increase in Al_2O_3, CaO and decrease in FeO, MgO, TiO_2 and K_2O in the melt. However, during dehydration melting plagioclase becomes stable and amphibole becomes unstable. There is linear relationship between thermal stability of amphibole and P_{H2O}, whereas, pyroxene becomes unstable under high P_{H2O} condition (Spear, 1981; Gilbert et al., 1982; Beard and Lofgrren, 1991).

Rapp et al. (1991) and Rapp and Watson (1995) had carried out experiments on partial melting (10-40%) of mafic source over a pressure range of 0.8-3.2 GPa under vapour absent (i.e. $P_{fluid} < P_{total}$) condition. At 0.8 GPa and $T < 1000^0C$, the residual mineralogy is dominated by amphibole + plagioclase with minor orthopyroxene ± quartz ± Fe-oxide ± biotite, and above 1050^0-1075^0 C amphibole gets dissolved giving rise to basaltic andesite and the residue consists of plagioclase + clinopyroxene ± olivine ± orthopyroxene. At 1.6 GPa and 1000^0 C temperature, a tonalite-trondjhemite melt forms in equilibrium with residue consisting of garnet ± clinopyroxene ± plagioclase ± amphibole ± orthopyroxene ± Fe-oxides. However, at 2.2 and 3.2 GPa melt of similar composition coexists with garnet + clinopyroxene ± rutile residue.

Arth (1972), Rudnick and Taylor (1986), Rapp et al. (1991) and Rapp and Watson (1995) suggest that partial melting of tholeiitic basalt can give rise to tonalite-trondhjemite melts leaving granulite or eclogite residue. Quartz monzodiorites occurring to the west of the Hutti schist belt are associated with tholeiitic rocks. Therefore, it is possible that partial melting of these tholeiitic rocks gives rise to quartz monzodiorite-granodiorite rock suite. An

attempt is made to model the trace element and REE abundance in melts formed by partial melting of tholeiites and compared it with the quartz monzodiorites.

Experimental studies under a variety of P, T, and X_{H2O} conditions suggest that 25 to 50% melting of basalts is required in order to attain relatively high ferro-magnesian elements and silica abundance in the melt (Green and Ringwood, 1968, 1970; Holloway and Burnham, 1972; Helz, 1976; Stern and Wyllie, 1978; Gill, 1981). Average Sr and Ba content of the basalt would be 100 ppm and 125 ppm, respectively, whereas, quartz monzodiorites contain 500 ppm Sr and 1000 ppm Ba. To obtain these levels of Sr and Ba in a melt of average basalt source the degree of melting should be less than 15% (Stern et. al., 1989). Furthermore, if plagioclase is present in the residue, significant enrichment of Sr is not possible. The average Ni and Cr content of a basalt are in the range of 150 ppm and 250 ppm, respectively. Using Nielsen's (1985, 1988) modeling calculations, Stern et al. (1989) show that liquid after 40% fractional crystallization of average basalt has 54 wt.% SiO_2 but only 5 ppm Ni and 14 ppm Cr. In contrast, the quartz monzodiorites in the Hutti schist belt contain 65 ppm Ni and 140 ppm Cr. Since partial melting or fractional crystallization of basalt will leave phases like amphibole, pyroxene or garnet, the bulk distribution coefficient (D) for Ni and Cr will be much greater than 1. Therefore, partial melting of a basaltic parent cannot generate the magmas of quartz monzodiorite of Hutti area.

For modeling the REE abundance in the melts, an amphibolite of the Hutti schist belt (GH-10) is considered as the source and the partial melting of this source leaving amphibolite residue (plagioclase and hornblende in equal proportion) is considered. The calculated chondrite normalized REE patterns on 10% and 30% partial melting show Ce enrichment only and a depletion of Nd to Yb giving rise to concave upward chondrite normalized REE patterns for the melts (Fig. 5.3a). Figure. 5.3a shows that as the melting increases the REE concentration in the melt further decreases. However, the chondrite normalized REE patterns of the melt do not match with that of quartz monzodiorite. Melts formed by 10 to 30% partial melting of this tholeiitic parent leaving amphibolite residue has a lower REE abundance than that of quartz monzodiorite. The REE concentration in quartz monzodiorites is so high that it cannot be achieved by even very low extents of partial melting of the tholeiitic parent similar in composition to that of Hutti amphibolite (GH-10).

A similar modeling exercise is carried out leaving granulite as residue (plagioclase:orthopyroxene:clinopyroxene:olivine:garnet in the ratio of 30:33:20:10:7,

respectively). The REE abundance in melts formed on 5 to 30% partial melting of the tholeiitic parent leaving the granulite mineral assemblage as residue are calculated. It reveals that the chondrite normalized REE patterns of the melt are sub-parallel to that of the quartz monzodiorites (Fig. 5.3b). The REE abundance in the melts formed by partial melting of the tholeiitic source are, however, much lower than the REE abundance in the quartz monzodiorites.

The high MgO content as well as high Mg# of quartz monzodiorites suggest that they could have been derived by partial melting of a source similar in composition to that of a primitive mantle. On the basis of experimental studies several workers (Mysen and Boettcher, 1975; Green, 1976; Wyllie, 1977; Mysen, 1979, 1982; Kuroda et al., 1978; Green, 1980; Takahasi and Khushiro, 1983) suggest that partial melting of peridotite between 1.0-2.0 Gpa pressure can give rise to magmas with intermediate SiO_2 content.

To test this hypothesis, a primitive mantle having Ce = 1.75 ppm and Yb = 0.49 ppm (Sun and McDough, 1989) with chondrite normalized flat REE pattern is considered as a source. Since garnet is stable only at pressure greater than 2.0 GPa (Olafasson and Eggler, 1983), it is not considered as an important residual mineral. REE abundance in the residual melts are calculated on 0.1 to 5% partial melting of this primitive mantle leaving 55% olivine + 25% orthopyroxene + 20% clinopyroxene as residue and the chondrite normalized REE pattern of these melts are plotted (Fig. 5.3c). Despite the fact that the chondrite normalized REE patterns of these melts are sub-parallel to that of quartz monzodiorites (except for LREEs) the REE abundance in the calculated melts are much lower than the REE abundance in the quartz monzodiorites. Furthermore, the modeled melt contains very low abundance of trace elements such as Ba (203 ppm), Sr (183 ppm) and Zr (62 ppm) as compared to that in the quartz monzodiorites even at a very low percent (0.2%) of melting of the primitive mantle source. Therefore, even low extents of melting of primitive mantle cannot give rise to magma similar in composition to that of the quartz monzodiorites.

Thus, quartz monzodiorites of Hutti schist belt can neither be derived by partial melting of tholeiitic basalt, nor by fractional crystallization of the basalt with or without assimilation. Even low extents of partial melting of primitive mantle cannot explain the REE enrichment of the quartz monzodiorite melt. The parents for quartz monzodiorite must have had higher MgO contents than the Archean tholeiitic basalt. They might have been derived from a mixture of peridotite and tholeiitic parent. Incompatible trace element including LILEs

and REEs might have been enriched in the source by processes like fluid metasomatism prior to melting (Gastil, 1982; Tatsumi et al., 1986; Drumand and Defant, 1990).
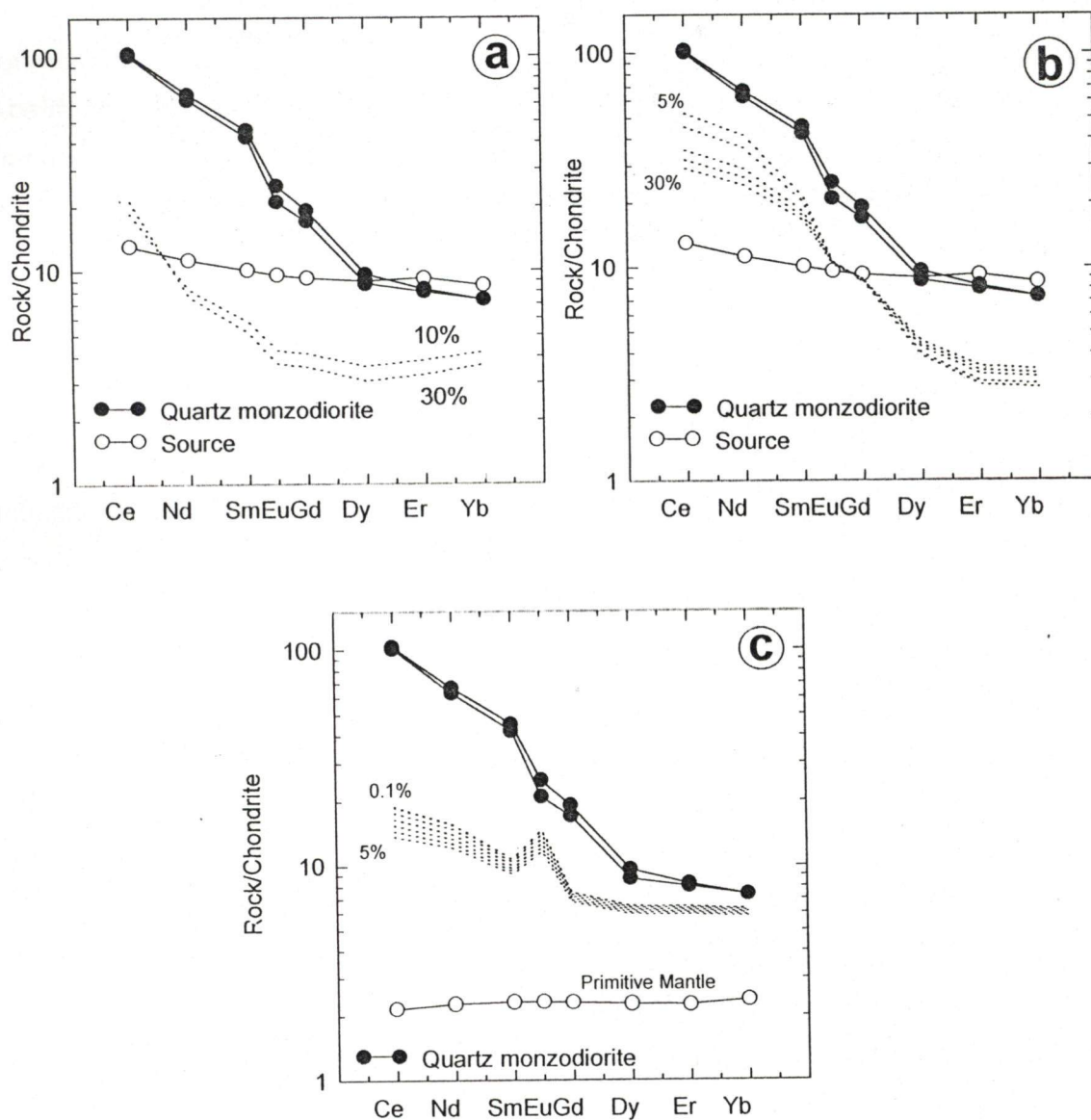
Fig. 5.3 Calculated chondrite normalized REE patterns for partial melting of a tholeiitic source, GH-10 and primitive mantle (dotted lines represent the chondrite normalized REE patterns of the melts). a) For 10% and 30% partial melting of the tholeiitic source leaving equal proportion of plagioclase and hornblende in the residue. b) For 5 to 30% partial melting of the tholeiitic source leaving a granulite residue (plagioclase:orthopyroxene:clinopyroxene:olivine:garnet = 30:33:20:10:7). c) For 0.1 to 5% partial melting of a primitive mantle leaving olivine, orthopyroxene and clinopyroxene in 55:25:20 ratio. Note that the REE abundance in quartz monzodiorite are much higher than that in the calculated melts.

5.2.3 Mixing Model

Yogodzinski et al. (1995) suggest a mixing model for origin of high magnesian andesite. They suggest that andesite magma can be produced by fractional crystallization of silica undersaturated phases such as olivine, clinopyroxene in appropriate proportion from a mixture of slab melts and basaltic magma. Quartz monzodiorites are silica saturated and contain high amount of Fe, Mg and Ba but low amount of Sr than that of magnesian andesite. Their REE abundance are comparable to that of ADAK type (Yogodzinski et al., 1995) though the latter is having more fractionated chondrite normalized REE pattern.

[Mg]-[Fe] Modeling

Based on olivine saturation concept of Roeder and Emsile (1971), Hanson and Langmuir (1978) proposed [Mg]-[Fe] melt field in which olivine is in equilibrium with the melt. The MgO and FeO contents of the melt can be determined from equilibrium distribution coefficient of MgO and FeO between olivine and melt by considering that olivine is in equilibrium with the melt. The equilibrium distribution coefficient depends on pressure, temperature, oxygen fugacity and composition of the melt. Rajamani et al. (1985) have modified the "melt-field" by applying correction for pressure and composition, and discussed the usefulness of this diagram in assessing the processes and physical condition of magma generation.

The compositionally corrected cation mole% of MgO and FeO at 1.5 Gpa pressure are plotted in figure 5.4a & b assuming garnet-lherzolite (PHN-1611) of Takahashi and Scarfe (1985) and komatiite (18-15) of Rajamani et al. (1985), as the sources, respectively, from which parent liquid of Hutti tholeiites were derived. Rajamani et al. (1989) have shown that as the pressure and solidus temperature increases the [Mg]-[Fe] field contracts. Quartz monzodiorites plot more close to the melt field than most of the tholeiitic amphibolites of Hutti schist belt, because quartz monzodiorites have higher [Mg]/[Fe]% values than the tholeiites. Therefore, fractional crystallization or partial melting of these tholeiites cannot give rise to quartz monzodiorites.

The Mg# for quartz monzodiorites ranges between 0.6 to 0.65 and falls close to one of the relatively more primitive Hutti tholeiites (GH-10) in [Mg]-[Fe] diagram. In general, quartz monzodiorites have higher Mg# than that of common Hutti tholeiites. Fractional

crystallization of olivine and clinopyroxene will reduce the MgO content and increase the FeO content in the residual melt.
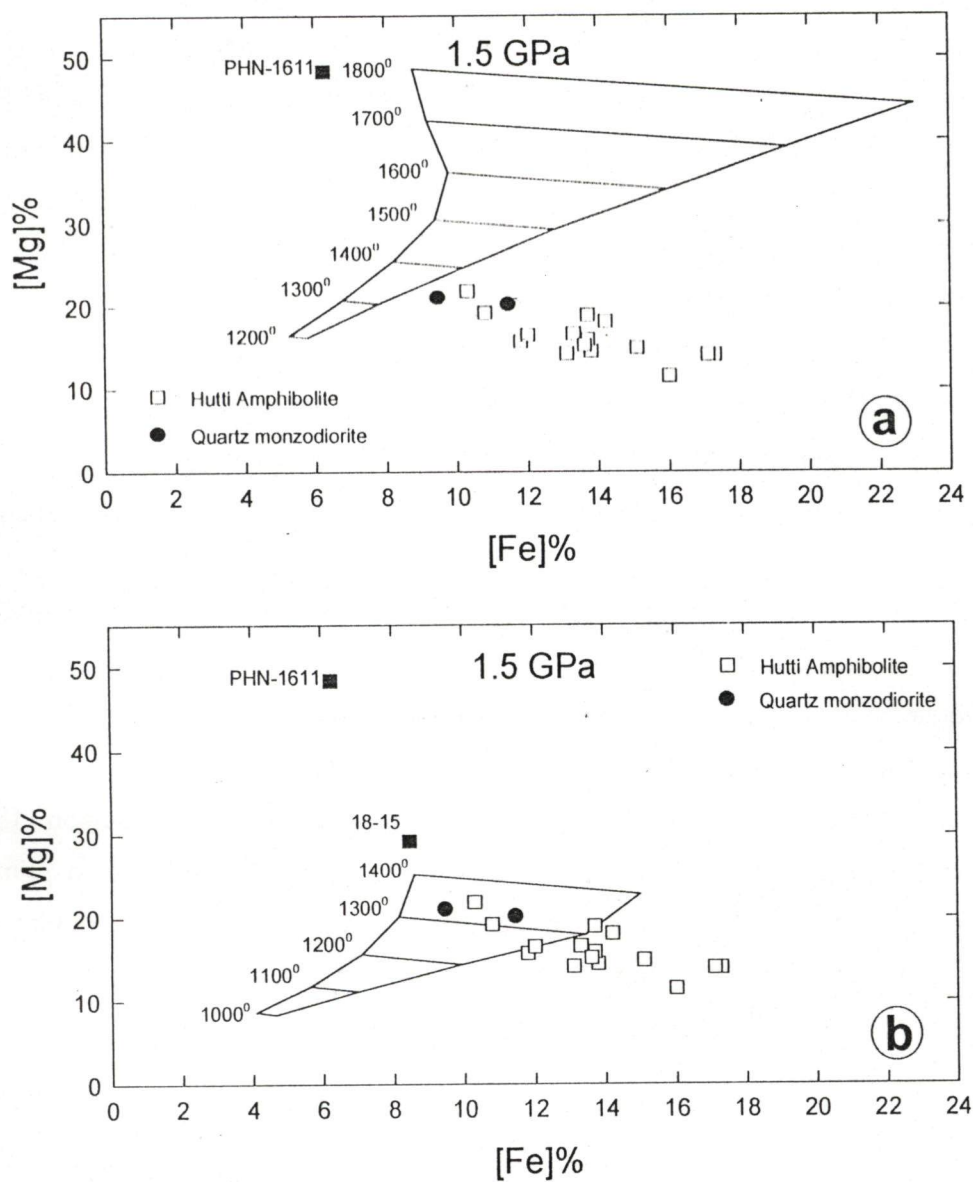
Fig. 5.4 [Mg]-[Fe] systematic for quartz monzodiorites and amphibolites of the study area. [Mg]-[Fe] values are in cation mole%, which is calculated using the Ford et al. (1983) equation. The calculated melt field is for 1.5 Gpa pressure. a) From a garnet-lherzolite source, PHN-1611 (Takahasi and Scarfe, 1985). b) From a komatiite source, 18-15 (Rajamani et al., 1985). PHN-1611 is also plotted for comparison. Quartz monzodiorites plot inside the melt field. See text for detail.

The magma representing quartz monzodiorites could not have been generated by partial melting of mantle sources similar in composition to that of garnet-lherzolite as they plot outside the "melt field". The source for quartz monzodiorite magma must have been enriched in Fe relative to the PHN-1611. It is possible that the sources for the quartz monzodiorites as well as tholeiites could have had similar major element composition. From the figure 5.4, it may be inferred that the Fe/Mg ratio of the source must be lying between the garnet-lherzolite (PHN-1611) and tholeiites. A sample of komatiitic amphibolites (18-15 from Rajamani et al., 1985) from Kolar schist belt has Fe and Mg cation mole% values lying between the garnet-lherzolite and tholeiites. This sample is assumed as a potential source and the melt field is calculated. The quartz monzodiorite samples plot well within the "melt-field". Thus, quartz monzodiorite magma could have been generated by partial melting of mixed sources formed by mixing of komatiites and garnet-lherzolite. The source for quartz monzodiorite, however, must have been enriched in incompatible trace elements including LREE prior to melting.

To know the trace element (including REEs) abundance of the possible source/sources for quartz monzodiorites, inverse modeling is attempted. One of the two quartz monzodiorite samples (QMD-1) that has higher Mg# is considered as the product and the abundance of trace elements as well as REEs are calculated at different extents of melting under suitable experimental P-T conditions as outlined by Rapp and Watson (1995). It is observed that the assumed sources show enrichment of LREEs relative to primitive mantle and parallel chondrite normalized REE pattern to that of quartz monzodiorite (Fig. 5.5). The possible source would have had 55-103 ppm Ba and 36-64 ppm Sr, assuming that quartz monzodiorites were formed by 5 to 10% partial melting (Table. 5.1).

5.3 GRANODIORITES

The granodiorites around the Hutti schist belt show large variation in the major, trace and REE chemistry. The granodiorites occurring to east of the belt designated as Kavital granodiorite by Srikantia (1995) have higher MgO, FeO, TiO$_2$, Ni, Cr content and higher Mg# as compared to the granodiorites occurring to the west of the belt. The Northern granodiorites are similar to eastern Kavital granodiorites in their major and trace element chemistry but they have distinct chondrite normalized REE patterns.

The granodiorite samples plotted in Harker variation diagram show that there is systematic variation between TiO$_2$, FeO, MgO, CaO against SiO$_2$ but no correlation exists
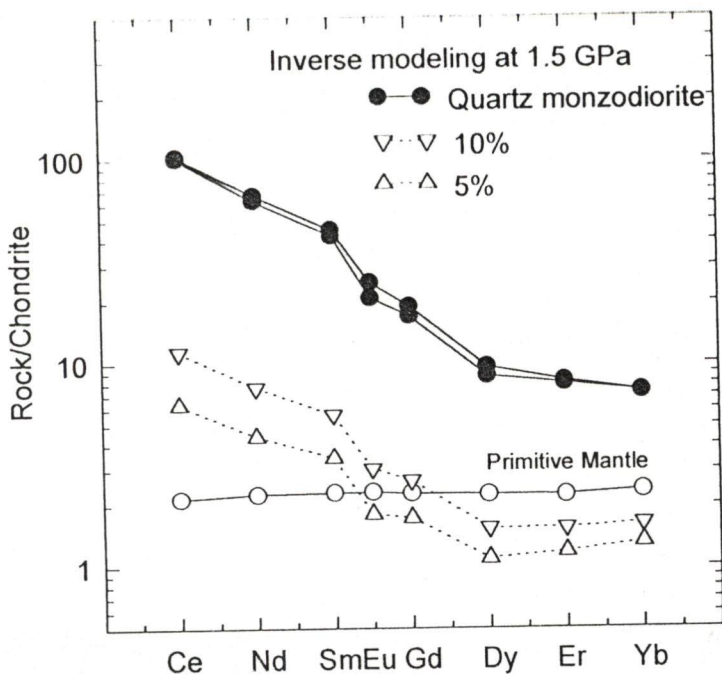
Fig. 5.5 Inverse modeling of the sources for quartz monzodiorite assuming that its magmas are derived by 5% and 10% partial melting of shallow mantle sources leaving 40% olivine, 30% spinel and 30% orthopyroxene in the residue. REE pattern of primitive mantle is also shown for comparison. The assumed sources have higher LREE and lower HREE abundance than that in the primitive mantle.

	PM	S-1	S-2	QMD-1
Ce	1.755	5.138	9.289	84
Nd	1.354	2.629	4.591	39.9
Sm	0.444	0.66	1.083	8.7
Eu	0.168	0.13	0.219	1.81
Gd	0.596	0.449	0.686	4.96
Dy	0.737	0.355	0.501	3.12
Er	0.48	0.251	0.33	1.75
Yb	0.493	0.273	0.339	1.52
Ba	21.1	36.215	63.888	968
Sr	6.989	55.628	103.648	562

Table 5.1 Calculated incompatible trace elements and REE abundance in the assumed sources for quartz monzodiorite. PM=primitive mantle, S=assumed source, QMD-1=quartz monzodiorite.

74

between Na_2O, K_2O against SiO_2 (Fig. 5.6). In the Harker variation diagram, the granodiorites from different parts of the Hutti schist belt show similar variation but they differ in REE chemistry. For this reason, the granodiorites occurring to east, west and north of the belt have been treated separately.

5.3.1 Western Granodiorites

Granodiorites occurring to west of the Hutti schist belt are closely associated with the amphibolites. It is necessary, therefore, to test the possibility of evolution of these granodiorites by fractional crystallization or partial melting of the Hutti amphibolite. The Western granodiorites do not show any systematic variation between Ni and Cr with respect to MgO content (Fig. 5.6). Assimilation of upper crustal rocks cannot change the Ni and Cr concentration of the Western granodiorites as the Ni and Cr contents in these granodiorites are more or less same as that in the upper crustal rocks. From the chemical data, it seems that fractional crystallization of silica undersaturated phases such as olivine and hornblende/pyroxene can increase the SiO_2 content of the residual melt. In general, Sr content of granodiorites is high as compared to amphibolites, and they have LREE enriched fractionated chondrite normalized REE patterns with slight or no Eu anomaly. Plagioclase fractionation is not plausible because it depletes Sr as well as it gives rise to negative Eu anomaly in the residual melts.

5.3.1.1 Partial Melting

Partial melting of the amphibolite of the Hutti schist belt can give rise to melts similar in composition to Western granodiorites. To test this hypothesis, a common Hutti tholeiite (GH-10) is assumed as a possible source. Trace elements as well as REEs abundance of the melts formed by 5 to 30% partial melting of this source leaving amphibolite residue (plagioclase:hornblende = 40:60) are calculated. The chondrite normalized REE patterns of the melts are concave upward (Fig. 5.7a), and their REE abundance are lower than that of the granodiorites.

A similar exercise of partial melting of the same tholeiitic source leaving eclogite residue is considered. The residual assemblage consists of 55% clinopyroxene, 35% plagioclase and 10% garnet. Low degree partial melting (5 to 20%) of this tholeiitic source gives rise to a fractionated chondrite normalized REE patterns that are parallel to that of the
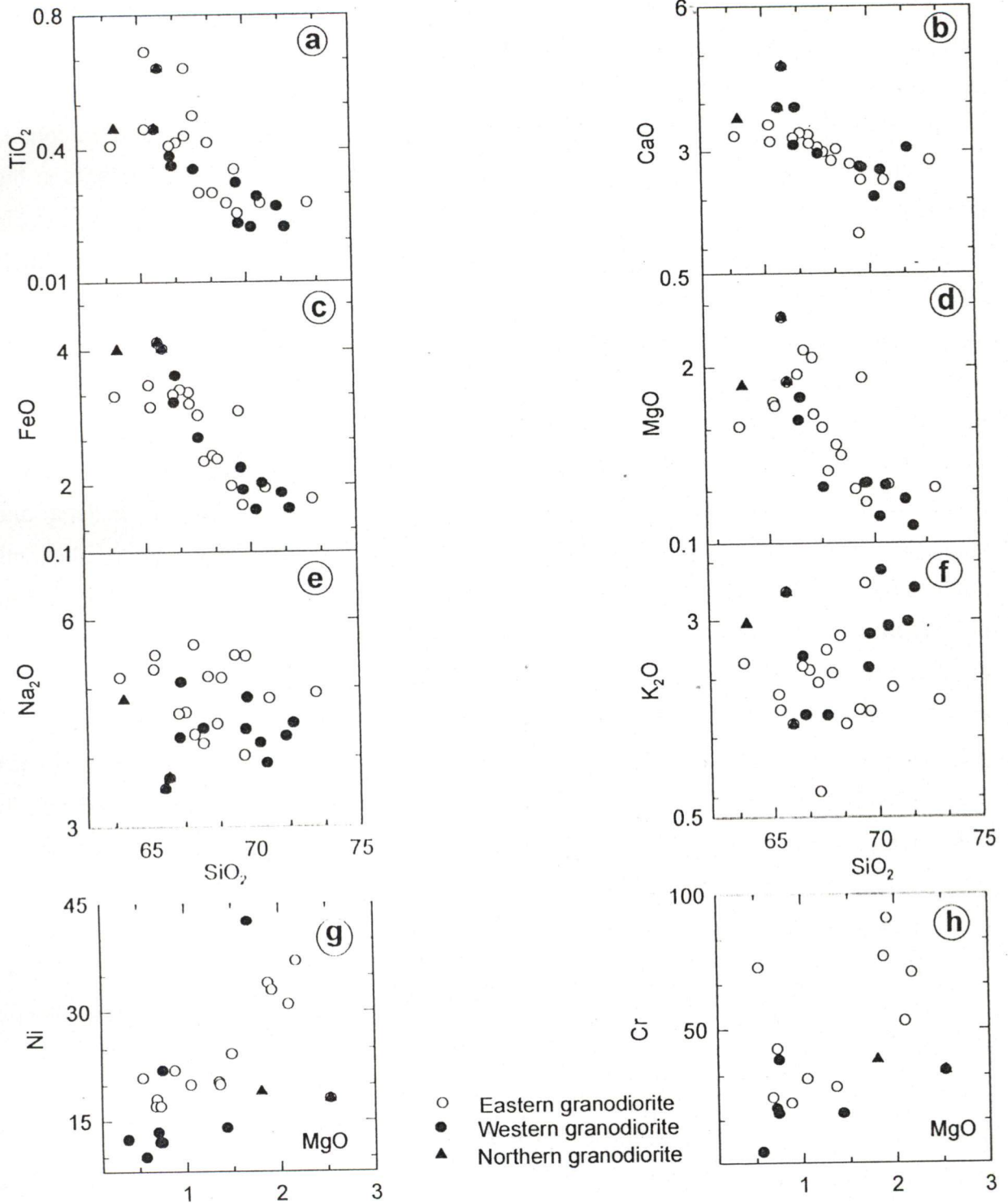
Fig. 5.6 Harker's variation diagrams showing the behaviour of different major element oxides with SiO_2 (a to f). Variation diagrams showing the behaviour of Ni and Cr with MgO (g & h).

granodiorites (Fig. 5.7b). However, the abundance of the REEs in the calculated melts are much lower than those in the granodiorites. Furthermore, as the melting proceeds there is a decrease in Sr and Ba contents in the generated melts. If 5% partial melting of tholeiitic source leaving an amphibolite residue is considered, the melt would have Sr and Ba content of the order of 101 ppm and 323 ppm, respectively, whereas, Sr and Ba contents in the granodiorites are of the order of 600 ppm and 1000 ppm, respectively. Alternatively, if 5% partial melting of the same source is considered leaving eclogite residue, the melts would have Sr and Ba content 151 and 576 ppm, respectively which are very low as compared to the granodiorites. Therefore, partial melting of tholeiitic parent leaving amphibolite or eclogite residue cannot give rise to magmas that will have Ba, Sr and REE abundance similar to that of the granodiorites of the Hutti schist belt.

Granitic magma equilibrates with many minor and trace minerals such as, sphene, zircon, allanite, apatite, rutile in addition to major constituent minerals like alkali feldspar and plagioclase feldspars, quartz, amphiboles, biotite. The significance of trace elements particularly the REE abundance in minor and trace minerals in petrogenetic modeling has been elaborated by Hanson (1980). Gromet and Silver (1983) have shown that more than 80 to 90% of the total REE abundance of the granodiorite are found in sphene (titanite) and allanite. Fractional crystallization as well as partial melting leaving sphene as one of the residual minerals significantly lowers the REE concentration in the residual magmas (Simmons and Hedge, 1978; Basir and Balakrishnan, 1999). Based on empirically determined sphene-melt K_d values for REEs Cocherie et al. (1994) show that sphene plays an important role during fractional crystallization in controlling the resultant REE pattern of the residual granitic melts.

Since, one of the granodiorite suites represented by sample GRD-21 is closely associated with quartz monzodiorite (of QMD-1 type), it can be possible that partial melting or fractional crystallization of quartz monzodiorite leaving sphene as one of the minor residual minerals gives rise to granodiorite magmas similar in composition to that of Western granodiorites. To test this hypothesis, trace element abundance are calculated assuming QMD-1 as source on 10 to 25% partial melting of this source. It is found that 10 to 25% partial melting of QMD-1 leaving 40% hornblende + 30% clinopyroxene + 29% plagioclase + 1% sphene gives rise to more fractionated chondrite normalized REE patterns as compared to the granodiorites (Fig. 5.7c). However, one of the granodiorite samples (GRD-4) from
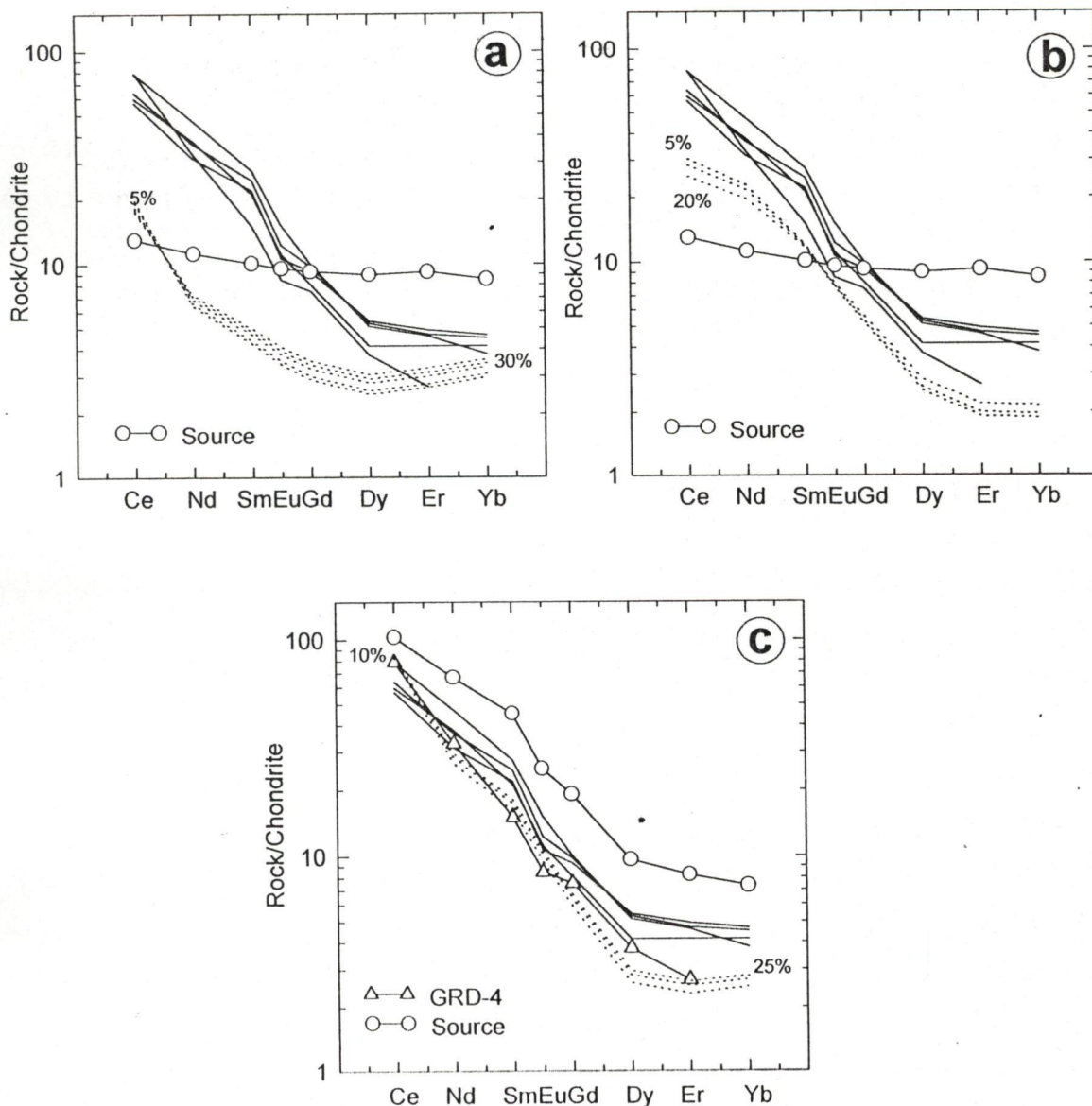
Fig. 5.7 Calculated chondrite normalized REE patterns for melts derived by partial melting of a tholeiitic source and an intermediate source (dotted lines represent the REE patterns of the melts). a) For 5 to 30% partial melting of a tholeiitic source (GH-10), leaving an amphibolite residue (plagioclase:hornblende = 40:60). b) For 5 to 20% partial melting of a tholeiitic source (GH-10), leaving clinopyroxene, plagioclase and garnet in 55:35:10 ratio in the residue. c) For 10 to 25% partial melting of an intermediate source (QMD-1) leaving 29% plagioclase, 40% hornblende, 30% clinopyroxene and 1% sphene in the residue. Note that the chondrite normalized REE pattern of granodiorite, GRD-4 is similar to the modeled melts.

Gurgunta has a chondrite normalized REE pattern very similar to the modeled melts. Though this model can explain the Sr (568 ppm on 10% partial melting) abundance of the granodiorites but the calculated melts have much higher Ba abundance (3948-2609 ppm on 10 to 25% partial melting) than what is observed in the granodiorites (500-1000 ppm). Therefore, the Western granodiorites of the Hutti schist belt cannot be derived by partial melting of quartz monzodiorite.

5.3.1.2 Fractional Crystallization

Fractional crystallization is considered to be one of the most important processes in the evolution of melts, and it can be constrained by geochemical modeling using simple thermodynamic calculations. As mentioned earlier, quartz monzodiorite and granodiorite occurring side by side in the Lingusugur area inspite of the lack of distinct field evidence to suggest their relative age relationship. Modal mineralogy of these two rock suites shows that the percentage of ferro-magensian minerals is lower in the granodiorite suite. Their major, trace as well as REE chemistry suggest that fractional crystallization of quartz monzodiorite can be a plausible mechanism by which these two rock types can be related. Further, there is a decrease in TiO_2 and an increase in SiO_2 in granodiorite as compared to that of quartz monzodiorite, which is very much expected when hornblende and biotite constitute the fractionation phase. It is most likely that clinopyroxene, hornblende, biotite, plagioclase and sphene would constitute the fractionation assemblage. To test this possibility trace element and REE modeling is carried out.

Fractional crystallization of plagioclase, hornblende and biotite in equal proportion from the quartz monzodiorite parent magma is considered. The trace element abundance (Sr and Ba) are calculated for the residual melts formed on 5% fractional crystallization and are found in agreement with the Western granodiorite values. But the REE abundance in and chondrite normalized patterns of granodiorites do not agree with those calculated for the melts (Fig. 5.8a).

If hornblende and biotite are assumed as the secondary products, then fractionation of clinopyroxene may be considered as viable mechanism to generate granodiorite from quartz monzodiorite. Clinopyroxene fractionation can increase the SiO_2 content of the melt because it has lower SiO_2 than quartz monzodiorite and this possibility is tested. On 5 to 20% fractional crystallization of clinopyroxene the residual melts contain 576-626 ppm Sr

and 1012-1175 ppm Ba, which are well within the limit of granodiorites of the belt. Although the major and the trace element chemistry allow the fractionation of clinopyroxene from quartz monzodiorite, the chondrite normalized REE patterns do not support such a mechanism (Fig. 5.8b).

As mentioned earlier that accessory minerals such as sphene, monazite, allanite contain most of the REE in the granitiod rocks. Therefore, it is important to consider the effect of fractional crystallization of these minerals along with major minerals. It is in this context that sphene along with plagioclase, hornblende, biotite is considered as fractionating phase to give rise to granodiorite magmas on fractional crystallization from quartz monzodiorite parent. It is observed that on 5 to 15% fractional crystallization of these phases can explain the trace elements such as Ba and Sr content in the melts ranges between 1014 to1122 ppm and 574 to 601 ppm, respectively and these concentrations are in agreement with the Ba and Sr content in granodiorites. The REE abundance calculated for this case, and the chondrite normalized REE patterns are similar to those of Western granodiorites (Fig. 5.8c).

5.3.1.3 Liquid Immiscibility Model

Liquid immiscibility is one of the viable petrogenetic processes for the diversification of magma. Experimental studies have demonstrated that it can occur in two types of silicate melts:

1) In highly Fe-rich basaltic melts
2) In highly alkaline melts

Clearly two immiscibile liquids must initially co-exist as droplets of the minor phase suspended in the major phases. Thus, texturally immiscibility can be recognized by the presence of rounded globules of one phase in a matrix of other.

If mantle derived magmas do intersect fields of immiscibility during their differentiation, liquid immiscibility has the potential to generate significant volumes of oversaturated crustal materials directly from silica undersaturated to moderately oversaturated melts.

When a magma undergoes liquid immiscibility process, it splits into two parts, one enriched in mafic components and, other relatively depleted in mafic (Roedder, 1956; Ryerson and Hess, 1978; Hanson, 1980, 1981; Bender et al., 1982). Quartz monzodiorites
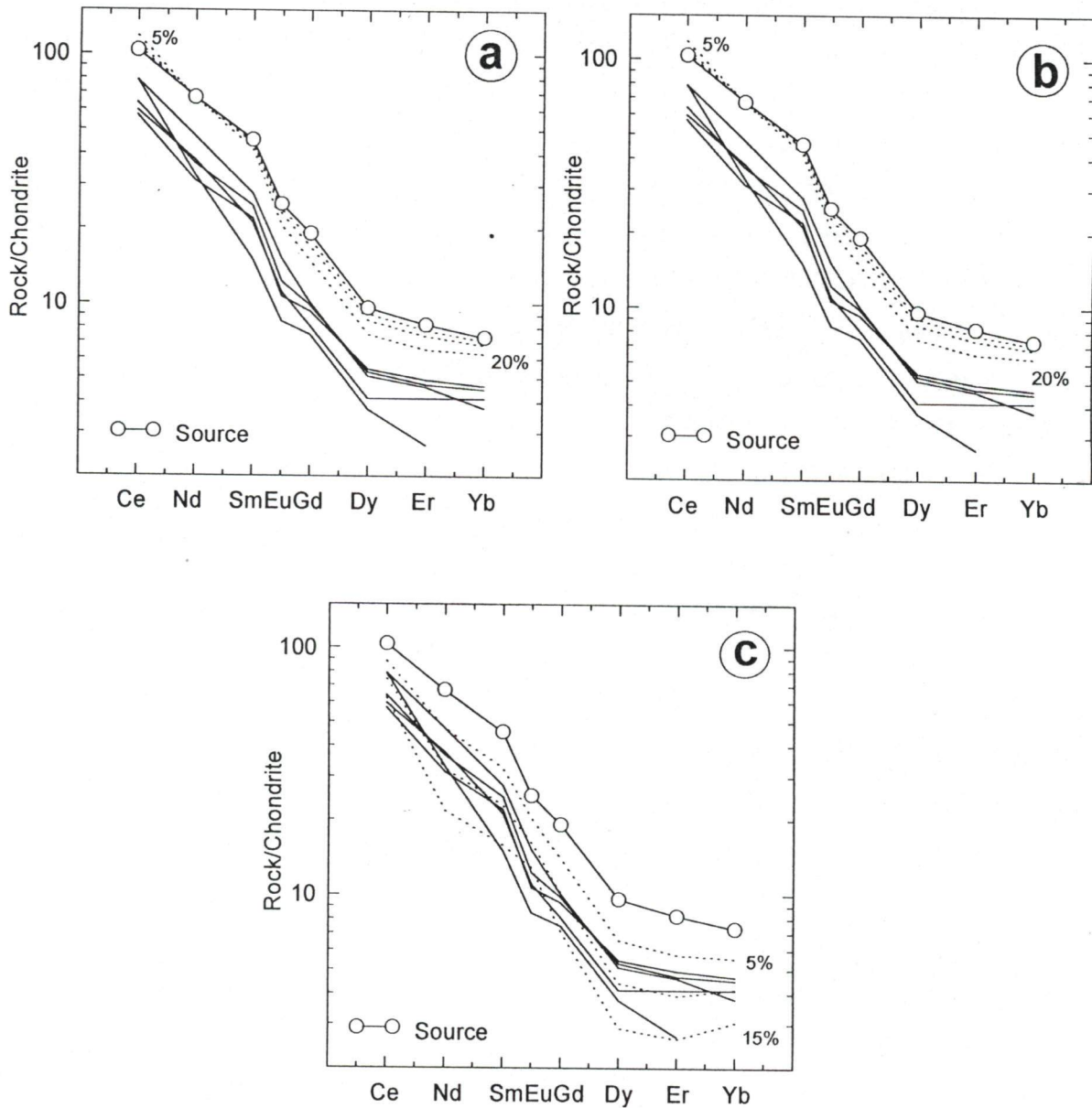
Fig. 5.8 Calculated chondrite normalized REE patterns for fractional crystallization of different minerals from an intermediate source, QMD-1 (dotted lines represent the REE patterns of fractionally crystallizing melts). a) for 5 to 20% fractional crystallization of plagioclase, hornblende and biotite in equal proportion. b) for 5 to 20% fractional crystallization of clinopyroxene. c) 5 to 15% fractional crystallization of 20% plagioclase, 40% hornblende and 5% sphene.

of Hutti schist belt are enriched in MgO, FeO, TiO$_2$, P$_2$O$_5$ and depleted in SiO$_2$ as compared to the Western granodiorites (Fig. 5.9). Therefore, it may be possible that these two rock types could have been formed by liquid immisibilty processes.

Experimental work by Roedder (1956) suggests that felsic magmas can be produced by liquid immiscibility processes. Though the field defined by quartz monzodiorites and Western granodiorites of Hutti schist belt (Fig. 5.9) does not coincide totally with that of two liquid field of Greig's (1927, after Philpots, 1994) they are close to each other. Most granodiorites have chondrite normalized REE patterns parallel to that of the quartz monzodiorites but with lower abundance. These observations only support the possibility of magma immiscibility for the origin of quartz monzodiorite and granodiorite but do not prove it alone.
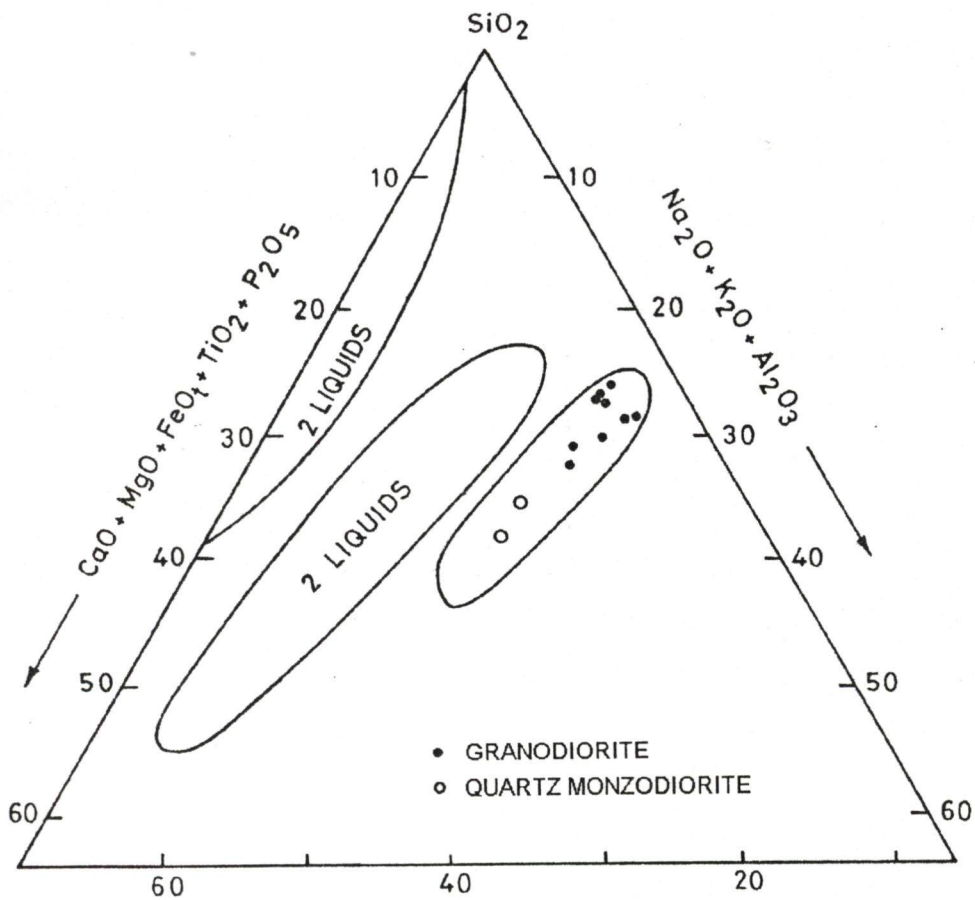
Fig. 5.9 Greig's (1927) pseudo-ternary phase diagram showing the experimentally determined two liquid fields. Quartz monzodiorite and Western granodiorite samples plot towards right of the two liquid fields. Granodiorites are more evolved than quartz monzodiorites.

Experimental studies show that the REE are strongly and nearly equally partitioned into the mafic melts and they have more concentration of P and Zr as compared to the coexisting felsic melts (Watson, 1976; Ryerson and Hess, 1978). K_d values for all the trivalent REE between mafic and felsic liquids are approximately 5 and therefore the felsic liquid, equally depleted in REEs, gives rise to sub-parallel to parallel REE pattern with the mafic components. The magnitude of depletion of REE in the felsic liquid depends on the relative proportion of mafic and felsic liquids that are separated from each other (Hanson, 1980). Based on the Sr abundance between immiscibile silicate melts Bender et al. (1982) show that Eu is less strongly partitioned into the mafic melt than the trivalent REEs and the felsic melts generated by the progressive separation of an immiscibile mafic melt has a larger positive Eu anomaly due to decrease in REE content. The lack of Eu anomalies may indicate that the variation in composition within the near liquid suite is the result of the separation of relatively small amounts of a basic immiscibile melts. There will not be a significant change in Sr concentration in the two liquids because the K_d values for Sr is about 1.5 as it lies between the mafic and felsic liquids (Hanson, 1981).

If liquid immiscibility has produced variation within near-liquid suite from the Lingusugur granitoids, then the samples with the greatest abundance of high field strength-elements will have the chemical characteristics closest to those of the parental liquid(s) bulk composition. The parental magmas are required to have similar Mg# and REE patterns with similar shape, and higher abundance than those of the near liquid composition.

From the above discussion, it may be inferred that most of the Western granodiorites can be derived by fractional crystallization of plagioclase, hornblende, biotite and sphene and/or liquid immisibility processes from magmas similar in composition to that of quartz monzodiorites.

5.3.2 Eastern Granodiorites

The granodiorites that occur to east and southeast of the belt are called Kavital granodiorites (Srikantia, 1995). They have ca. SiO_2 = 67 wt.%, TiO_2 = 0.4 wt.%, FeO = 3.2 wt.%, MgO = 1.5 wt.%, Na_2O = 4.5 wt.%, K_2O = 2.35 wt.%. These granodiorites have chondrite normalized REE patterns that are more LREE enriched and fractionated as compared to the other granodiorites of the belt. Their Mg# (0.4-0.48) is the highest amongst

all the granodiorites. The outcrops of Kavital granodiorites near Pamankallur, Hire Guda and Kavital represent more primitive magma characteristics.

It has been shown that partial melting or fractional crystallization of Hutti tholeiites leaving either amphibolite or granulite residue (plagioclase, clinopyroxene, hornblende, biotite etc. or a combination of these phases) cannot give rise to magmas represented by the Western granodiorites. The Kavital granodiorites have more LREE enriched and HREE depleted chondrite normalized REE patterns than that of the Western granodiorites and hence, their magmas cannot be generated by partial melting of Hutti tholeiitic rocks. Their magmas can also not be derived by partial melting of primitive mantle as they have relatively higher silica, alkalis, and lower Mg# than the quartz monzodiorites.

The Kavital granodiorites require a source that is silica enriched and has LREE enriched chondrite normalized REE pattern, and has a Mg# $\geq$ 0.60. As the intermediate rocks such as sanukitoids, high magnesian andesite and adakites fulfil these requirements they may be considered as possible sources for the Kavital granodiorites. The quartz monzodiorite (QMD-1) also has major and trace element chemistry similar to the above intermediate rocks. Hence, partial melting of quartz monzodiorite source is tested. It is observed that 5 to 40% partial melting of a source similar in composition to that of quartz monzodiorite (QMD-1) leaving 10% hornblende, 40% biotite, 48.5-49% plagioclase and 1.5-1% sphene, can give rise to magmas with chondrite normalized REE patterns similar to of Kavital granodiorites (Fig. 5.10a & b). The resultant melts have 447 ppm Sr and 475 ppm Ba that are comparable to that of the Kavital granodiorites, having ca.500 ppm and 600 ppm Sr and Ba, respectively.

The Kavital granodiorite occurring further south (near Bhagalvad village) has slightly lower REE abundance and negative Eu anomaly than that of more primitive granodiorites. The more evolved granodiorites are represented by samples GRD-26 and GRD-27. The magmas representing these samples could have been derived by fractional crystallization of more primitive granodiorite magma similar in composition to that of GRD-28. To test this hypothesis, 10 to 25% fractional crystallization of hornblende and biotite in 65:35 ratio from parent magma similar in composition to that of GRD-28 is considered. The resultant residual melt has REE abundance similar to that of GRD-26 and GRD-27 (Fig. 5.11).

Minor variation in the major and trace element chemistry may be expected in a large composite pluton such as the Kavital granodiorites. This is due to different extents of partial
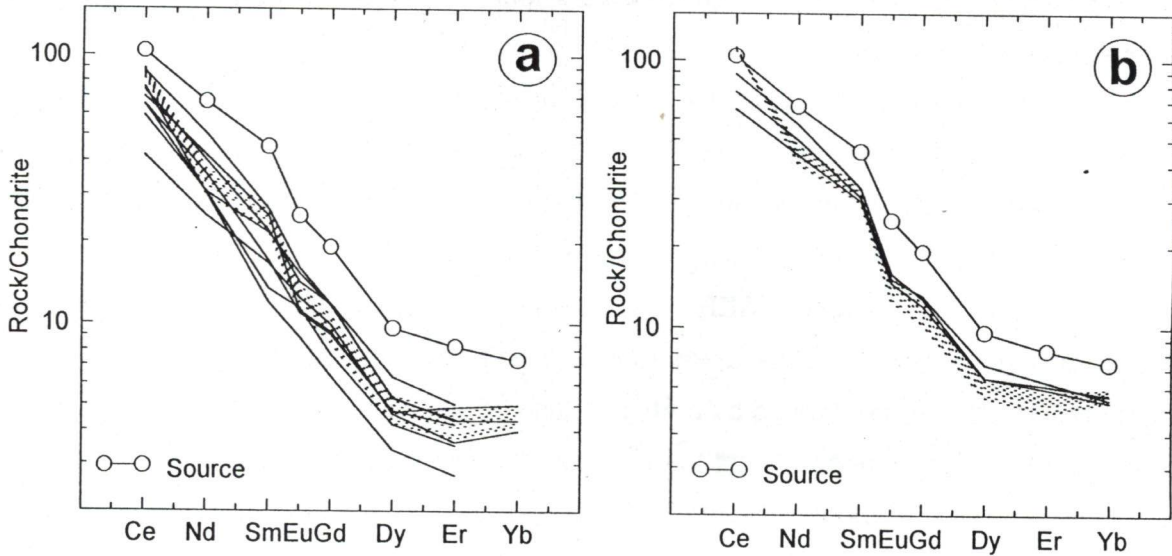
Fig. 5.10 Calculated chondrite normalized REE patterns of the melts derived by 5 to 40% partial melting of an intermediate source, QMD-1 (dotted lines represent REE patterns of the melts), leaving a residue of hornblende, biotite, plagioclase and sphene in a) 10:40:48.5:1.5 and b) 10:40:49:1 ratios.
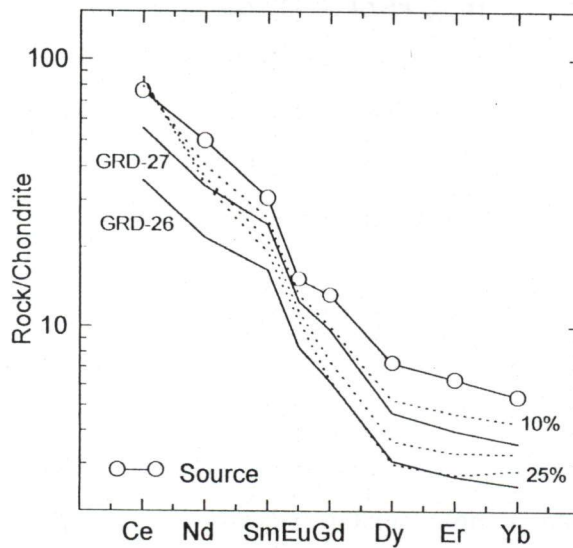
Fig. 5.11 Calculated chondrite normalized REE patterns for 10 to 25% fractional crystallization of hornblende and biotite in 65:35 ratio from a granodiorite source, GRD-28 (dotted lines represent REE patterns of the fractionally crystallizing melts).

melting of intermediate sources (such as adakites or high magnesian andesites) or small degrees of fractional crystallization.

It may be inferred from the above discussion that magmas representing granodiorites occurring to the east of the Hutti schist belt around Kavital and southeast of Kavital (near Bhagalvad village) are generated by partial melting of intermediate sources similar in composition to that of quartz monzodiorite. The formers (the granodiorites occurring near Kavital) are the products of partial melting of the quartz monzodiorite, whereas, the later are the more evolved phase derived by fractional crystallization of hornblende and biotite from a melt that is compositionally similar to Kavital granodiorites.

5.3.3 Northern Granodiorites

Amongst the granodiorites of the Hutti schist belt, the Northern granodiorites have distinct field, petrographic and geochemical characteristics from that of others. They have megacrysts of K-feldspars and often have enclaves of hornblende schist. These enclaves range in size from few centimetres to tens of metres. The Northern granodiorites occur as massive body occupying a large area to the north of the Hutti schist belt (Fig. 3.1). Their chondrite normalized REE patterns that are less fractionated with negative Eu anomaly quite distinct from the chondrite normalized REE patterns of Eastern and Western granodiorites (Fig. 4.8). Their relatively low Mg# (0.4-0.48), and high SiO_2 suggest that they cannot be derived by partial melting of primitive mantle sources.

5.3.3.1 Fractional Crystallization

Fractional crystallization of mafic magmas corresponding to the Hutti tholeiites may give rise to Northern granodiorites. In such a case, ferro-magnesian minerals like olivine, pyroxenes, hornblende along with plagioclase would be the probable fractionating phases for Hutti tholeiitic magmas. The SiO_2 content of Northern granodiorites is of the order of 64 and 68 wt.%. To account such a large proportion of SiO_2 from Hutti tholeiites (SiO_2 content < 50 wt.%), a large degree of fractional crystallization of ferro-magnesian phases is required. This will result in extreme lowering of Mg# which is not observed in the Northern granodiorites. Moreover, if plagioclase is one of the dominant phase during fractional crystallization there will be large depletion of Sr. Furthermore, fractional crystallization of plagioclase and clinopyroxene cannot increase the SiO_2 content in the residual magma as

these minerals have higher SiO_2 than the parent tholeiite magmas. If plagioclase and hornblende are the fractionally crystallizing phases from a parent similar in composition to that of the Hutti tholeiite (GH-10) then the residual melts will be enriched in REE relative to the tholeiitic parent up to 30% fractional crystallization and after that there is only Ce enrichment and large depletion of HREE (Fig. 5.12a). However, the Northern granodiorites have much higher REE abundance than that of calculated for residual melts formed by fractional crystallization of plagioclase and hornblende from mafic magmas like that of Hutti tholeiites. Therefore, fractional crystallization of tholeiitic magmas is not capable of producing a magma similar in composition to that of the Northern granodiorites.

Fractional crystallization of plagioclase, hornblende and biotite in equal proportion from quartz monzodiorite magmas, produces the residual melts that are more depleted in HREE and show more fractionated chondrite normalized REE patterns than the parent magma as well as the Northern granodiorites (Fig. 5.12b). The magmas represented by Northern granodiorites, therefore cannot be derived by fractional crystallization of parent magmas having composition similar to that of intermediate rocks (such as quartz monzodiorite).
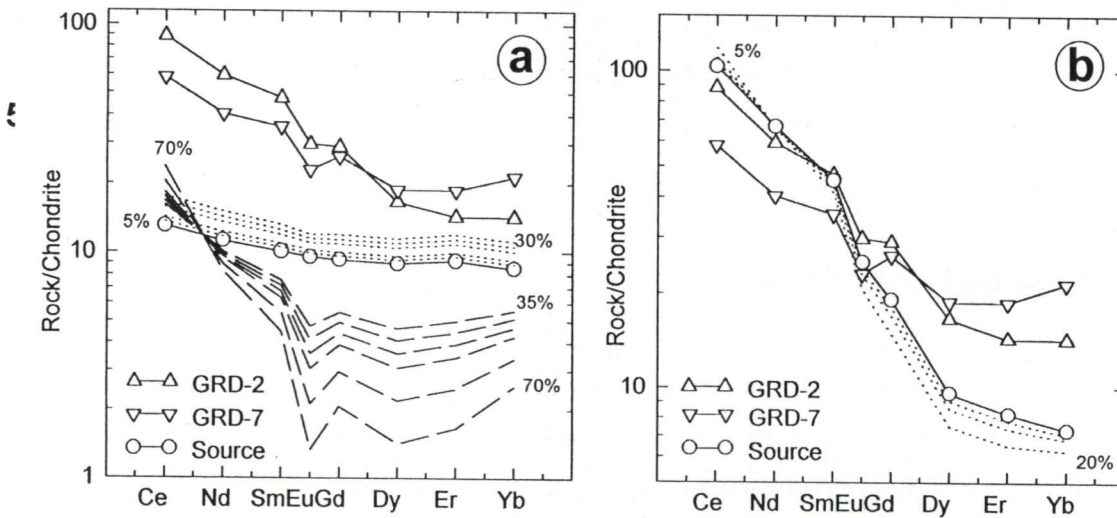
Fig. 5.12 Calculated chondrite normalized REE patterns for fractional crystallization from a tholeiitic source and an intermediate source (dotted lines represent 5 to 30% and dashed lines represent 35 to 70% fractional crystallization). a) For 5 to 70% fractional crystallization of plagioclase and hornblende in 60:40 ratio from a tholeiitic source (GH-10). b) For 5 to 20% fractional crystallization of plagioclase, hornblende and biotite in equal proportion from an intermediate source (QMD-1).

87

5.3.3.2 Partial Melting

Partial melting of intermediate rocks gives rise to magmas having chondrite normalized REE patterns parallel to that of the source (Fig. 5.10) but the REEs are relatively lower in abundance in the magmas than the source. However, the Northern granodiorites have higher, and less fractionated chondrite normalized REE patterns compared to that of quartz monzodiorite. The REE patterns of Northern granodiorite are also quite distinct from that of Eastern as well as Western granodiorites. Hence, they cannot represent magmas derived by partial melting of quartz monzodiorite.

It is suggested that low extents of partial melting of oceanic crust (basaltic component) may give rise to granitic magmas (Arth, 1972; Arth and Hanson, 1975; Rudnick and Taylor, 1986) at about 2.2-3.0 GPa pressure and $> 1000^0$ C temperature (Tatsumi and Eggins, 1995). To test this hypothesis, partial melting of a Hutti tholeiite is modeled. The residual mineralogy (20% plagioclase + 25% orthopyroxene + 30% clinopyroxene + 10% hornblende + 15% garnet) is approximated as outlined in the experimental studies on partial melting of amphibolites by Rapp and Watson (1995). The trace elements and REE abundance of the melt are calculated, and the chondrite normalized REE patterns of the melt along with the source rock are shown in figure 5.13. It is observed that the REE abundance of the melt are not at all comparable to that of Northern granodiorites and there is greater depletion of HREE in the melt. Rapp and Watson (1995) suggest more than 30% garnet in the residual mineralogy along with other phases (as mentioned above) at 2.2-3.0 GPa pressure. This condition will lead to further depletion of HREE in the melt. Therefore, partial melting of basaltic tholeiites in the subducting slab (where 2.2-3.0 Gpa pressure is normally expected) cannot give rise to magmas similar in REE abundance to that Northern granodiorites.

The Hutti tholeiites are inferred to have formed in the island arc environment (Giritharan and Rajamani, 1998). It may be possible that partial melting of these tholeiites at shallower level can give rise to magmas similar in composition to that of Northern granodiorites. It is in this context that 20% partial melting of Hutti tholeiites leaving plagioclase and clinopyroxene in 32:68 ratio is investigated. As the REE abundance as well as chondrite normalized REE patterns are variable in the Hutti tholeiites, two samples of the Hutti tholeiites, *viz.,* GH-7 and HB-5B are considered as sources. It is observed that the chondrite normalized REE patterns of the calculated melts are parallel to that of Northern

granodiorites but with lower REE abundance (Fig. 5.14a & b). The modeling of trace element including REEs suggest that Northern granodiorites require a parent that is 30 to 20
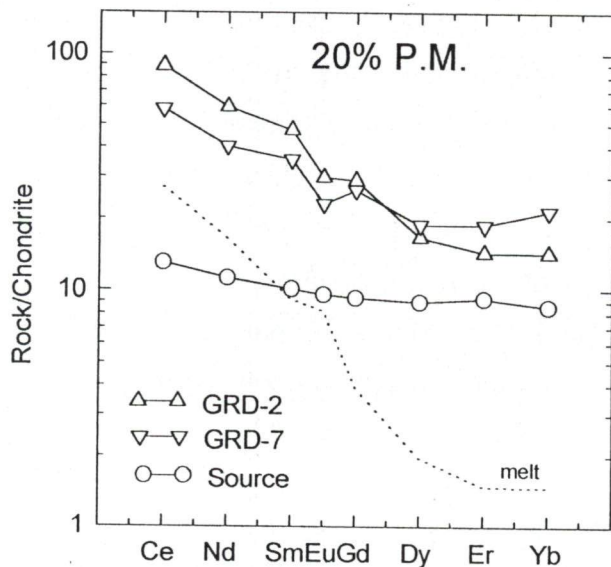
Fig.5.13 Calculated chondrite normalized REE pattern of the melt derived by 20% partial melting of a tholeiitic source (GH-10), leaving 20% plagioclase, 25% orthopyroxene, 30% clinopyroxene, 10% hornblende and 15% garnet in the residue.
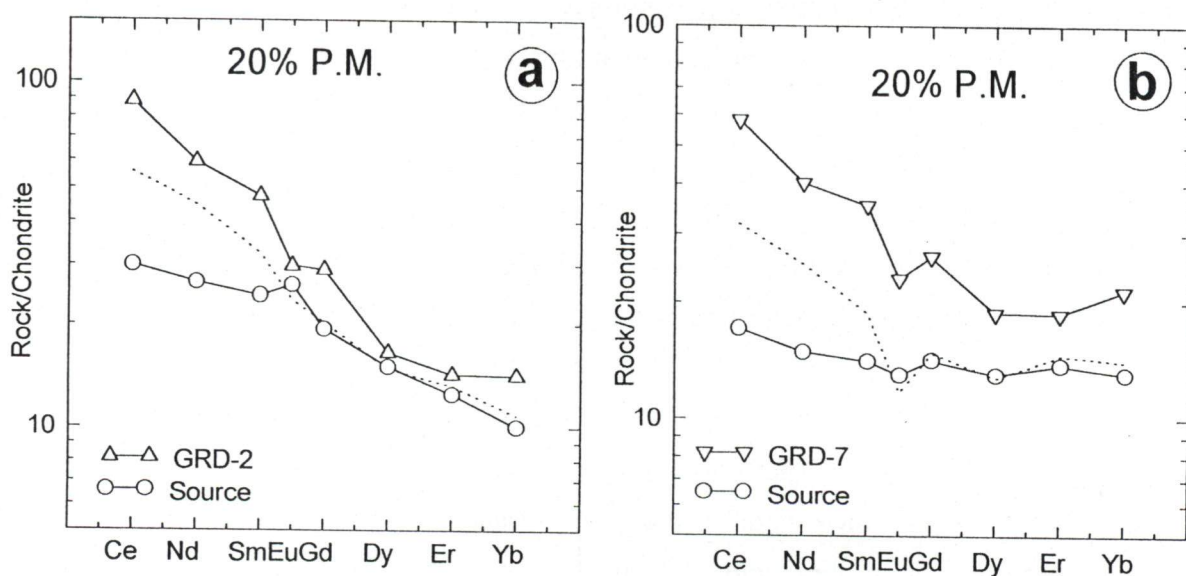
Fig. 5.14 Calculated chondrite normalized REE patterns of melts derived by 20% partial melting of tholeiitic sources leaving plagioclase and clinopyroxene in 32:68 ratio in the residue. a) GH-7 as source. b) HB-5B as source.

times more enriched in Ce and Yb, respectively, as compared to chondrites. Tholeiite metabasalts with the above REE abundance are commonly found in the Archean schist belts of eastern Dharwar craton like Hutti, Ramagiri and Kolar (Rajamani et al., 1985; Zachariah et al., 1996, 1997; Giritharan and Rajamani, 1998) as well as in the present day island arcs (Wilson, 1989, Tatsumi and Eggins, 1995). Thus, the geochemical modeling indicates that the magmas represented by Northern granodiorites could have been formed by low pressure partial melting of island arc tholeiites.

5.4 GRANITES

The granites mostly occur to northwest and northeast of the Hutti schist belt and are called as Western granites and Eastern granites, respectively. Aplite veins cutting older granodiorite gneiss occur to northwest of the belt, near Gurgunta village. The Western granites are leucocratic, fine to medium grained, consisting of < 5% ferro-magnesian minerals. They have $\geq$ 74 wt.% SiO_2, and Mg# 0.25-0.33. The Eastern granites have 4.6 to 6.1 wt.% K_2O, and higher K_2O/Na_2O ratios than that of Western granites. Both the granites have typical LREE enriched chondrite normalized REE patterns with distinct negative Eu anomalies of different magnitudes (Fig. 4.6). They also have much lower Sr (129-226 ppm) and lower Ba (296-547 ppm) abundance than the granodiorites of the Hutti schist belt. They are found as intrusives into the granodiorites (Kasamdoddi village, near sample location GR-5) as well as into the schist belt (Kurkundi village, near sample location GR-4). Therefore, it may be possible that their magmas might have been derived by partial melting of crustal rocks such as basalt or granodiorite (Rapp and Watson, 1995). The chondrite normalized REE patterns for these granites are quite different from that of hypothetical melts generated by partial melting of tholeiitic sources (refer figures for Northern granodiorites). Hence, partial melting of tholeiitic basalt similar in composition to that of Hutti tholeiites cannot give rise to magmas representing the Hutti granites.

The granites of the Hutti schist belt are plotted in $NaAlSi_3O_8$-K $AlSi_3O_8$-SiO_2-H_2O (Ab-Or-Qz-H_2O) system with phase relationship indicated for melting under hydrous conditions at 0.5 GPa and 3.0 GPa pressure. In this system when melting takes place under hydrous conditions (with excess H_2O), the granite melts are formed within a narrow temperature interval and lie close to the eutectic (Huang and Wyllie, 1975) The Western granites plot on

left hand side of the eutectic and very close to it, whereas, the Eastern granites plot on the right hand side of eutectic and they are close to the coetectic (Fig. 5.15)
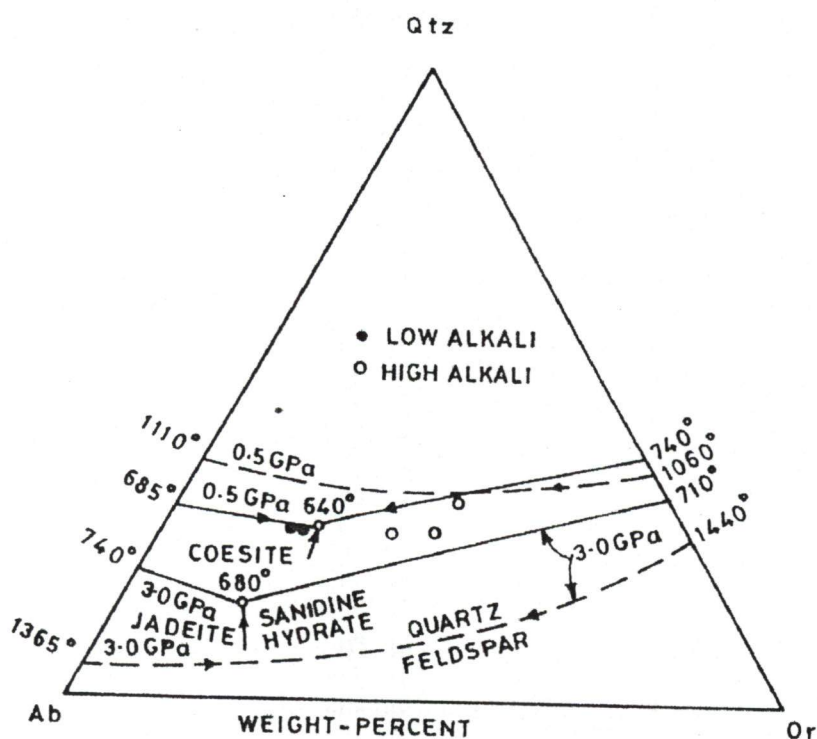
Fig.5.15 Comparison of field boundaries in systems Ab-Or-Qtz-H₂O and Ab-Or-Qtz two pressures, 0.5 and 3.0 Gpa. Solid lines represent excess water and dott lines represent dry conditions (data and estimates as described by Huang a Wyllie, 1975; after Wyllie, 1977).

Partial melting of granodiorite, such as, Kavital granodiorite may give rise to magmas similar in composition to that of granites of the study area. Since the Kavital granodiorites have variable REE abundance, two of the Kavital granodiorite samples, *viz.,,* GRD-19 and GRD-26 are tested as parents. 10% partial melting of these sources under H_2O saturated conditions are investigated and the abundance of trace elements including REEs in the melts have been calculated. The REE abundance of melts formed by 10% partial melting of a source such as granodiorite GRD-26 leaving 1% and 2% sphene (along with other minerals namely 63-64% plagioclase, 25% biotite and 10% K-feldspar) in the residue are quite similar to the REE abundance in the Western granites *viz.,* GR-2 and GR-6 (Fig. 5.16a). The Eastern granites *viz.,* GR-1, GR-4 and GR-5 have REE abundance similar to that of melts formed by 10% partial melting of granodiorite GRD-19 leaving 1% to 2% sphene (along with other minerals) in the residue (Fig. 5.16b).
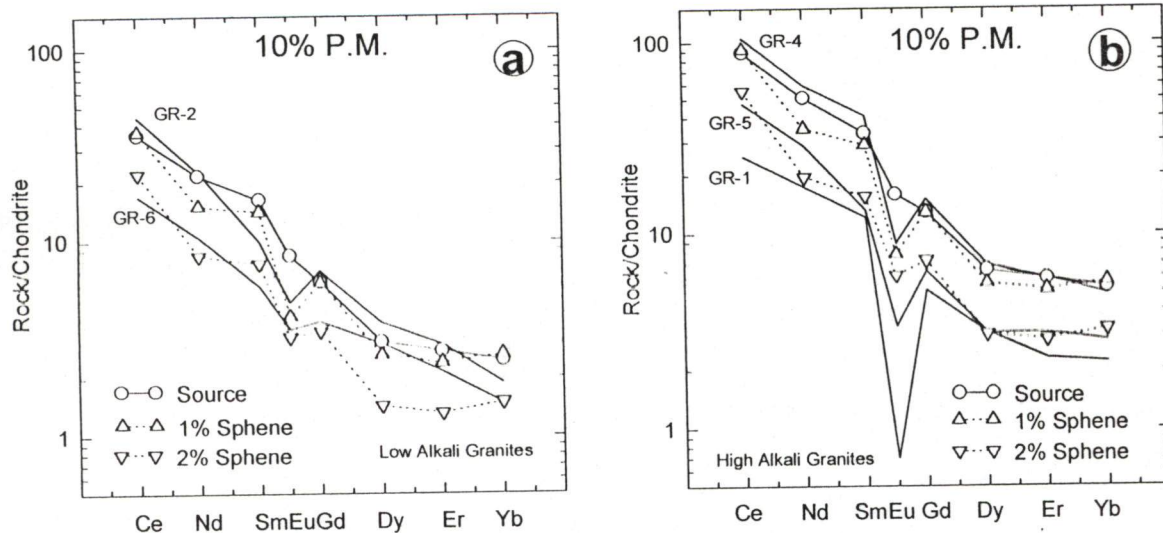
Fig. 5.16 Calculated chondrite normalized REE patterns of melts derived by 10% partial melting of granodiorite leaving 1% and 2% sphene in the residue. a) Granodiorite, GRD-26 as source. b) Granodiorite, GRD-19 as source.

Granite GR-1 (from Galaga area) has the most pronounced negative Eu anomaly (Fig. 5.16) and the lowest Sr (129 ppm) and Ba (296 ppm) abundance, which can be as a result of its magma equilibrating with feldspars dominated in the residue. Alternatively, this magma could have been originated by partial melting at granite eutectic (at lowest possible temperatures) under $P_{H2O} = P_{total}$ conditions.

Thus, partial melting of granodiorites having fractionated chondrite normalized REE patterns but with varying REE abundance, and leaving different proportion of feldspars, Ferro-magnesian minerals along with sphene in the residue under H_2O saturated conditions can give rise to granite magmas with the observed variations.

5.5 MONZODIORITES

A multiple set of veins of granitoid rocks occurs at Kotekalu (east of Kavital) area. The contact between the vein is distinct. A series of five samples *viz.*, GRD-8, GRD-9, GRD-10, GRD-11 and MZD-2, one from each vein, have been collected. Out of these five samples, one sample (MZD-2) plot in monzodiorite field of "TAS" classification diagram (Fig. 4.5). Its major and trace element abundance, and chondrite normalized REE pattern (Fig. 5.17a) imply that it can be derived by the similar processes like that of Kavital granodiorite (i.e., by partial melting of a parent similar in composition to that of intermediate rocks).

Alternatively, magmas representing these vein samples can be generated by varying extents of fractional crystallization from an intermediate parent magma having chondrite normalized REE patterns parallel to that of MZD-2 but higher in abundance.

One of the samples (MZD-1) from the complex granitoid outcrop, near Gurgunta, is classified as monzodiorite on the basis of "TAS" classification diagram (Fig. 4.5). The trace element including REE abundance imply that this monzodiorite (MZD-1) cannot be derived by partial melting of intermediate rocks. It is possible that it may be derived by partial melting of basaltic tholeiites like that of Hutti schist belt. To test this hypothesis, partial melting of one of the Hutti tholeiites (GH-10) at shallower level leaving plagioclase, orthopyroxene, clinopyroxene, hornblende and garnet in the residue is investigated and the REE abundance of the melt are calculated. The calculated chondrite normalized REE pattern of the melt is parallel to that of the monzodiorite (Fig. 5.17b), and the REE abundance are also comparable to that of that monzodiorite. It can therefore, be inferred that partial melting of Hutti tholeiites could give rise to magma similar in composition to that of monzodiorite (MZD-1) occurring near Gurgunta village.
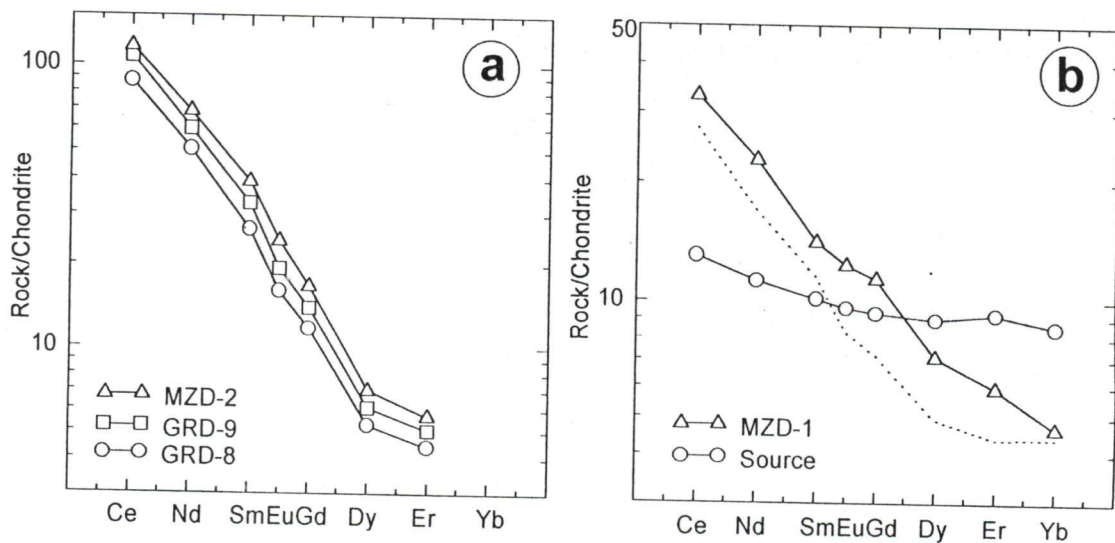
Fig. 5.17 a) Chondrite normalized REE pattern of Eastern monzodiorite (MZD-2). The REE patterns of granodiorite samples namely GRD-8 and GRD-9 are also plotted for comparison. b) Calculated chondrite normalized REE pattern of the melt derived by 20% partial melting of a tholeiitic source (GH-10), leaving 27% plagioclase, 25% orthopyroxene, 35% clinopyroxene, 10% hornblende and 3% garnet in the residue.

CHAPTER 6

DISCUSSION

The Hutti schist belt consists of pillowed metabasalts, felsic volcanic and metasediments. The belt is surrounded by granitoids on all sides. The mineralogical assemblage and the coexistence of hornblende and chlorite indicate that the schist belt rocks have undergone greenschist to amphibolite facies metamorphism (Ananta Iyer and Vasudev, 1979; Biswas, 1990; Riyazullah et al., 1996). The rocks of the schist belt have been subjected to two major episodes of co-axial folding that are responsible for its hook-shaped geometry (Roy, 1979).

The petrogenetic studies corroborated by geochemistry have been carried out to categorize the granitoids surrounding the schist belt and put constraints on the various models proposed for the evolution of the eastern Dharwar craton.

6.1 QUARTZ MONZODIORITES

Quartz monzodiorites are the intermediate rocks that are geochemically quite similar to sanukitoids and high magnesian andesites. It is argued that simple partial melting of basalts at different metamorphic conditions or fractional crystallization of different phases in different proportions from the basaltic magmas cannot give rise to magmas parental to quartz monzodiorites. The geochemical modeling reveals that quartz monzodiorite magmas have been derived by partial melting of sources that are more enriched in LILEs and LREEs and more siliceous and Fe enriched than the primitive mantle. The enrichment of incompatible trace elements including LILEs and LREEs is possible by fluid or melt interaction or by both (Tatsumi et al., 1986; Eggler, 1987; Kelemen, et al., 1993; Yogodizinski, et al., 1995; Tatsumi and Eggins, 1995). Yogodizinski, et al. (1995) further

suggest that slab melt is the main factor responsible for enrichment of LILEs and LREEs for high magnesian andesite of Aleutian region. They show that the addition of small percentage of slab melts to the magma source could result in enrichment of incompatible trace elements. It is suggested that addition of sediment component in the form of fluids can also enrich the source in trace elements (White and Patchet, 1984; Tatsumi et al., 1986). Kay and Kay (1988, 1994) argue that transportation of large ion lithophile elements like Ba and Th by hydrothermal fluid to the mantle wedge is doubtful.

Experimental studies by Tatsumi (1982) on high magnesian andesite of Setouchi volcanic belt indicate that melts of sanukitoid composition could represent primary magmas formed by partial melting of mantle sources. But Shirey and Hanson (1984) suggested a metasomatized mantle source for the sanukitoids.

In the [Mg]-[Fe] modeling of quartz monzodiorites of Hutti area reveals that they require sources with higher Fe/Mg ratio than the garnet-lherzolite and their partial melting at pressure of about 1.5 GPa. It is observed that a mixture of the lherzolite and picrite or even tholeiites can give rise to composite sources similar in composition to komatiites. Partial melting of this source may give rise to magmas compositionally similar to quartz monzodiorites. But the trace element modeling suggests that the source should be enriched in incompatible trace elements prior to melting. This composite source in mantle wedge can be enriched in LILEs and LREEs by reaction with aqueous fluids and/or hydrous siliceous melts derived from subducted oceanic crust. Therefore, it is argued that the parental magma to quartz monzodiorites could be derived by partial melting of composite lithospheric mantle sources similar in composition to komatiite enriched in incompatible trace elements under low pressure conditions.

6.2 GRANODIORITES

The granodiorites occurring to the east, west and north of the Hutti schist belt are classified in three groups with distinct geochemical characteristics. They are named as Kavital granodiorites, Western granodiorites and Northern granodiorites, respectively.

The Kavital and Northern granodiorites have higher FeO, MgO, TiO_2, Ni and Cr than the Western granodiorites. Though the Kavital granodiorites have comparable major and trace element abundance comparable to that of Northern granodiorites, the latter is characterized by less fractionated chondrite normalized REE patterns with distinct negative

Eu anomaly. The magmas parental to Kavital granodiorites are generated by partial melting of intermediate rocks similar in composition to that of quartz monzodiorite.

The Northern granodiorites have distinct field, petrographic and trace element characteristics. Their less fractionated chondrite normalized REE patterns with prominent negative Eu anomaly differ them from that of the granodiorites occurring east and west of the schist belt. It has been established that they cannot be derived either by partial melting of primitive mantle or intermediate rocks or by fractional crystallization of common tholeiites or andesitic magmas. Geochemical modeling suggests that their magmas can be derived by low-pressure partial melting of island arc basalts similar to that of Hutti tholeiitic metabasalts.

Western granodiorites have lower REE abundance than the quartz monzodiorites. These rocks have chondrite normalized REE patterns that are parallel to that of the quartz monzodiorites, and they lack Eu anomaly. On the basis of geochemical modeling it is argued that they can represent residual magmas formed by fractional crystallization processes (including liquid immiscibilty) from the quartz monzodiorite magmas.

Balakrishnan and Rajamani (1987) suggest a liquid immisibilty model for the origin of Dod-Dosa gneisses occurring to west of the Kolar schist belt. To explain the geochemical variation of Rose Town Complex granodiorites Bender et al. (1982) advocate liquid immisibilty as the main process, but Stern and Hanson (1991) argue that they are derived by fractional crystallization of dolerite cumulates. Western granodiorites of Lingusugur area are closely associated with quartz monzodiorites and all gradations between the granodiorites and quartz monzodiorites are observed. Their major, trace and REE abundance suggest that liquid immisibilty might have played a significant role in the evolution of Western granodiorites.

6.3 GRANITES

The granites are confined to northeast and northwest of the study area and they intrude into the surrounding rocks. They have typical LREE enriched chondrite normalized REE patterns with pronounced negative Eu anomaly. In the Q-Ab-Or diagram they plot close to the eutectic and cotectic for granite melting at 0.5 GPa pressure under water saturated conditions. Geochemical modeling shows that the magmas parental to these granites might have been derived by low extents of partial melting of granodiorites similar in composition to the Kavital granodiorites under hydrous conditions.

6.4 MONZODIORITES

Two granitoid samples that are grouped into monzodiorites have comparable major element chemistry but differ significantly in their REE abundance as well as chondrite normalized REE patterns. Interestingly, these two samples represent two outcrops that are located on opposite sides of the belt, and their source rocks are also different. From petrogenetic considerations, it is inferred that magmas parental to monzodiorite (MZD-2) occurring to the east of the belt are derived by partial melting of intermediate rocks. On the contrary, the monzodiorite (MZD-1, from Gurgunta outcrop) occurring to the west of the belt is derived by shallow level partial melting of tholeiites similar in composition to that of Hutti tholeiites.

6.5 TECTONIC EVOLUTION

In an island arc settings the magmas could be derived by (I) partial melting of subducting slab, (II) partial melting of mantle wedge and/or, (III) partial melting of both. The present day geothermal gradient at the subduction zone indicates that although it is difficult to melt the slab (Tatsumi and Eggins, 1995; Wilson, 1989), the slab may undergo dehydration and release volatiles into the mantle wedge. In the present day island arc settings the mantle wedge is considered as the source region for the arc magmas (Kay et al., 1993).

Petrogenetic modeling indicates that the quartz monzodiorites were derived from a composite mantle source metasomatically enriched in incompatible trace elements. The Eastern and Western granodiorites of the Hutti schist belt were also directly or indirectly derived from such enriched mantle sources. Enriched mantle sources are likely to be found in the mantle wedge above the subducting slab in the island arc tectonic settings. The Northern granodiorites represent melts generated by partial melting of island arc basalts under low pressure conditions. The petrogenetic studies of granitoids surrounding the Hutti schist belt indicate that none of them can be generated by partial melting of the slab. If the geothermal gradient would have higher than the present day one then partial melting of the slab component would be possible. The absence of granitoids that represent slab melts in the study area indicates that during the late Archean the geothermal gradient must have been similar to what is found in the subducting environments in the present day.

97

6.5.1 Granitoids of Hutti-, Kolar- and Ramagiri- schist belts

On the basis of field, petrographic and geochemical studies, it has been suggested that granitoids occurring to east and to west of the Kolar schist belt are quite different from each other. Further, on the basis of isotopic age data on granitoids surrounding the Kolar schist belt, it has been inferred that the Western granitoids (2636 Ma) are older than the Eastern granitoids (2530 Ma; Krogstad, et al., 1989, 1995). These authors have suggested that graniotoids occurring to east and to west of the Kolar schist belt represent two disparate granitic terranes, each having its own evolutionary history. Balakrishnan et al. (1990) have assigned an age of 2700 Ma for the schist belt rocks and suggested that the schist belt may form the boundary between these two unrelated granitic terranes.

The granitoids surrounding Ramagiri schist belt have also been studied in detail. The granitoids occurring east, west and central of the Ramagiri schist belt have distinct geochemical characteristics and on the basis of major and trace element modeling, they have been considered as three unrelated granitoid terranes separated by the Ramagiri schist belt (Zachariah, et al., 1995, 1996; Mohanta, 1998). Zachariah et al. (1995) have assigned an age of 2746 $\perp$ 66 Ma for the schist belt rocks. The U-Pb isotope study by Balakrishnan et al. (1999) on zircon and titanite of the granitoids suggest that the ages of the granitoids occurring east, west and central of Ramagiri schist belt are 2650 $\pm$ 7 Ma, 2613 $\pm$ 7 Ma and 2558 $\pm$ 1 Ma, respectively. They also assign an age of 2707 $\pm$ 18 Ma for zircon from pyroclastic unit occurring in the Ramagiri schist belt. Post kinematic veins cutting the granitoids have titanite ages of 2468 $\pm$ 4 Ma, which is considered to be the time of accretion of all the terranes.

A complex rock association of quartz monzodiorite, granodiorite, monzodiorite and granite similar to that of Kolar schist belt occur in the western side of the Hutti schist belt. The association as well as trace element characteristics suggest that they are comparable to that of the Dod-Dosa gneisses of Kolar schist belt. To the eastern side of the Hutti schist belt, the rocks are mainly granodiorites (Kavital granodiorites) with small intrusions of post tectonic granites. These are comparable with the Khamba gneisses occurring to east of the Kolar schist belt. However, the Khamba gneisses show migmatitic and/or agmatitic structure, and it is possible that they represent deeper level of crustal exposure.

Northern granodiorites (YG) of Hutti schist belt contain megacrysts of K-feldspars and mafic enclaves of various sizes. Their megascopic characteristics as well as REE chemistry are similar to that of the Central block of the Ramagiri schist belt.

6.5.2 Model for the Evolution

Chadwick et al. (1996) propose an intra-arc basin model for the evolution of the eastern Dharwar craton. They consider that the granitoids surrounding the schist belts in the eastern Dharwar craton form one large batholith and the schist belts (*viz.* Sandur, Hutti, Kolar etc.) were evolved with the Dharwar batholith. This batholith is thought to have accreted onto the older Archean continent with its marginal or back-arc, volcano-sedimentary basins (Dharwar Supergroup) in western Karnataka during Late Archean plate convergence. But the study of granitoids around Hutti schist belt as well as earlier studies of granitoids surrounding Kolar and Ramagiri schist belts establish that the granitoids surrounding these belts do not represent a single batholith. The granitoids occurring to east and to west of Kolar and Hutti schist belts are not comparable to those surround the Ramagiri schist belt. Furthermore, the granitoids occurring to west of the Kolar schist belt are older (~100 Ma) than those occurring to west of the Ramagiri schist belt. On the contrary, granodiorites occurring to east of the Kolar schist belt are younger (~30 Ma) than those occurring to east of the Ramagiri schist belt. Significant variation in the ages of different granitoids surround the schist belts argues against the regional accretionary model for the evolution of the eastern Dharwar craton.

It is now well established that many Archean terranes evolved by accretionary processes in different shield areas of the world. For example, the Superior Province of Canada was assembled together between 2725 and 2695 Ma (Card, 1990), the Nuuk region of Greenland includes three distinct terranes, each of its own geological history were assembled together by 2700 Ma (Friend et al., 1996) and various granite-greenstone terranes were assembled between 2670 and 2650 Ma to make up the Yilgran craton of western Australia (Mysers, 1997). Because, the granitoids occurring to east of Hutti Ramagiri and Kolar schist belts cannot be considered to form one unit (a linear belt) and those occurring to west of these belts form the other unit. Geochemical and geochronological evidence imply that each granitoid complex surrounding the individual schist belt of eastern Dharwar craton, has its own evolutionary history and they were accreted together towards the end of Archean to form the eastern part of the Dharwar craton.

CHAPTER 7

CONCLUSIONS

❧   The granitoid rocks surrounding the Hutti schist belt have been divided into four categories on the basis of geochemical characteristics, *viz.* Monzodiorite, Quartz monzodiorite, Granodiorite and Granite. In general, these granitoids are meta-aluminous in nature and show calc-alkaline trend.

❧   The quartz monzodiorites were derived by partial melting of LILEs and LREEs enriched composite sources in the mantle wedge similar in composition to that of komatiite under hydrous conditions.

❧   Eastern granodiorites (Kavital granodiorites) were derived by partial melting of intermediate rocks, whereas, the Western granodiorites were derived by fractional crystallization processes including liquid immiscibility from quartz monzodiorite. Northern granodiorites represent magmas derived by low extents of partial melting of island arc basalts under low pressure conditions.

❧   Monzodiorites were derived by partial melting of intermediate rocks such as quartz monzodiorite, as well as island arc tholeiites similar to those occurring in the Hutti schist belt.

❧   The magmas parental to granitoids surrounding the Hutti schist belt must have been formed by partial melting of sources such as the mantle wedge or the oceanic arc crust. None of them were derived by partial melting of subducting slab.

     The granitoid terranes occurring to east, west and north of the Hutti schist belt have distinct field, petrographic and geochemical characteristics. They may represent three disparate granitic terranes with their own evolutionary histories. These three unrelated granitic terranes were assembled together towards the end of late Archean and Hutti schist belt may define the boundary between them.

     Granites surrounding the Hutti schist belt are post-tectonic and could have been derived by low extent partial melting of granodiorites under hydrous conditions.

REFERENCES

Anantha Iyer, G.V. and Vasudev, V.N. 1979. Geochemistry of the Archean metavolcanic rocks of Kolar and Hutti Gold Fields, Karnantaka, India. Jour. Geol. Soc. India, 20, 419-432.

Anantha Iyer, G.V., Vasudev, V.N. and Jayaram, S. 1980. Rare earth element geochemistry of metabasalts from Kolar and Hutti gold-bearing volcanic belts, Karnataka craton, India. Jour. Geol. Soc. India, 21, 603-608.

Arth, J.G. 1972. Quartz diorites derived by partial melting of eclogite or amphibolite at mantle depths. Contrib. Mineral. Petrol., 37, 161-174.

Arth, J.G. and Hanson, G.N. 1975. Geochemistry and origin of the early Precambrian crust of northeastern Minnesota. Geochem. et. Cosmochim. Acta, 4, 325-362.

Arth, J.G.F., Barker, F., Peterman, Z.E. and Friedman, I. 1978. Geochemistry of the gabbro-diorite-tonalite-trondhjemite suite of southwest Finland and its implications for the origin of tonalitic and trondhjemitic magmas. Jour. Petrol., 19, 289-316.

Balakrishnan, S. 1982. Geochemistry of felsic rocks around Kolar Schist Belt, Karnataka. Unpub. M. Phil. Thesis, Jawaharlal Nehru University, New Delhi.

Balakrishnan, S. and Rajamani, V. 1987. Geochemistry and petrogenesis of granitoids around Kolar schist belt, south India: Constraints for the evolution of the crust in the Kolar area. Jour. Geol., 95, 219-240.

Balakrishnan, S., Hanson, G.N. and Rajamani V. 1990. Pb and Nd isotope constraints on the origin of high Mg and tholeiitic amphibolites, Kolar schist belt, south India. Contrib. Mineral. Petrol., 107, 279-292.

Balakrishnan, S., Rajamani, V. and Hanson, G.N. 1985. REE abundances and Nd isotopic characteristics of komatiitic rocks-implications to the formation of an Archean greenstone belt in the Karnataka craton. Proc. 3rd National Sym. Mass Spectrometry: RRL, Hyderabad, E7/1-2.

Balakrishnan, S., Rajamani, V. and Hanson, G.N. 1999. U–Pb ages for zircon and titanite from the Ramagiri area, southern India: Evidence for accretionary origin of the eastern Dharwar craton during the late Archean. Jour. Geol., 107, 69-86.

Ballal, N.R.R., 1975. The geology of Pamidi and Penukonda-Ramagiri schist belt and the surrounding Archean gneisses and granites, Anantapur district, Andhra Pradesh. Geol. Surv. India Misc. Pub., 23, Part 1, 97-104.

Barker, F. 1979. Trondhjemite: definition, environment and hypotheses of origin. In Trondhjemites, Dacites, and Related Rocks, edited by F. Barker, Elsevier, New York, 1-12.

Barker, F. and Arth, J.G. 1976. Generation of trondhjemitic-tonalitic liquids and Archaean bimodal trondhjemite-basalt suites. Geol., 4, 596-600

Basir, S.R. and Balakrishnan, S. 1999. Geochemistry of sphene from granodiorites surrounding the Hutti-Maski schist belt: Significance to rare earth element (REE) modeling. Jour. Geol. Soc. India, 54, 107-119.

Beard, J.S and Lofgren, G.E. 1991. Dehydration melting and water saturated melting of basaltic and andesitic Greenstones and amphibolites at 1, 3 and 6.9 Kb. Jour. Petrol., 32, 365-401.

Beckinsale, R.D., Drury, S.A. and Holt, R.W. 1980. 3360 Ma old gneisses from the south Indian craton. Nature, 283, 469-470.

Beckinsale, R.D., Reeves-Smith, G., Gale, N.H., Holt, R.W. and Thompson, B. 1982. Rb-Sr and Pb-Pb whole rock isochron ages and REE data for Archean gneisses and granites, Karnataka state, south India. Indo-US workshop on Precambrian of south India, Hyderabad, Abstracts.

Bender, J.F., Hanson, G.N and Bence, A.E. 1982. The Cortlandt Complex: Evidence for large scale liquid immisibility involving granodiorite and diorite magmas. Earth Planet. Sci. Lett., 58, 330-344.

Bhalla, N.S., Gupta, J.M., Chabria. T. and Vasudeva, S.G. 1978. Rb-Sr geochronology of the rocks from the Kolar schist belt, south India. In Archean Geochemistry, edited by B.F. Windley and S.M. Naqvi, Elsevier, Armsterdom, 79-84.

Bhaskar Rao, Y.J., Sivaraman, T.V., Pantulu, G.V.C., Gopalan, K. and Naqvi, S.M. 1992. Rb-Sr ages of late Archean metavolcanics and granites, Dharwar craton, south India and evidence of early Proterozoic thermotectonic event(s). Precambrian Res., 59, 145-170.

Biswas, S.K. 1990. Gold mineralisation on Uti Block of Hutti-Maski supracrustal belt, Karnataka. Jour. Geol. Soc. India, 36, 79-89.

Biswas, S.K., Prabhakaran, K. and Rao, P.S. 1985. Preliminary exploration of auriferous lodes of Hutti-Maski schist belt, Karnataka, India. U.N. Regional seminar on gold exploration and development, Bangalore, Sect.II, 1-29.

Buddington, A.F. 1959. Granite emplacement with special reference to North America. Geol. Soc. Am. Bull., 70, 671-747.

Burke, K., Dewey, J.F. and Kidd, W.S.F. 1976. Dominance of horizontal movements, arc and microcontinental collisions during the later permobile regime. In The Early History of the Earth, edited by B.F. Windley, John Wiley, New York, 113-129.

Card, K.D. 1990. A review of the Superior Province of the Canadian shield, a product of Archean accretion. Precambrian Res., 48, 99-106.

Chadwick, B., Ramakrishnan, M., Viswanatha, M.N. and Sreenivasa Murthy, V. 1978. Structural studies in the Archean Sargur and Dharwar supracracrustal rocks of the Karnataka craton. Jour. Geol. Soc. India, 19, 531-542.

Chadwick, B., Vasudev, V.N. and Ahmed, N. 1996. The Sandur schist belt and adjacent plutonic rocks: Implications for late Archean crustal evolution in Karnataka. Jour. Geol. Soc. India, 47, 37-57.

Clarke, D.B. 1992. Granitoid rocks. Chapman and Hall, India, 283p.

Cocherie, A., Rossi, PH., Fouillac, A.M. and Vidal, PH. 1994. Crust and Mantle contribution to granite genesis - an example from the Variscan batholith of Corsica, France, studied by trace element and Nd-Sr-O-isotope systematics. Chem. Geol., 115, 173-211.

Condie, K.C. 1981. Archaean greenstones. Elsevier, Amsterdam, 434p.

Condie, K.C. 1986. Origin and early growth rate of continents. Precambrian Res.,32, 261-278.

Condie, K.C. 1988. Plate tectonics and Crustal evolution. 3rd ed., Pergamon Press, New York, 476p.

Condie, K.C. and Hunter, D.R. 1976. Trace element geochemistry of Archean granitic rocks from the Barberton region, South Africa. Earth Planet. Sci. Lett., 29, 389-400.

Crock, J.G., Lichte, F.E. and Wildeman, T.R. 1984. The group separation of the rare earth elements and Yttrium from geologic materials by cation exchange chromatography. Chem. Geol., 45, 149-163.

Curtis, L.C., Radhakrishna, B.P. and Naidu, G.K. 1990. Hutti Gold Mine with a Future. Geol. Soc. India Pub., 123p.

Drummond, M.S. and Defant, M.J. 1990. A model for trondhjemite-tonalite-dacite genesis and crustal growth via slab melting : Archean to modern comparisons. Jour. Geophy. Res., 95, 21503-21521.

Eggler, D.H. 1987. Solubility of major and trace elements in mantle metasomatic fluids : Experimental constraints. In Mantle metasomatism, edited by M.A.Menzies and C.J. Hawkesworth, Academic Press, Lond., 21-41.

Flood, R.H. and Vernon, R.H. 1988. Microstructural evidence of orders of crystallization in granitoid rocks. Lithos, 21, 237-245.

Ford, C.E., Russel, D.G. and Frisk, M.R., 1983. Oivine-liquid equilibria: temperature, pressure and composition dependence of the crystal/liquid partition coefficients for Mg, Fe, Ca and Mn. Jour. of Petrol. 4, 56-265.

Friend, C.R.L., Nutman, A.P., Baadsgaard, H., Kinny, P.D. and McGregor, V.R. 1996. Timing of late Archean terrane assembly, crustal thickening and granodiorite emplacement in the Nuuk region, southern west Greenland. Earth Planet. Sci. Lett., 142, 353-365.

Gastil, G. 1982. Symposium on subduction of oceanic plates: Summary. Geol. Soc. Am. Bull., 93, 464-467.

Ghosh, S.K. and Sengupta, S. 1985. Superposed folding and shearing in the western quartzite of Kolar Gold Fields. Indian Jour. Earth Sci., 12, 1-8.

Gilbert, M.C., Heltz, R.T., Popp, R.K. and Spear, F.S. 1982. Experimental studies of amphibole stability. In Amphiboles: Petrology and experimental Phase relations, edited by D.R. Velblenand and P.H. Ribbe, Mineral. Soc. Am. Rev. Mineral., 9b, 229-354.

Gill, J.B. 1981. Orogenic andesites and plate tectonics. Springer-Verlag, New York, 385p.

Giritharan, T.S. and Rajamani, V. 1998. Geochemistry of the metavolcanics of the Hutti-Maski Schist Belt, South India: Implications to gold metallogeny in the eastern Dharwar craton. Jour. Geol. Soc. India, 52, 583-594.

Glikson, A.Y. 1979. Early Precambrian tonalite-trondhjemite sialic nuclei. Earth-Sci. Rev., 15, 1-73.

Goodwin, A.M. 1974. Precambrian belts, plumes and shield development. Am. Jour. Sci., 274, 987-1028.

Green, 1976. Experimental testing of "equilibrium" partial melting of peridotite under water-saturated, high pressure conditions. The Canadian Mineralogist, 14, 255-268.

Green, D.H. and Ringwood, A.E. 1970 Mineralogy of peridotitic compositions under upper mantle conditions. Physics of the Earth and Planetary Interiors, 3, 359-371.

Green, T.H and Pearson, N.J. 1983. Effect of pressure on rare earth element partition coefficients in common magmas. Nature, 305, 414-415.

Green, T.H. 1980. Island arc and continent-building magmatism - A review of petrogenetic models based on experimental petrology and geochemistry. Tectonophysics, 63, 367-385.

Green, T.H. and Ringwood, A.E. 1968. Genesis of the calc-alkaline igneous rock suite. Contrib. Mineral. Petrol., 18, 105-162.

Greig, J.W. 1927. Immiscibility in silicate melts. Am. Jour. Sci., 5th ser., XIII(73), 1-44 and XIII(74), 133-154.

Gromet, L.P. and Silver, L.T. 1983. REE distributions among minerals in a granodiorite and their petrogenetic implications. Geochem. et. Cosmochim. Acta, 47, 925-939.

Hamilton. J.V. and Hodgson, C.J. 1986. Mineralization and structure of the Kolar Gold Fields, India. Proceeding gold'86 symposium, edited by A.J. Macdoland, 270-283.

Hanson, G. N. 1980. Rare earth elements in petrogenetic studies of igneous systems. Ann. Rev. Earth Planet Sci. Lett., 8, 371-406.

Hanson, G.N. 1981. Geochemical constraints on the evolution of the early continental crust. Philos. Trans. R. Soc. Lond., 1430, 423-442.

Hanson, G.N. and Langmuir, C.H. 1978. Modelling of major elements: In mantle-melt system using element approaches. Geochem. et. Cosmochim. Acta, 42, 725-741.

Hanson. G.N., Krogsatd, E.J., Rajamani, V. and Balakrishnan, S. 1986. The Kolar schist belt: A possible Archean suture zone: Lunar Planet. Inst. Tech. Rep., 86-10, 111-113.

Harris, N.B.W. and Jayaram, S. 1982. Metamorphism of cordierite gneisses from the Bangalore region of the Indian craton. Lithos, 15, 89-98.

Helz, R.T. 1976. Phase relations of basalts in their melting ranges at P_{H2O} = 5 kb. Part II Melt compositions. Jour. Petrol., 17, 139-193.

Holloway, J.R. and Burnham, C.W. 1972. Melting relations of basalt with equilibrium water pressure less than total pressure. Jour. Petrol., 13, 1-30.

Huang, W.L. and Wyllie, P.J. 1975. Melting reactions in the system $NaAlSi_3O_8$-$KAlSi_3O_8$-SiO_2 to 35 kilobars, dry and with excess water. Jour. Geol., 83, 737-748.

Iyengar, B.R.C. and Jayaram, B.N., 1970. Stratigraphy of the 'Dharwar' rocks of Mysore. Jour. Ind. Geosci. Assoc., 12, 1-4.

Jayaram, S., Venkatasubramanian, V.S. and Radhakrishna, B.P. 1976. Rb-Sr ages of cordierite-gneisses of southern Karnataka. Jour. Geol. Soc. India, 17, 557-561.

Jayaram, S., Venkatasubramanian, V.S. and Rajagopalan, P.T. 1984. Geochemistry and petrogenesis of the Peninsular Gneisses, Dharwar Craton, India. Jour. Geol. Soc. India, 25, 570-584.

Kay, R.W. and Kay, S.M. 1988. Crustal recycling and Aleutian arc. Geochim. et Cosmochim. Acta, 52, 1351-1359.

Kay, S.M. and Kay, R.W. 1994. Aleutian magmas in space and time. In The geology of Alaska: Boulder, Colrado, edited by G. Plafker and H.C. Berg, Geol. Soc. Am., Geology of North America, G-1, 687-722.

Kay, S.M., Ramos, V.A. and Marquez, Y.M. 1993. Evidence in Cerro Pampa volcanic rocks for slab melting prior to ridge-trench collision in southern America. Jour. Geol.,101, 703-714.

Kelemen, P.B., Shimizu, N. and Dunn, T. 1993. Relative depletion of niobium in some arc magmas and the continental crust: partitioning of K, Nb, La, Ce during melt / rock interaction in the upper mantle. Earth Planet. Sci. Lett., 120, 111-134.

Kramers, J.D. 1988. An open-system fractional crystallization model for very early continental crust formation. Precambrian Res., 38, 281-295.

Krishna Murthy, M. 1974. Tectonomagnetic history of the Precambrians in the Bellary district, Mysore state. Jour. Geol. Soc. India, 15, 37-47.

Krishna Murthy, M. 1978. Geology and mineral resources of Bellary district, Karnataka (Mysore) state. Geol. Surv. India, Mem. 180, 98p.

Krogstad, E.G., Balakrishnan, S., Mukhopadhyay, D.K., Rajamani, V. and Hanson, G.N. 1989. Plate tectonics 2.5 billion years ago: Evidence at Kolar, south India. Science, 243, 1337-1340.

Krogstad, E.J., Hanson, G.N. and Rajamani, V. 1986. U-Pb zircon and sphene ages of discrete, juxtaposed, late Archean terrains, south India. EOS., 67, 400.

Krogstad, E.J., Hanson, G.N. and Rajamani, V. 1995. Source of continental magmatism adjacent to the late Archean Kolar suture zone, south India: distinct isotopic and elemental signatures of two late Archean magmatic series. Contrib. Mineral. Petrol., 122, 159-173.

Krogstad, E.J., Hanson. G.N. and Rajamani. V. 1991. U-Pb ages of zircon and sphene for two gneissic terranes adjacent to the Kolar schist belt, south India: constraints for the evolution of the crust in the Kolar area. Jour. Geol., 95, 219-240.

Krogstad, E.J., Hanson. G.N. and Rajamani. V. 1992. Archean sutures marked by schist belts, east Dharwar craton, south India. EOS, 73, 332.

Kumar, A., Bhaskar Rao, Y.J., Sivaraman, T.V.and Gopalan, K. 1996. Sm-Nd ages of Archean metavolcanics of the Dharwar craton, south India. Precambrian Res., 80, 205-216.

Kurien, T.K. 1980. Geology and mineral resources of Andhra Pradesh. Geol. Surv. India Bull., Ser. A, 44, 242p.

Kuroda, N., Shiraki, K. and Urano, H. 1978. Boninite as a possible calc-alkalic primary magma. Volcanol. Bull., 41, 563-575.

Le Bas, M.J. and Streckeisen, A.L. 1991. The IUGS systematics of igneous rocks. Jour. Geol. Soc., Lond.,148, 825-833.

Mahmood, G. and Hildreth W. 1983. Large partition coefficients for trace elements in high silica rhyolites. Geochem. et. Cosmochim. Acta, 47, 11-30.

Marmo, V. 1971. Granite Petrology and the Granite Problem. Elsevier, Amsterdam, 244p.

Martin, H. 1987. Petrogenesis of Archean trondhjemites, tonalites and granodiorites from eastern Finland: Major and trace element geochemistry. Jour. Petrol., 28, 921-953.

Martin, R.F. and Piwinskii, A.J. 1972. Magmatism and tectonic setting. Jour. Geophs. Res., 77, 4966-4975.

Meen, J.K., Rogers, J.J.W. and Fullagar, P.D. 1992. Lead isotopic compositions of the western Dharwar craton, southern India: Evidence for distinct middle Archean terranes in late Archean craton: Geochem. et. Cosmochim. Acta, 56, 2455-2470.

Menon. A.G., Venkatasubramanian, V.S., Vasudev, V.N. and Anantha Iyer, G.V. 1981. Sulphur isotope abundance variations in sulphides of the Dharwar craton – Part III, Hutti. Jour. Geol. Soc. India, 22, 448-450.

Mohanta, M.K. 1991. Geochemistry of granitic rocks around the Ramagiri Gold Fields, Andhra Pradesh. Unpub. M. Phil. Thesis, Jawaharal Nehru University, New Delhi.

Mohanta, M.K. 1998. Geochemistry and nuclear energy potential of the granitic gneisses around Ramagiri gold fields. Unpub. Ph.D Thesis, Jawaharal Nehru University, New Delhi.

Mohanty, S.C. and Raju, K.K. 1974. Geology and methods of working at Hutti Gold Mines. Golden Jublee volume, The Geological, Mining and Metallurgical Soc. India.

Mookherjee, A. and Philip, R. 1979. Distribution of copper, cobalt and nickel in ores and host rocks, Ingaldhal, Karnataka, India. Mineralium Deposita, 14, 33-55.

Muhkopadhyay, D.K. and Haimanot, B.W. 1989. Geometric analysis and significance of mesoscopic shear zones in the Precambrian gneisses around the Kolar schist belt, south India. Jour. Struc. Geol., 11, 569-581.

Mukherjee, M.M., Natarajan, W.K. and Shashidharan, K. 1986. Tectonically-controlled gold mineralization in Chigaragunta area, south Kolar schist belt, Chittor district, Andhra Pradesh. Jour. Geol. Soc. India, 27, 517-526.

Mukhopadhyay, D. 1986. Structural pattern in the Dharwar craton. Jour. Geol., 94, 167-186.

Mukhopadhyay, D. and Baral, M.C. 1985. Structural geometry of the Dharwar rocks near Chitradurga. Jour. Geol. Soc. India, 26, 547-566.

Mukhopadhyay, D. and Ghosh, D. 1983. Superposed deformation in the Dharwar rocks of the southern part of the Chitradurga schist belt near Dodguni, Karnataka. In Precambrian of south India, edited by S.M. Naqvi and J.J.W. Rogers, Geol. Soc. India, Mem., 4, 275-292.

Mukhopadhyay, D.K. 1988. Structural evolution of Kolar schist belt, south India. Jour. Geol. Soc. India, 31, 94-96.

Mukhopadhyay, D.K. 1989. Significance of small-scale structures in the Kolar scist belt, south India. Jour. Geol. Soc. India, 33, 291-308.

Mukhopadhyay, D.K. 1990. Deformational history of the Precambrian Kolar schist belt, south India: Constraints for the tectonic evolution. Proc. Ind. Aca. Sci. (Earth and Planet. Sci.), 99, 201-213.

Mysen, B.O. 1979. Trace element partitioning between garnet peridotite minerals and water rich vapour: Experimental data from 5 to 30 kb. The American Mineralogist, 64, 274-287.

Mysen, B.O. 1982. The role of mantle anatexis. In andesites, edited by R.S.Thorpe, John Willey & Sons, New York, 489-522.

Mysen. B.O. and Boettcher, A.L. 1975. Melting of a hydrous mantle, I, Phase relations of natural peridotite at high pressures and temperatures with controlled activities of water, CO_2 and H. Jour. Petrol., 16, 520-548.

Mysers, J.S. 1997. Preface: Archean geology of the eastern Goldfields of western Australia-regional overview. Precambrian Res., 83, 1-10.

Naha, K. and Chatterjee, A.K. 1982. Axial plane folding in the Bababudan hill ranges of Karnataka. Ind. Earth Sci., 9, 37-43.

Naha, K., Srinivasan, R., Gopalan, K., Pantulu, G.V.C., Subba Rao, M.V., Vrevsky, A.B. and Bogomolov, Y.S. 1993. The nature of the basement in the Archaen Dharwar craton of southern India and the age of the Peninsular Gneiss: Proc. Ind. Acad. Sci. (Earth Planet. Sci.), 102, 547-565.

Naqvi, S.M. 1973. Geological structure and aeromagnetic and gravity anomalies in the central part of the Chitradruga schist belt, Mysore, India. Geol. Soc. Am. Bull., 84, 1721-1732.

Naqvi, S.M. 1976. Pysico-chemical conditions during the Archean as indicated by Dharwar geochemistry. In The Early History of the Earth, edited by B.F. Windley, John Wiely, New York, 289-298.

Naqvi, S.M. and Rogers, J.J.W. 1987. Precambrian Geology of India. Oxford Monograph on Geology and Geophysics No. 6. Clarendon Press/Oxford University Press.

Narayanan Kutty, T.R. and Anantha Iyer, G.V., 1977a. Chemical petrology of calc-silicate rocks and associated metamorphics around Sakarasanahalli, Kolar. Ind. Jour. Earth Sci., 4, 141-159.

Narayanan Kutty, T.R. and Anantha Iyer, G.V., 1977b. Mineralogy of coexisting zoisite-clinozoisite and epidote from Sakarasanahalli, Kolar, Karnataka. Jour. Geol. Soc. India, 18, 78-89.

Nash, W.P.and Crecraft, H.R. 1985. Partition coefficients for trace elements in silisic magmas. Geochem. et. Cosmochim. Acta, 49, 2309-2322.

NGRI. 1992. Antiquity of the Dharwar craton. National Geophysical Research Institute (NGRI), Hyderabad, Annual report from 1991-1992, 19-20.

Nielsen, R.L. 1985. EQUIL: a program for the modeling of low-pressure differentiation processes in natural mafic magma bodies. Computer and Geosciences, 11, 531-546.

Nielsen, R.L. 1988. TRACE. FOR: a program for the calculation of combined major and trace-element liquid lines of descent fro natural magmatic systems. Computer and Geosciences,14, 15-35.

Nisbet, E.G. 1987. The Young Earth. Allen and Unwin, Boston, Mass., 402p.

Nutman, A.p., Chadwick, B., Krishna Rao, B. and Vasudev, V.N. 1996. SHRIMP U/Pb zircon ages acid volcanic rocks in the Chitradurga and Sandur Groups, and granites adjacent to the Sandur schist belt, Karnataka. Jour. Geol. Soc. India, 41, 153-164.

Nutman, A.P., Chadwick, B., Ramakrishnan, M. and Viswanatha, M.N. 1992. SHRIMP U-Pb ages of detrital zircon in Sargur supracrustal rocks in western Karnataka, southern India. Jour. Geol. Soc. India, 39, 367-374.

Olafsson, M. and Eggler, D.H. 1983. Phase relations of amphibole, amphibole-carbonate and phlogopite - carbonate peridotite: Petrologic constraints on the asthenosphere. Earth Planet. Sci. Lett., 64, 305-315.

Parson, B.A. and Sclater, J.G. 1977. An analysis of the variation of ocean floor bathymetry and heat flow with ages. Jour. Geophys. Res.,82, 802-827.

Peucat, J.J., Bouhallier, H., Fanning, C.M. and Jayananda, M. 1995. Age of Holenarsipur greenstone belt, relationships with the surrounding gneisses, Karnataka, south India. Jour. Geol., 103, 701-710.

Philpotts, A.R. 1994. Principles of Igneous and Metamorphic Petrology. Prentice-Hall of India Pvt. Ltd.

Potts, P.J. 1987. A Handbook of Silicate Rock Analysis. Blackie Glasgow, 622p.

Raase, P., Raith, M., Ackermand, D. and Lal, R.K. 1986. Progressive metamorphism of mafic rocks from greenschist to granulite facies in the Dharwar craton of south India. Jour. Geol., 94, 261-282.

Radhakrishna, B.P. 1954. On the nature of certain cordierite-bearing granulites bordering the Closepet granites of Mysore. Mysore Geol. Deptt. Bull., 21, 25p.

Radhakrishna, B.P. 1967. Reconsideration of some problems in the Archean complex of Mysore. Geol. Soc. India, 8, 102-109.

Rajamani, V., Shirey, S.B. and Hanson, G.N. 1989. Fe-rich Archaean tholeiites derived from melt enriched mantle sources: evidence from the Kolar Schist Belt, south India. Jour. Geol., 97, 487-501.

Rajamani, V., Shivakumar., K., Hanson, G.N. and Shirey, S.B. 1985. Geochemistry and petrogenesis of amphibolites, in the Kolar schist belt, south India: evidence for komatiitic magma derived by low percentage of the melting of the mantle. Jour. Petrol., 26, 92-123.

Rapp, R.P. and Watson, E.B. 1995. Dehydration melting of metabasalt at 8-32 kbar: Implications for continental growth and crust-mantle recycling. Jour. Petrol.,36, 892-931.

Rapp, R.P., Watson, E.B. and Miller, C.F. 1991. Partial melting of amphibolite/eclogite and the origin of Archean trondhjemites and tonalites. Precambrian Res., 51, 1-25.

Rathi, M.S., Khanna, P.P. and Mukherjee, P.K. 1991. Determination of ten rare-earth elements and yttrium in silicate rocks by ICP-AES without separation and preconcentration. Talanta, 38, 329-332.

Rathi, M.S., Khanna, P.P., Mukherjee, P.K., Purohit, K.K. and Saini, N.K. 1994. Working values for major, minor and trace elements for meta-basic reference sample (MB-H). Jour. Geol. Soc. India, 43, 295-303.

Read, H.H. 1948 Granites and Granites. Geol. Soc. Am., Mem., 28, 1-19.

Reddy, K.N., Dutta, S.K. and Palaniappan, K. 1992. Assessment of gold resources in Ramagiri-Penakacherla schist belt, Anantapur district, Andhra Pradesh. Rec. Geol. Surv. India, 125, part 5, 27-29.

Riazullah, M.S., Pathan, A. and Maaskant, P. 1996. The characterization of metamorphic facies of metabasalts of Hutti greenstone belt. Jour. Geol. Soc. India, 47, 547-554.

Roedder, E. 1956. The role of liquid immiscibility in igneous petrogenesis: A discussion. Jour. Geol., 64, 84-88.

Roeder, P.L. and Emsile, R.F. 1971. Olivine- liquid equilibrium. Contrib. Mineral. Petrol., 22, 275-289.

Rollinson, H.R., Windley, B.F. and Ramakrishnan, M., 1981. Contrasting high and intermediate pressures of metamorphism in the Archean Sargur schists of southern India. Contrib. Mineral. Petrol., 76, 420-429.

Roy, A. 1979. Polyphase folding deformation in the Hutti-Maski Schist Belt, Karnataka. Jour. Geol. Soc. India, 20, 598-607.

Roy, A. and Biswas, S.K. 1979. Metamorphic history of Sandur schist belt, Karnataka. Jour. Geol. Soc. India, 20, 179-187.

Roy, A. and Biswas, S.K. 1982. A note on the volcanic conglomerate'/pyroclast horizon near Palkhanmaradi in the Hutti schist belt, Karnataka. Jour. Geol. Soc. India, 506-510.

Rudnick, R.L. and Taylor, S.R. 1986. Geochemical constraints on the origin of tonalitic-trondhjemitic rocks and implication for lower crustal compositon. In The nature of the lower Continental Crust Dawson, edited by J.B., Carswell, D.A., Hall, J. and Wedepohl, K.H, Geol. Soc. Spec. Pub., 24, 179-91.

Ryerson, F.J. and Hess, P.C. 1978. Implications of liquid distribution coefficients to mineral-liquid partitioning. Geochem.et Cosmochim. Acta, 42, 921-932.

Safonav, Yu. G., Radhakrishna, B.P., Krishna Rao, M., Vasudev, V.N., Krishna Raju, K., Nosik, L.P. and Pashkov, Y.N. 1980. Mineralogical and geochemical features of epigene gold and copper deposits of south India. Jour. Geol. Soc. India, 21, 365-378.

Safonov, Yu.G., Genkin, A.D., Vasudev, V.N., Krishna Rao, B. And Anantha Iyer, G.V. 1984. Genetic features of gold ore deposit at Kolar, Dharwar craton, India. Jour. Geol. Soc. India, 25, 145-154.

Sahoo, J. and Balakrishnan, S. 1994. Geochemistry and Petrogenesis of Kolar Dolerite Dykes in and around Kolar schist belt, south India. Jour. Geol. Soc. India, 43, 511-528.

Satyanarayana, K., Srinivasan, G., Malhotra, R.K. and Tikoo, B.N. 1989. Determination of rare-earth elements and yttrium in some uranium and thorium rich geological materials by inductively coupled plasma emmision spectrometry. Expl. Res. Atomic Min., 2, 235-245.

Shapiro, L. and Brannock, W.W. 1962. Rapid analyses of silicate, carbonate and phosphate rocks. USGS, Bull., 1144A.

Shaw, H.R. 1965. Comments on viscosity, crystal settling, and convection in granitic magmas. Am. Jour. Sci., 263, 120-152.

Shirey, S.B. and Hanson, G.N. 1984. Mantle-derived Archaean monzodiorites and trachyandesites. Nature, 310, 222-224.

Simmons, E.G. and Hedge, C.E. 1978. Minor-element and Sr-isotope geochemistry of Tertiary Stocks, Colorado mineral belt. Contrib. Mineral. Petrol., 67, 379-396.

Siva Siddaiah, N. and Rajamani, V. 1989. The geologic setting, mineralogy, geochemistry, and genesis of gold deposit of the Archean Kolar schist belt, India. Eco. Geol., 84, 2155-2172.

Sivaprakash, C. 1983. Petrology of quartzo-feldspathic schists/phyllites associated with manganese formation of north Kanara and Kumsi Karnataka. Jour. Geol. Soc. India, 24, 571-587.

Sleep, N.H and Windley, B.F. 1982. Archean plate tectonics: Constraints and inference. Jour. Geol., 90, 363-379.

Smeeth, W.F. 1916. Outline of geological history of the Mysore. Mysore Geol. Dept., Bull ,6.

Spear, F.S. 1981. An experimental study of hornblende stability and compositional variability in amphibole. Am. Jour. Sci., 281, 697-734.

Srikantia, S.V. 1995. Geology of Hutti-Maski Greenstone belt, In: Hutti Gold Mine, into the 21st century. Geol. Soc. India, Min. Res. India, No.8, 8-27.

Stern, C.R. and Wyllie, P.J. 1978. Phase compositions through crystallization intervals in basalt-andesite-H_2O at 30 kbar with implications for subduction zone magmas. Am. Mineral., 63, 641-663.

Stern, R.A. and Hanson, G.N. 1991. Archean high Mg Granodiorite : A derivative of Light Rare Earth Element enriched Monzodiorite of mantle origin. Jour. Petrol., 32, 201-238

Stern, R.A., Hanson, G.N. and Shirey, S.B. 1989. Petrogenesis of mantle-derived Archean monzodiorites and trachyandesites (sanukitoids) in southwestern Superior Province. Can. Jour. Earth Sci., 26, 1688-1712.

Strekeisen, A. 1976. To each plutonic rock its proper name. Earth Sci. Rev., 12, 1-33.

Stroth, P.T., Monrad, J.R., Fullagar, P.D., Naqvi, S.M. and Hussain, S.M. 1983. 3,000 m.y-old Halekote trondjemite: a record of stabilization of the Dharwar craton. In Precambrian of south India, edited by S.M. Naqvi and J.J. Rogers, Geol. Soc. India Mem., 4, 365-376.

Sun, S.S. and McDonough, W.F. 1989. Chemical and isotopic systematics of oceanic basalts: Implications for mantle composition and processes. In Magmatism in the ocean basins, edited by A.D. Sanders and M.J. Norry, Geol. Soc. Lond., Spc. Pub., 42, 313-345.

Swaminath, J. and Ramakrishnan, M. (Eds) 1981. Early Precambrian supracrustals of southern Karnataka. Geol. Surv. India, Mem.,112, 1-350.

Swaminath, J., Ramakrishnan, M. and Viswanathan, M.N. 1976. Dharwar stratigraphic model and Karnataka craton evolution. Rec. Geol. Surv. India, 107, 149-179.

Takahasi, E. and Kushiro, I. 1983. Melting of a dry peridotite at high pressures and basalt magma genesis. The Am. Mineralogist, 68, 850-879.

Takahasi, E. and Scarfe, C.M. 1985. Melting of Peridotite to 14 GPa and the genesis of komatiite. Nature, 315, 566-568.

Tarney, J., Dalziel, W.D. and DeWit, M.J. 1976. Marginal basin 'Rocas Verdes' complex from S. Chile: A model for Archean greenstone belt formation. In The Early History of the Earth, edited by Windley, John Wiley, New York, 131-146.

Tatsumi, Y. 1982. Origin of high magnesian andesites in the Setouchi volcanic belt, southwest Japan, II. Melting phase relations at high pressures. Earth Planet. Sci. Lett., 60, 305-317.

Tatsumi, Y., Hamilton, D.L. and Nesbit, R.W. 1986. Chemical characteristics of fluid phase released from a subducted lithosphere and origin of arc magmas: Evidence from

high pressure experiments and natural rocks. Jour. Volcano. Geoth. Res., 29, 293-309.

Tatsumui, Y. and Eggins, S. 1995. Subduction zone magmatism. Blackwell Science, Ltd., 211p.

Taylor, P.N., Chadwick, B., Friend, C.R.L., Ramakrishna, M., Moorbath, S. and Viswanatha, M.N. 1988. New age data on the geological evolution of southern India. Workshop on the deep continental crust of south India. Jour. Geol. Soc. India, 31, 155-158.

Taylor, S.R. and Mclennan, S.M. 1981. The composition and evolution of the continental crust: Rare earth element evidence from sedimentary rocks. Phil. Trans. R. Soc. Lond., 301A, 381-399.

Thompson, A.B. 1992. Water in the earth's upper mantle. Nature, 358, 295-302.

Trendall., A.F., de Laeter, J.R., Nelson, D.R. and Bhaskar Rao, Y.J. 1997. Further zircon U-Pb age data for the Daginkatte Formation, Dharwar Supergroup, Karnataka craton. Jour. Geol. Soc. India, 50, 25-30.

Vasudev, V.N. and Naganna, C. 1973. Mineralogy of gold-quartz-sulfide reefs of Hutti Gold Mines, Raichur district, Mysore State. Jour. Geol. Soc. India, 14, 378.

Viswanatha, M.N. and Ramakrishnan, M. 1981. Kolar belt. Geol. Surv. India Mem., 112, 221-245.

Viswanatha, M.N. and Ramakrishnan, M. 1981. Sargur and allied belts. In early Precambrian of supracrustals of southern Karnataka, edited by J. Swaminath and M. Ramakrishnan, Geol. Soc. India, Mem., 112, 41-59.

Walsh, J.N., Buckley, F. and Barker, J. 1981. The simultaneous determination of the rare earth elements in rocks using inductively coupled plasma source spectrometry. Chem. Geol., 33, 141-153.

Watson, E.B. 1976. Two liquid partition coefficients: experimental data and geochemical implications. Contrib. Mineral. Petrol., 56, 119-134.

White, W.M. and Patchett, J. 1984. Hf-Nd-Sr isotopes and incompatible element abundances in Island arcs: Implications for magma origins and crust-mantle evolution. Earth Planet. Sci. Lett., 67, 167-185.

Wilson, M., 1989. Igneous Petrogenesis- A global tectonic approach, Unwin Hyman Ltd. 466p.

Wilson, M., Downes, H. and Cebria, J. 1995. Contrasting fractionation trends in co-existing continental alkaline magma series; Cantal, Massif Central, France. Jour. Petrol., 36, 1729-1753.

Windley, B.F. 1984. The evolving Continents. John Wiley, New York, 399p.

Working Group of GSI. AMD. and NGRI. 1977. The geology and geochemistry of Kolar schist belt with special reference to the early history of crustal development of southern Peninsular shield of India. Archean Geochemistry Sym., Hyderabad., 12-20, Abstract.

Wyllie, P.J. 1977. Experimental studies on biotite and muscovite granites and some crustal magmatic sources, in Migmatites, melting and metamorphism. In proceedings of the Geochemical Group of the Mineralogical Society, edited by M.P. Atherton and C.D. Gibble, Shiva publishing Ltd., Nantwich, 12-26.

Yogodzinski, G.M., Kay, R.W., Volynets, O.N., Koloskov, A.V. and Kay, S.M. 1995. Magnesian andesites in the western Aleutian Komandorsky region: Implication for slab melting and processes in the mantle wedge. Geol. Soc. Am. Bull., 107, 505-519.

Zachariah, J.K., Hanson, G.N. and Rajamani, V. 1995. Post crystallization disturbances in the Nd and Pb isotope systematics of metabasalts from the Ramagiri schist belt, south India. Geochem. et. Cosmochim. Acta, 59, 3189-3203.

Zachariah, J.K., Mohanta, M.K. and Rajamani, V. 1996. Accretion evolution of the Ramagiri schist belt, eastern Dharwar craton, Jour. Geol. Soc. India, 47, 279-291.

Zachariah, J.K., Rajamani, V. and Hanson, G.N. 1997. Petrogenesis and source characteristics of metatholiites fromthe Archean Ramagiri schist belt, eastern part of Dharwar craton, India. Contrib. Mineral. Petrol., 129, 87-104.

Zachariah, Z.K. 1992. Geochemistry and Petrogenesis of amphibolites of Ramagiri Gold Fields, south India. Unpub Ph.D Thesis, Jawaharal Nehru University, New Delhi.

Ziauddin, M. and Narayanaswamy, S. 1974. Gold Resources of India. Geol. Surv. India Bull., 38, 114-116.

APPENDIX

Table 1

	REE abundance in granodiorites and sphenes (in ppm.)													
	B-5			B-7			B-8			St & Ha'91		Gr & Si'83		CHR
	WR	Sp	Sp/WR	WR	Sp	Sp/WR	WR	Sp	Sp/WR	Sp	Sp/WR	Sp	Sp/WR	
Ce	48.2	3377.9	70.1	34.2	2685.7	78.51	123.0	1193.6	9.7	9704	77.5	3305	51.2	0.813
Nd	18.3	2362.2	129.1	12.1	1811.7	149.7	51.0	1503.2	29.5	5313	97.1	2680	107.2	0.597
Sm	4.1	450.6	109.9	3.2	416.1	130.0	10.0	534.9	53.5	877	102.0	655	152.3	0.192
Eu	1.1	68.0	61.8	0.9	82.2	91.3	2.1	128.9	61.4	157	87.2	165	150.0	0.0722
Gd	3.0	262.8	87.6	2.5	273.0	109.2	6.1	428.3	70.2	531	100.2	564	165.9	0.259
Dy	1.7	182.7	107.4	1.5	178.6	119.0	3.3	359.3	108.9	311	103.6	470	180.7	0.213
Er	0.9	93.3	103.6	0.8	84.3	105.4	1.5	168.4	112.2	138	98.6	237	182.3	0.208
Yb	0.9	71.0	78.9	0.8	58.9	73.6	0.9	119.8	133.1	114	95.0	207	188.8	0.208
Total	78.2	6868.5	-	56.0	5590.5	-	197.9	4436.4	-	17145	-	8283	-	-

The analytical uncertainties for the REE data are within ± 5% except for Nd and Er for which the uncertainties are within ± 10% of the amount reported.
WR = Whole Rock; Sp = Sphene Sp/WR = approximated as K_d values of sphene for REEs
St & Ha'91 = Stern and Hanson (1991)
Gr & Si'83 = Gromet and Silver (1983)
CHR = REE abundance in chondrite used for the normalization as given in Hanson (1980).
Sphene data from Basir and Balakrishnan (1999)

REE abundance in Hutti tholeiites			
	GH-7	GH-10	HG-5B
Ce	24.33	10.59	13.92
Nd	15.9	6.71	8.9
Sm	4.68	1.94	2.71
Eu	1.89	0.69	0.94
Gd	5.03	2.4	3.68
Dy	4.9	2.9	4.23
Er	2.67	1.96	2.94
Yb	2.09	1.77	2.72

Data from Giritharan and Rajamani (1998).

Table 2

	Olivine	OPX	CPX	HB	PLAG	GT	BIOTITE	KF	Sphene
				K_d values for granodiorite melt					
Ce	0.0069	0.03	0.508	0.899	0.24	0.35	0.037	0.044	70.1
Nd	0.0066	0.047	0.645	2.89	0.17	0.53	0.044	0.025	129.1
Sm	0.0066	0.082	0.954	3.99	0.13	2.66	0.058	0.018	109.9
Eu	0.0068	0.069	0.681	3.44	2.11	1.5	0.145	1.13	61.8
Gd	0.0077	0.132	1.35	5.48	0.09	10.5	0.082	0.011	87.6
Dy	0.0096	0.212	1.46	6.2	0.086	28.6	0.097	0.006	107.4
Er	0.011	0.314	1.33	5.94	0.084	42.8	0.162	0.006	103.6
Yb	0.014	0.438	1.3	4.89	0.077	39.9	0.179	0.012	78.9
Sr	0.014	0.032	0.033	0.022	2.84	0.015	0.12	3.87	
Ba	0.0099	0.013	0.04	0.044	0.36	0.017	6.36	6.12	

	Olivine	OPX	CPX	HB	PLAG	GT	BIOTITE	Sphene
				K_d values for basaltic melt				
Ce	0.0069	0.02	0.15	0.2	0.12	0.03	0.034	70.1
Nd	0.0066	0.03	0.31	0.33	0.081	0.07	0.032	129.1
Sm	0.0066	0.05	0.5	0.52	0.067	0.29	0.031	109.9
Eu	0.0068	0.05	0.51	0.4	0.34	0.49	0.03	61.8
Gd	0.0077	0.09	0.61	0.63	0.063	0.97	0.03	87.6
Dy	0.0096	0.15	0.68	0.64	0.055	3.17	0.03	107.4
Er	0.011	0.23	0.65	0.55	0.063	6.56	0.034	103.6
Yb	0.014	0.34	0.62	0.49	0.067	11.5	0.042	78.9
Sr	0.014	0.04	0.06	0.46	1.83	0.012	0.081	
Ba	0.0099	0.013	0.026	0.42	0.23	0.023	1.09	

OPX = Orthopyroxene, CPX = Clinopyroxene, HB = Hornblende, PLAG = Plagioclase, GT = Garnet